FABRICATION, SWELLING, AND BIOLOGICAL PROPERTIES OF SURFACE-PATTERNED HYDROGELS BASED ON POLY(2-HYDROXYETHYL METHACRYLATE)

By

HASANI G. J. JAYSINGHE ARACHCHIGE DONA

Bachelor of Science in Chemistry
University of Kelaniya
Sri Lanka
2010

Submitted to the Faculty of the
Graduate College of the
Oklahoma State University
in partial fulfillment of
the requirements for
the Degree of
DOCTOR OF PHILOSOPHY
December, 2018

FABRICATION, SWELLING, AND

BIOLOGICAL PROPERTIES OF

SURFACE-PATTERNED HYDROGELS BASED ON

POLY(2-HYDROXYETHYL METHACRYLATE)

Dissertation Approved:

Dr. Yolanda Vasquez

Dissertation Adviser

Dr. Barry K. Lavine

Dr. Frank D. Blum

Dr. Toby Nelson

Dr. Sundar V. Madihally

ACKNOWLEDGEMENTS

I would like to express my sincere gratitude to my research adviser Dr. Yolanda Vasquez for her immense support and guidance toward the success of my degree at Oklahoma State University. I am truly grateful to my graduate advisory committee Dr. Barry K. Lavine, Dr. Frank D. Blum, Dr. Toby Nelson (Department of Chemistry, OSU), and Dr. Sundar V. Madihally (Department of Chemical Engineering, OSU) for their valuable comments and suggestions given to my research, and support extended during the difficult times in my time at OSU.

I extend my special thanks to the Faculty and staff members of the Department of Chemistry, OSU for their support and guidance during my stay at OSU. As well, I am sincerely thankful to our collaborator Dr. Mughees Khan, as well as Dr. Kenneth D. Berlin and Dr. Jeffery L. White for their support with the manuscript and publication of research work. I would also like to thank the staff members of OSU Microscopy Laboratory and Oklahoma Animal Disease Diagnostic Laboratory (OADDL), Center for Veterinary Health Sciences, OSU, for their assistance in my research. I acknowledge the financial support from Department of Chemistry, OSU, and National Science Foundation. Also, I would like to thank my former and current lab mates for creating a friendly environment in the lab.

I humbly appreciate my undergraduate adviser Dr. K. A. S. Pathiratne and the other professors at the University of Kelaniya, Sri Lanka, for their guidance and advice provided during my undergraduate studies and all my teachers at Sirimavo Bandaranaike Vidyalaya, Colombo 7, Sri Lanka, for providing me a strong primary and secondary education.

I express my highest appreciation to my father (late Mr. Piyasiri Jayasinghe), mother (Mrs. Jayantha Jayasinghe), and sister (Ms. Manori Jayasinghe) for their unconditional love, encouragement, and tremendous support, which inspired me to be who I am today. Also, I am very much grateful to my loving husband, Mr. Ujith S. K. Madduma-Bandarage, without whom I would have never accomplished this goal. As well, I wish to extend many thanks to my in-laws' family for their love and help during this journey. Finally, I would like to thank all my friends in Stillwater for making this time happy and joyful.

Name: HASANI G. J. JAYSINGHE ARACHCHIGE DONA

Date of Degree: DECEMBER, 2018

Title of Study: FABRICATION, SWELLING, AND BIOLOGICAL PROPERTIES OF SURFACE-PATTERNED HYDROGELS BASED ON POLY(2-HYDROXYETHYL METHACRYLATE)

Major Field: CHEMISTRY

Abstract:

Hydrogels are networks of hydrophilic polymers which can retain large amounts of water. Poly(2-hydroxyethyl methacrylate) [poly(HEMA)] is a synthetic hydrogel well known for various biomedical applications due to excellent biocompatibility, high retention of water, and high mechanical and chemical stability, but, has limited applications in tissue engineering because of low cell-adhesion properties. Patterning surfaces of hydrogels with microscale features changes the surface properties and enables the regulation of functions of cultured cells. However, generating patterns of intricate microstructures onto the hydrogel surfaces remains challenging. In this work, arrays of micropillars were successfully patterned onto a hydrogel based on 2-hydroxyethyl methacrylate by using soft lithography technique. The self-delamination of the hydrogel induced by swelling in solvents such as phosphate buffered saline, deionized water, 60% ethanol, and absolute ethanol facilitated the reproducible replication of the pattern. The swelling, mechanical properties, and structural parameters of the hydrogel were studied in detail. The biological properties of the hydrogel were evaluated using HeLa cells and human mesenchymal stem cells. It was revealed that the attachment of cells on the intrinsically non-adhesive hydrogel was enhanced by the micropillars. As well, the stem cells tend to form aggregates on the hydrogel and the size and number of cell aggregates can be tuned by changing the height of the micropillars. The fabricated material was not cytotoxic and did not inhibit the chondrogenic and adipogenic differentiation of stem cells at the composition used in synthesis.

TABLE OF CONTENTS

Chapter Page

Chapter Page

LIST OF TABLES

LIST OF FIGURES

Figure Page

Figure Page

Figure Page

LIST OF SCHEMES

Scheme Page

CHAPTER I

INTRODUCTION

Hydrogels are three-dimensional, hydrophilic network polymers which have chemical or physical cross-links.[1,2] The chemical cross-links can be either ionic or covalent while the chain entanglements or interactions such as hydrogen bonding and van der Waals forces are considered as physical cross-links.[3] The hydrophilic nature of polymer chains allows penetration of water into the network while the cross-linked structure imparts flexibility so that the integrity of the polymer remains intact and chemical stability.[4,5] As a consequence, the polymer swells by retaining a large quantity of water and forms a hydrogel. The water absorbed soft hydrogels possess the mechanical properties similar to the soft tissues and hence resemble the natural tissue environment. When synthesized from biocompatible monomers, the hydrogels find tremendous applications in the biomedical field as drug delivery systems[6-8] and scaffolds in tissue engineering.[9,10]

Characterization of the network structure of a hydrogel is important because these structural features affect the properties of the material in the aforementioned applications. The parameters which define the structure of a swollen hydrogel include volume fraction of the polymer in the swollen state, the cross-linking density, the average molecular weight between cross-links, and the network mesh or pore size.[1,11]

Poly(2-hydroxyethyl methacrylate) (poly(HEMA)) is a widely studied synthetic hydrogel which has excellent biocompatibility, high retention of water, as well as high chemical and mechanical stability.[12-14] During past few decades, HEMA has been copolymerized with various synthetic and natural monomers to acquire properties desirable for target applications; for instance, HEMA was copolymerized with N-isopropylacrylamide (NIPAAm) for temperature sensitivity,[15] 2-(diisopropyl-amino)ethyl methacrylate (DPA)[16] or acrylic acid (AA)[17] for pH sensitivity, N,N-(dimethylamino-ethyl)methacrylate (DMAEMA) for both pH and temperature sensitivity,[18] methyl methacrylate (MMA) to tune the swelling properties,[19] and hemicellulose[20] or polycaprolactone[21] to increase biodegradability.

Poly(HEMA)-based hydrogels have a broad range of biomedical applications that include soft contact lenses,[22] artificial corneas,[23] artificial skin,[24] as a bone composite material,[25] and as a dentin bonding agent.[26] However, applications of poly(HEMA) hydrogels as scaffolds in tissue engineering where the cells are grown directly on the hydrogel are limited due to poor cell adhesion which is caused by the lack of cell binding domains.[27,28] According to previous studies, the cell adhesion properties of non-adhesive poly(HEMA) hydrogel can be improved by copolymerization of HEMA with hydrophobic monomers i.e. ethyl methacrylate (EMA),[28,29] or by modification of the hydrogel surface with extracellular matrix (ECM) components such as collagen,[30,31] and fibronectin.[31] Furthermore, adhesion of cells onto intrinsically non-adhesive poly(HEMA)-based hydrogels was enhanced by introducing topographic features onto the surface.[32]

Patterning hydrogel surfaces with micro to nanoscale topographic features changes the surface properties such as wettability[33] and adhesion.[34] Surface-patterned hydrogels can be fabricated by using the soft lithography technique where the features originally produced on a silicon wafer are transferred to the hydrogel surface with the aid of an intermediate elastomeric mold,

i.e. poly(dimethylsiloxane) (PDMS) mold.[35] However, the mechanical properties of the hydrogel, adhesion between the hydrogel and the mold, as well as the dimensions of the features may result in the incomplete transfer of pattern and low fidelity;[36] thus, patterning of hydrogel surfaces remains challenging.

The combination of properties of patterned-surfaces with hydrogels provides an excellent platform to regulate functions of cells, especially in tissue engineering applications. Tissue engineering is an emerging, interdisciplinary field that combines principles of life sciences and engineering to improve or regain functions of malfunctioning tissues.[37] The main tissue engineering strategies utilize incorporation of suitable types of cells with materials that can be used as a platform to grow cells *in vitro* or as delivery devices to carry growth factors.[38] The two main types of cells used in tissue engineering are embryonic stem cells (ES) and human mesenchymal stem cells (hMSCs).[38] Human mesenchymal stem cells are undifferentiated, primary cells which can be isolated from various tissues or organs including bone marrow, umbilical cord, adipose tissue, placenta etc. The mesenchymal stem cells can be differentiated *in vivo* and *in vitro* into other specialized cell types such as osteoblasts (cells in bone tissue), chondrocytes (cells in cartilage tissue), and adipocytes (cells in fat tissue).[39] The ability to self-renew, expand outside the body, and establish daughter cells make the mesenchymal stem cells desirable in tissue engineering applications.[40] Once cultured on a surface with good cell attachment (i.e. tissue culture plastic or polystyrene), these mesenchymal stem cells show fibroblast-like morphology having elongated shapes and grow as monolayers adherent to the surface.[41] It has been reported that the cells interact with the surrounding environment and the properties of the materials such as elasticity[42] as well as topographical features can influence their gene expression resulting changes in morphology, proliferation, and adhesion.[43] A study published by Bucaro et al. reported that the arrays of nanoscale pillars provided contact guidance to the stem cells directing their attachment, growth, and differentiation patterns.[44] Gunendiren et al. also has shown that the wrinkling patterns generated on the poly(HEMA) hydrogel surface can control the shape and the differentiation

of stem cells.[45] Jeon and Alsberg reported the control of viability, proliferation rate, and differentiation of adipose-derived stem cells on a poly(ethylene glycol) (PEG) hydrogel using micropatterns created by different cross-linking of the hydrogel.[46] Since previous studies evident that the surface features can determine the fate of stem cells, it is worthwhile to investigate the effect of topographical features and the dimensions of the pattern, patterned onto the surface of a non-adhesive hydrogel, on morphology, attachment, and differentiation of stem cells.

In this study, a poly(HEMA/DMAEMA/TEGDMA) (HEMA = 2-hydroxyethyl methacrylate, DMAEMA = N,N-(dimethylaminoethyl)methacrylate, and TEGDMA = tetraethylene glycol dimeth-acrylate) hydrogel patterned with hexagonal arrays of micropillars having dimensions of diameter (d) = 1 μm, height (h) = 2 μm or 6 μm, and interpillar spacing (d_{int}) = 3 μm was fabricated using soft lithography technique. Chapter 2 describes the fabrication of the surface-patterned poly(HEMA/DMAEMA/TEGDMA) hydrogel. Here, the polymer-PDMS composite was soaked in a solvent, until the hydrogel delaminated from the mold to successfully transfer the micropattern. The effect of functionalization of the PDMS mold, swelling solvent, and the dimensions of the mold was investigated with respect to the transfer of pattern. Also, the temperature dependency of swelling of the poly(HEMA/DMAEMA/TEGDMA) hydrogels and kinetics of sorption were evaluated. Not only that, the compatibility of the hydrogel with two common histological sectioning protocols, paraffin and cryosectioning, was also examined to figure out the best technique for analyzing the behavior of the stem cells cultured on the hydrogels.

The properties such as swelling, network parameters, and mechanical properties of poly(HEMA-/DMAEMA/TEGDMA) hydrogels have not been broadly investigated, especially, at the composition used here; hence it is important to explore the properties of the hydrogel post synthesis. Chapter 3 focuses on characterization of the fabricated polymer. The swelling of the hydrogel was studied in

four solvents: deionized water, phosphate buffered saline (PBS), 60% ethanol, and absolute ethanol, by means of solvent uptake. Since swelling of the polymer was crucial in the surface-patterning process, the swelling behavior was studied while the polymer was confined in the PDMS mold using a swelling-induced curvature of the hydrogel-PDMS composite and solvent uptake. Additionally, the mechanical properties, network parameters, solubility parameter, and biological properties of the polymer were also determined.

Previous studies show that poly(HEMA)-based hydrogels patterned with different topographical features have interesting biological applications in controlling tissue growth,[47] morphology, and differentiation lineage of cells.[45] Chapter 4 highlights a potential application of poly(HEMA-/DMAEMA/TEGDMA) hydrogel bearing micropillar arrays in biological studies. The goal of this work was to study the morphology, attachment, and differentiation of human mesenchymal stem cells (hMSCs) cultured on the fabricated hydrogels. As the cells tend to aggregate on the hydrogel, the effect of micropattern on the number and size of aggregates was investigated. As well, the differentiation potential of cells along chondrogenic and adipogenic lineages was also explored.

CHAPTER II

SWELLING INDUCED SELF-DELAMINATION OF HYDROGELS FOR GENERATING MICROPILLARS ON THE SURFACE

Note: Parts of this chapter was published in Jayasinghe, H. G, Tormos, C. J., Khan, M., Madihally, S., and Vasquez, Y., (2018), A soft lithography method to generate arrays of microstructures onto hydrogel surfaces; Journal of Polymer Science Part B: Polymer Physics, 56, 1144-1157, (published by John Wiley & Sons, Inc., NJ), (DOI:10.1002/polb.24634)

2.1. Introduction

Hydrogels are cross-linked networks of hydrophilic polymers that absorb large quantities of solvents without dissolution and, therefore, exhibit volume expansion or swelling.[2,4] Since swelling is a characteristic feature of a hydrogel, the swelling behavior of hydrogels has been broadly studied.[5,48-52] The swelling of a hydrogel depends on the properties of the polymer, solvent,[53] as well as the external factors such as pH,[54] temperature,[55] and ionic strength.[18] The key features of hydrogels including high retention of water, mechanical properties akin to the natural tissues, and biocompatibility support hydrogels to mimic the natural biological environment; thus the hydrogels have been studied in a broad range of biological applications such as delivery systems,[56] and scaffolds in tissue engineering.[9]

Surface properties of a hydrogel, such as hydrophobicity, can be altered by patterning the hydrogels with microscale features such as pillars, plates, and wrinkles.[33,47,57-59] The two most common techniques used for fabrication of surface-patterned hydrogels are photolithography[60] and soft-lithography.[35,60] Although photolithography has the advantage of generating high-resolution features on solid and semi-solid systems, drawbacks such as high cost, the requirement of special conditions i.e., a clean room facility and the limitation of using photosensitive materials restrict its broad use.[35,60] Soft lithography is a complimentary technique which uses an elastomeric mold or stamp as an intermediate template to transfer the topographical features originally created on silicon wafers by photolithography to the hydrogels or any other surface of interest. The use of an elastomeric mold allows patterning hydrogels with high fidelity and reproducibility.[35,61]

Poly(dimethylsiloxane) (PDMS) is widely used as the elastomeric material in soft lithography due to favorable properties like low surface energy, good thermal stability, optical transparency, and its non-hygroscopic nature.[35,62] After the polymerization of monomers in the PDMS mold, the hydrogel is removed from the mold, usually, by lifting off.[47] However, the mechanical release of the hydrogel from the mold may result in the poor transfer of features depending on the feature size as well as intrinsic properties of the hydrogel including low mechanical strength and adhesion.[63,64] In a study previously reported by Chiellini et al., swelling of the hydrogel was used to remove the surface-patterned hydrogel from a glass slide,[32] but has not been applied in soft lithography techniques for demolding the hydrogels from the elastomeric mold.

In this study, a surface-patterned hydrogel based on 2-hydroxyethyl methacrylate (HEMA), N,N-(dimethylaminoethyl methacrylate) (DMAEMA), and tetraethylene glycol dimethacrylate (TEGDMA), which is the poly(HEMA/DMAEMA/TEGDMA) hydrogel, was fabricated using the soft lithography technique. Here, the swelling was utilized to remove the hydrogel from the

PDMS mold and revealed that the hydrogel has to be swollen until it delaminates from the PDMS mold automatically. Therefore, swelling and the other factors affecting the self-delamination process were studied in detail. Moreover, it is anticipated that the poly(HEMA-/DMAEMA/TEGDMA) hydrogel will have potential biological applications. The use of this hydrogel in cell studies requires visualization techniques such as microscopy to better understand the behavior of the cells on the material. If the target application is in tissue engineering, hydrogel samples are generally evaluated by obtaining histological sections which provide information on interactions between cells and matrix, distribution of cells, growth patterns, and morphology of cells.[65] Paraffin sectioning and cryosectioning are the most common sectioning techniques used to section the biological samples for light microscopy. Both techniques involve several handling steps such as dehydration and embedding. Sectioning hydrogels using paraffin or cryosectioning may result in poor quality sections if the hydrogel is unable to withstand the conditions used and protocols have to be optimized for each system. Thus, in this study, the compatibility of the poly(HEMA/DMAEMA/TEGDMA) hydrogel with paraffin or cryosectioning protocols was also investigated.

2.2. Experimental

2.2.1. Materials

SYLGARD™ 184 silicone elastomer (PDMS) was purchased from Dow Corning (Midland, MI). The chemicals HEMA (97%), DMAEMA (98%), TEGDMA (≥ 90%), 2-hydroxy-2-methyl-propiophenone (97%), trichloro(1H, 1H, 2H, 2H-perfluorooctyl) silane, albumin from bovine serum (BSA), 2-phospho-L-ascorbic acid trisodium salt, and 10% neutral buffered formalin solution were obtained from Sigma-Aldrich (St. Louis, MO). Bone-marrow-derived human mesenchymal stem cells (hMSCs) at passage 2 were purchased from the Institute for Regenerative Medicine, Texas A&M University, College of Medicine (College Station, TX).

Minimum essential medium α (α-MEM) and ethylene glycol were obtained from Thermo Fisher Scientific (Waltham, MA). Fetal bovine serum–premium select (FBS) and ethanol (200 proof) were from Atlanta Biologicals (Flowery Branch, GA) and Pharmco-AAPER (Brookfield, CT), respectively. Gibco™ Penicillin Streptomycin (Pen Strep) and Dulbecco's phosphate buffered saline (PBS) powder were purchased from Life Technologies (Grand Island, NY). Corning ITS + Premix universal culture supplement was obtained from Corning Inc. (Corning, NY). Tissue-Tek® O.C.T. (optimal cutting temperature) compound, Sakura® Finetek was purchased from VWR (Radnor, PA). Water was deionized at a resistance of 18.1 Ω/cm using a Barnstead Nanopure™ water purification system.

2.2.2. Generation of micropatterns

The micropillar arrays were originally fabricated by UV projection lithography and Bosch Deep Reactive Ion Etching (DRIE) of single crystal silicon wafers. The hexagonal arrays of micropillars were generated with the following dimensions: diameter (d) = 1 μm, height (h) = 2 μm or 6 μm, and interpillar spacing (d_{int}) = 3 μm. In order to transfer the pattern onto the hydrogel, negative poly(dimethylsiloxane) (PDMS) molds of the original Si pattern were used. The PDMS molds were prepared as described elsewhere.[44,66,67] Briefly, Sylgard™ 184 silicone elastomer and curing agent were mixed thoroughly in a ratio of 10:1 wt. % and poured over the Si wafer, degassed in a vacuum to remove air bubbles, and thermally cured in an oven (Barnstead™) at 75 °C for 5 – 6 h.

2.2.3. Synthesis of poly(HEMA/DMAEMA/TEGDMA) and transfer of micropillar patterns

To synthesize the polymer, the monomers HEMA (the transduction monomer), DMAEMA (the functional co-monomer that makes the polymer pH sensitive), TEGDMA (the cross-linker) were thoroughly mixed with the initiator 2-hydroxy-2-methylpropiophenone in a ratio of 38:2:1:1 mol/mol respectively, and the solvent mixture containing water and ethylene glycol (1:1 mol/mol) (as adapted from work published by You et al.[68]). Then, the mixture was poured over the PDMS molds and cured with 365 nm UV light using a Dymax™ light curing system (225 mW/cm^2, Model 5000 Flood) for 90 s. After UV curing, the polymer-PDMS composites were cooled to room temperature and the polymer was peeled off or the composite was immersed in solvents to facilitate the pattern transfer. After delamination of the hydrogel from the PDMS mold, the hydrogel samples were serially dehydrated in a concentration series of ethanol, critical point dried (BAL-TEC CPD030), coated with Au/Pd (Balzers Union MED 010), and imaged using an Environmental Scanning Electron Microscope (FEI Quanta 600 FE – ESEM) to verify the transfer of the micropillar arrays. The unpatterned or *blank* hydrogel was prepared in the same manner, except for using a piece of an unpatterned or bare silicon wafer for the generation of PDMS molds.

The structure of the polymer was characterized by solution and solid-state nuclear magnetic resonance (NMR), and attenuated total reflectance Fourier transform infrared (ATR-FTIR) spectroscopy. The uncross-linked polymer (poly(HEMA/DMAEMA)) was dissolved in deuterated dimethylsulfoxide (DMSO-d_6) for the solution-state proton NMR (^{1}H NMR) while ^{13}C solid-state Magic Angle Spinning (MAS) NMR spectra and ATR-FTIR spectra were obtained for the dehydrated cross-linked poly(HEMA/DMAEMA/TEGDMA) (see sections 3.2.4 and 3.3.1 for detailed procedure and spectra.)

2.2.3.1. The effect of functionalization of the PDMS mold on the transfer of micropillar pattern

Prior to casting the hydrogel monomer mixture, the surface of the PDMS molds was functionalized with trichloro(1H, 1H, 2H, 2H-perfluorooctyl) silane as mentioned elsewhere.[61,62] Briefly, the PDMS molds were treated with a corona treater (Electro-Technic Products, BD-20) for 5 min and functionalized with trichloro(1H, 1H, 2H, 2H-perfluorooctyl) silane for 18 h in a vacuum desiccator. Here, an opened glass vial containing the silane (0.5 mL) was placed in the vicinity of the PDMS molds in the desiccator. The treated molds were used for fabrication of hydrogels. The polymer samples were mechanically released by peeling off from the molds.

2.2.3.2. The effect of swelling solvent on the transfer of micropillar pattern

The polymer-PDMS composites (*blank* and surface-patterned) were submerged in deionized water (DI water) for delaminating from the PDMS mold followed by refrigeration for 3 h. Also, the effect of pH of the swelling solvent toward pattern transfer was investigated. Here, the composites were immersed in buffer solutions of pH 3.0, 4.0, 5.0, and 6.0. The citrate buffer solutions (prepared from $C_6H_8O_7$ and $Na_3C_6H_5O_7$) were used to maintain pH at 3.0, 4.0, and 5.0 whereas the phosphate buffer (prepared from KH_2PO_4 and Na_2HPO_4) was used for pH 6.0. The delamination of the hydrogel from the mold was checked daily.

The composites were also immersed in ethanol solutions in water; the concentrations of ethanol solutions were 20%, 40%, and 60% (v/v). Swelling and delamination of the hydrogel from the mold were checked in 30 min time intervals. In each experiment, the pattern transfer was verified by imaging with SEM as mentioned above.

2.2.4. Factors affecting self-delamination of the hydrogel from the PDMS mold

Here, the effect of the dimensions of the well in the PDMS mold on self-delamination of the hydrogel was investigated. The length, width, and depth of the PDMS well were systematically changed as mentioned below. Since the self-delamination of hydrogel was fast, 60% ethanol solution was chosen as the swelling solvent in these experiments. The percent swelling, curvature of the hydrogel-PDMS composite, and time required for self-delamination were evaluated. The percent swelling (%Q) was determined, as the solvent uptake, from the **Equation (2-1)**;

$$\%Q = \frac{W_s - W_i}{W_i} \times 100 \qquad \textbf{(2-1)}$$

where W_i is the initial mass of the hydrogel and W_s is the mass of the swollen hydrogel.[18,71] Five samples were used for these experiments which were continued until at least three hydrogels were delaminated from the molds.

2.2.4.1. Length to width ratio (aspect ratio) of the well

The PDMS wells with different aspect ratios were prepared by changing the length and width of the pieces of bare silicon wafers while maintaining a constant thickness (**Table 2-1**).

Table 2-1. Length, width, and aspect ratio of the PDMS well

Length (cm)	Width (cm)	Aspect ratio
2.0	2.0	1.0
2.0	1.5	1.3
3.0	1.0	3.0
4.0	1.0	4.0
3.0	0.5	6.0

2.2.4.2. The depth of the well

The length, width, and depth of the PDMS well were changed to study the effect of depth on the self-delamination process. All three dimensions were changed so as to maintain the volume of the well (6.0 mL) constant (**Table 2-2**). The volume of the well determines the volume of the monomer mixture required to completely fill the well. At a constant volume, any effect that can be caused by the amount of material can be eliminated.

Table 2-2. Length, width, and depth of the PDMS well

Length (cm)	Width (cm)	Depth (mm)
3.0	2.0	10.0
4.0	2.0	7.5
4.0	3.0	5.0
6.0	4.0	2.5

2.2.5. Swelling of poly(HEMA/DMAEMA/TEGDMA) polymer at different temperatures

The *blank* poly(HEMA/DMAEMA/TEGDMA) polymer was swollen in DI water, PBS, and 60% ethanol at different temperatures: 25 °C, 30 °C, 40 °C, 50 °C, and 60 °C. The percent swelling was determined at each temperature, in each solvent for 24 h.

2.2.6. Sorption kinetics of poly(HEMA/DMAEMA/TEGDMA) hydrogel

The *blank* poly(HEMA/DMAEMA/TEGDMA) samples were immersed in DI water, PBS, 60% ethanol, and absolute ethanol after recording the initial mass. The mass of the swollen hydrogels was recorded in 12 min time intervals for 2 h and the swelling ratio in terms of solvent uptake was determined by **Equation (2-2)**;

$$Q = \frac{W_s - W_i}{W_i} \qquad \textbf{(2-2)}$$

where W_i is the initial mass of the hydrogel and W_s is the mass of the swollen hydrogel.

The sorption mechanism of the polymer samples can be evaluated by fitting the data into the following equation (**Equation (2-3)**);[18,72,73]

$$Q = kt^n \qquad \textbf{(2-3)}$$

Here, Q is the uptake of solvent at time t, k is a constant characteristic of the system, and n is the kinetic exponent which defines the type of sorption mechanism.

2.2.7. Investigation of compatibility of the poly(HEMA/DMAEMA/TEGDMA) hydrogel with sectioning protocols

To test the compatibility of the hydrogel with sectioning protocols, the human mesenchymal stem cells were cultured on the hydrogel samples (the cell experiments are described in details in **chapter 4**). Briefly, the *blank* and surface-patterned hydrogel samples were sterilized by autoclaving in PBS (30 min, 121 °C) and placed in the wells of 24-well plates for pre-incubation in complete culture media (α-MEM, supplemented with 16.7% FBS, and 1% Pen Strep (v/v)) overnight at 37 °C and 5% CO_2 in a CO_2 supplied humidified incubator (Symphony 5.3 A, VWR, Radnor, PA). Frozen hMSCs (5×10^5 cells/mL, 0.5 mL) at passage 3 were recovered and expanded in T125 flasks containing complete culture medium at 37 °C and 5% CO_2 to produce cells required for the experiments. At 70% confluency, the cells were detached from the flasks and seeded onto the samples (seeding density = 1.6×10^5 cells/cm^2). The cells were allowed to grow for two days and the spent media was replaced with either complete culture medium or chondrogenic differentiation medium (to promote the chondrogenic differentiation of cells – towards formation of cartilage tissue). The chondrogenic differentiation medium contained α-MEM provided with high glucose (4.5 g/L), 10% FBS, 1% Pen Strep, 1×10^{-7} M dexamethasone, 10% ITS + Premix tissue culture supplement, 50 µg/mL 2-phospho-L-ascorbic acid, and 10 ng/mL TGF β1. At the end of the experiment (after two weeks), the samples were fixed with 10% neutral buffered formalin solution for 30 min.

2.2.7.1. Paraffin sectioning

Prior to paraffin sectioning, the samples were serially dehydrated in ethanol (70% ethanol for 15 min, 80% ethanol for 20 min, 95% ethanol for 20 min, 95% ethanol for 30 min, 100% ethanol for 15 min, second 100% ethanol for 20 min, and third 100% ethanol for 30 min) and treated with toluene or xylene for 20 min, followed by a second toluene or xylene treatment for 30 min. Then the sample was embedded in molten paraffin for 20 min, followed by second and third molten paraffin embeds for 20 and 30 min respectively. Finally, the sample was embedded in molten paraffin for the fourth time followed by sectioning and staining with H & E (Hematoxylin and Eosin) and Alcian blue. [Note: The paraffin sectioning and related staining were performed at the Oklahoma Animal Disease Diagnostic Laboratory (OADDL), Center for Veterinary Health Sciences, OSU, Stillwater, OK.]

2.2.7.2. Cryosectioning

After fixing the cells, the samples were dehydrated in 30% sucrose (in PBS) overnight. The excess solution was wiped off and the sample was placed in a cryomold which was then completely filled with O.C.T (optimal cutting temperature) compound. The samples were allowed to equilibrate in O.C.T compound for ~2.5 h and frozen in liquid N_2 : pentane bath (Liquid N_2 : pentane bath maintains the temperature ~ -130 ºC, which helps to snap freeze the sample and minimize the formation of ice crystals). Immediately after freezing, the samples were stored in dry ice until sectioned. For sectioning, a cryoblock was fixed onto the sample holder using O.C.T compound and allowed to equilibrate at -20 °C in the cryostat for 1 h. Then the sections (7 µm thick) were cut and placed on the glass slides by touching the section with the glass slide at room temperature (this was done within 1 min to avoid freeze-drying of the sample). Normal glass slides or positively charged glass slides were used to collect sections.

2.3. Results and discussion

2.3.1. Factors affecting the transfer of micropillar patterns onto the hydrogel

2.3.1.1. Functionalization of the PDMS mold

Initial experiments showed that the mechanical detachment of the polymer from the PDMS mold without swelling resulted in the incomplete transfer of the pattern causing the pillars to be ripped off. The difficulty in transfer of the pattern was thought to result from the strong adhesion between the PDMS and poly(HEMA/DMAEMA/TEGDMA) polymer; therefore, the surface of PDMS molds was functionalized with trichloro(1H, 1H, 2H, 2H-perfluorooctyl) silane which is used as an anti-sticking agent in nanoimprint lithography[74] and soft lithography[75] to support the release of the mold. The corona treatment is expected to activate the surface groups on PDMS to ensure proper functionalization.[76,77] Even with the surface functionalization, the transfer of micropattern onto the hydrogel was not successful as seen in the SEM images (**Figure 2-1**). The SEM images of the side view confirm the dot-pattern present in the top-view images corresponds to the bases or remaining parts of the micropillars that were ripped off from the hydrogel surface. Since the hydrogels were peeled off from the PDMS molds, the pillars might be ripped off due to the mechanical force.

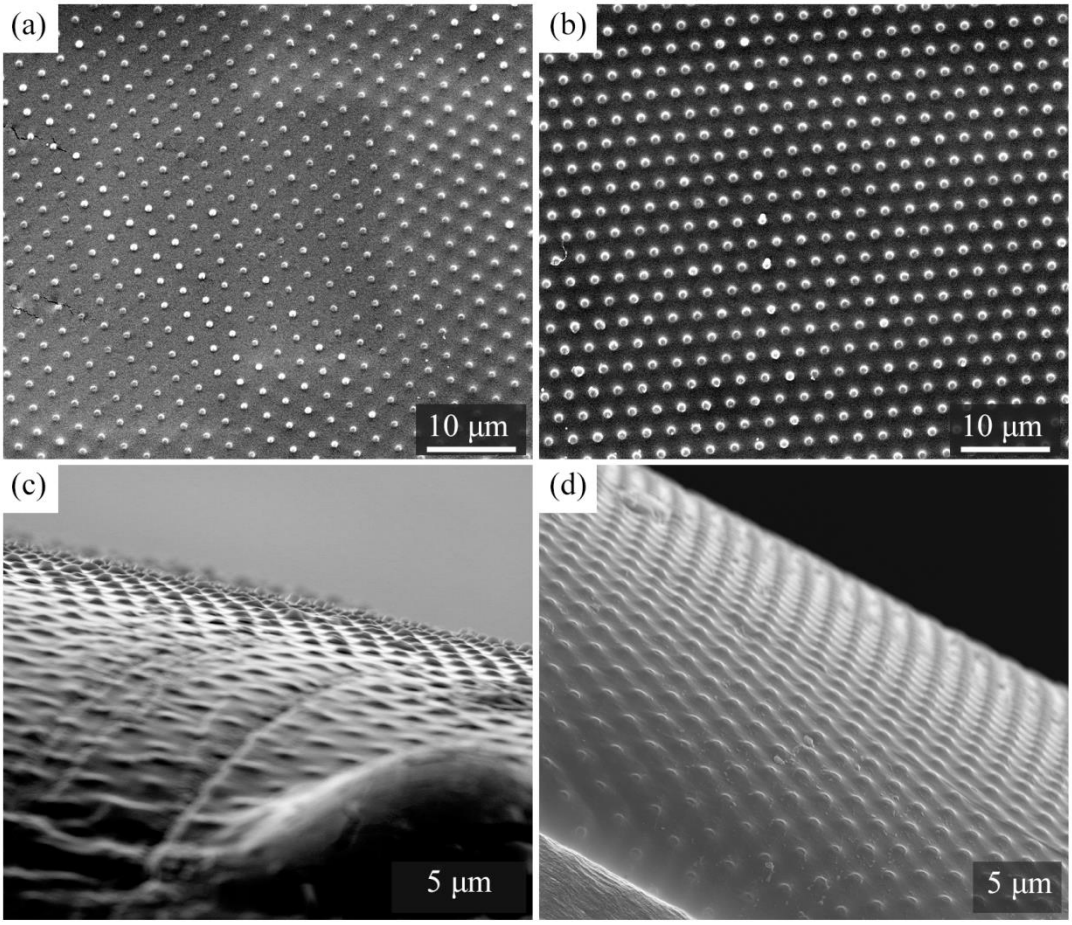

Figure 2-1. The SEM images of hydrogels patterned with (a, c) 2 μm pillars and (b, d) 6 μm pillars, (c) and (d) are SEM images of side views of (a) and (b); the PDMS molds were surface-functionalized prior to hydrogel fabrication.

2.3.1.2. Swelling solvent

The swelling of the polymer inside the PDMS mold induced a curvature of the hydrogel-PDMS composite, subsequently resulting delamination of the hydrogel from the PDMS mold. When immersed in DI water for 24 h, a curvature of the composite was observed and the hydrogels were detached from the edges of the well in the PDMS mold. Since the hydrogels were not completely detached, the composites were refrigerated for 3 h, while immersed in DI water, which supported the hydrogel to detach from the mold easily. The SEM analysis of the surface-patterned hydrogel

samples indicated the transfer of micropillars (**Figure 2-2(a)** and **Figure 2-2(b)**), but the pattern transfer was not reproducible (**Figure 2-2(c)** and **Figure 2-2(d)**).

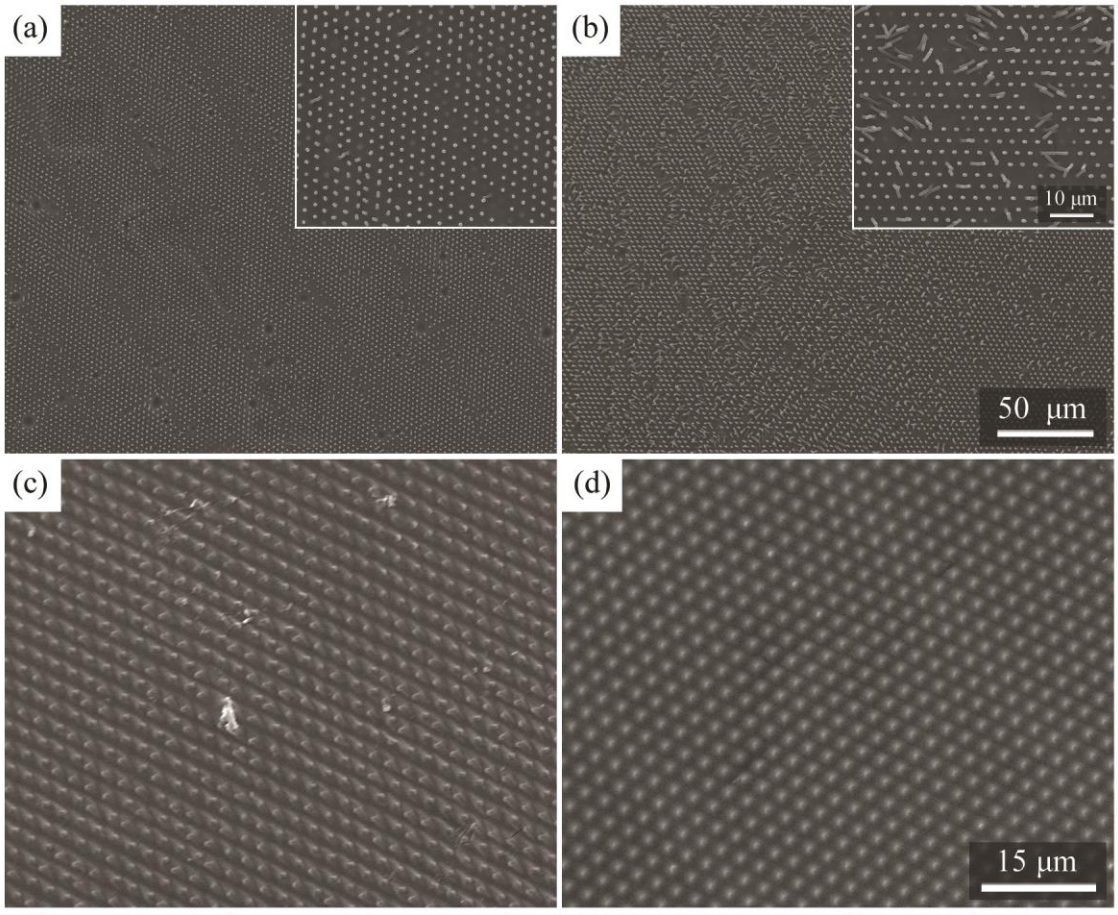

Figure 2-2. The SEM images of hydrogels patterned with (a, c) 2 µm pillars and (b, d) 6 µm pillars immersed in DI water followed by refrigeration.

Due to the presence of DMAEMA units, the swelling of the poly(HEMA/DMAEMA/TEGDMA) hydrogel changes as a response to the pH of the medium. Since the swelling in DI water was insufficient to completely transfer the micropillar patterns onto the hydrogels, the effect of pH of the medium was evaluated. The *blank* hydrogels were delaminated from the molds in each solution after one day, but not the patterned hydrogels. The experiment was continued at pH 6.0 for a week which resulted in detachment of the hydrogel from the edges. By applying a little

force, the hydrogels were completely detached from the mold. The SEM analysis of a hydrogel bearing 6 μm pillars indicated the transfer of micropillars onto the hydrogel sample (**Figure 2-3**).

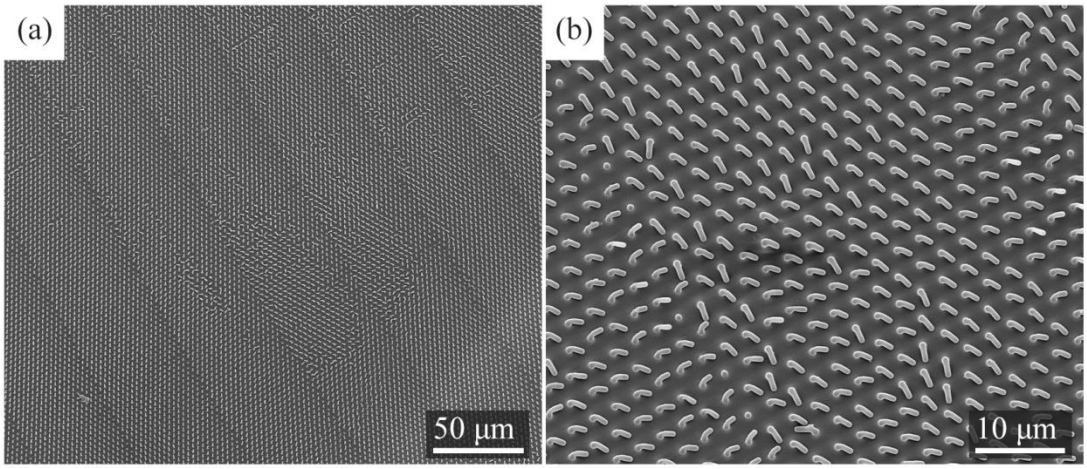

Figure 2-3. The SEM images of a hydrogel sample patterned with 6 μm pillars; the polymer-PDMS composites were immersed in phosphate buffer solution at pH 6.0 for a week.

The pattern transfer process in aqueous solutions was very time-consuming; therefore, the use of a good solvent in which the hydrogel can swell to a greater extent than in aqueous solutions was necessary to speed up the process. As previously reported, ethanol solutions are more compatible with poly(HEMA) hydrogel than water;[78] thus, it was worthwhile to test the pattern transfer in ethanol solutions. Here, the polymer-PDMS composites were left in different ethanol solutions (20%, 40%, and 60% ethanol), checking the curvature and detachment of the hydrogel in 30 min intervals. Neither curvature nor detachment was observed in any solution during 90 min. After 120 min and 240 min, the hydrogels were started to detach from the edges of the well, in 60% and 40% ethanol solutions, respectively. The hydrogels were completely delaminated from the molds upon overnight immersion in 60% ethanol, but not in 40% ethanol. Even though the composite was slightly curved in 20% ethanol, no detachment of hydrogels was observed at any time point. The SEM images in **Figure 2-4** clearly show that the pattern was successfully transferred in 60% ethanol. The high swelling obtained in 60% ethanol facilitated the self-delamination of the

hydrogel and the pattern transfer was successful and reproducible. The experiments performed in 60% ethanol revealed that the surface-functionalization of the PDMS mold is not necessary when the swelling of the hydrogel itself can promote self-delamination of the hydrogel.

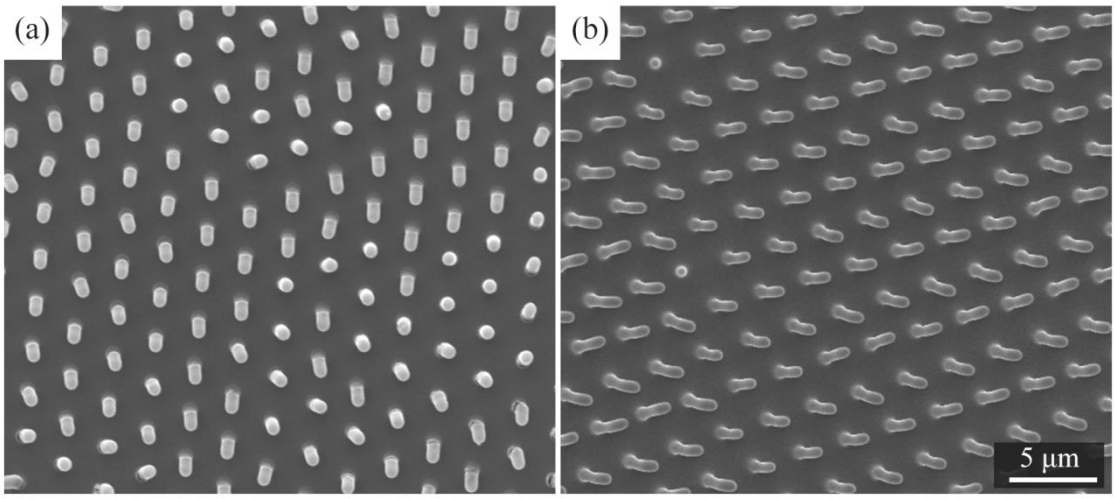

Figure 2-4. The SEM images of poly(HEMA/DMAEMA/TEGDMA) hydrogels patterned with (a) 2 µm pillars and (b) 6 µm pillars immersed in 60% ethanol overnight.

It is noteworthy that the hydrogels swelled in 60% ethanol solution were not stable upon storing in DI water as cracking of the hydrogel was observed in DI water. Although the hydrogel samples were transferred to DI water through a dilution series of ethanol (50%, 40%, 30%, 20% and 10%), after equilibrating in each solution, cracking was observed upon reaching 20% ethanol solution. Since storage of the hydrogel in the aqueous medium is essential for biological applications, the pattern transfer should be achieved in an aqueous solution. Thus, PBS was tested as a swelling solvent for pattern transfer, as the PBS solution has a pH of 7.4 which is equal to physiological pH. However, the swelling in PBS was insufficient to facilitate the self-delamination of the hydrogel from the PDMS mold, which is a key requirement for the successful transfer of micropillar arrays. To support the delamination of the hydrogel, the PDMS mold was immobilized onto a Petri dish prior to the fabrication step (**Figure 2-5**). As well, after immersing in PBS for ~48 h, the hydrogel was mechanically released from the edges to accelerate the

delamination process. The same method was used to successfully transfer the micropillar pattern in DI water.

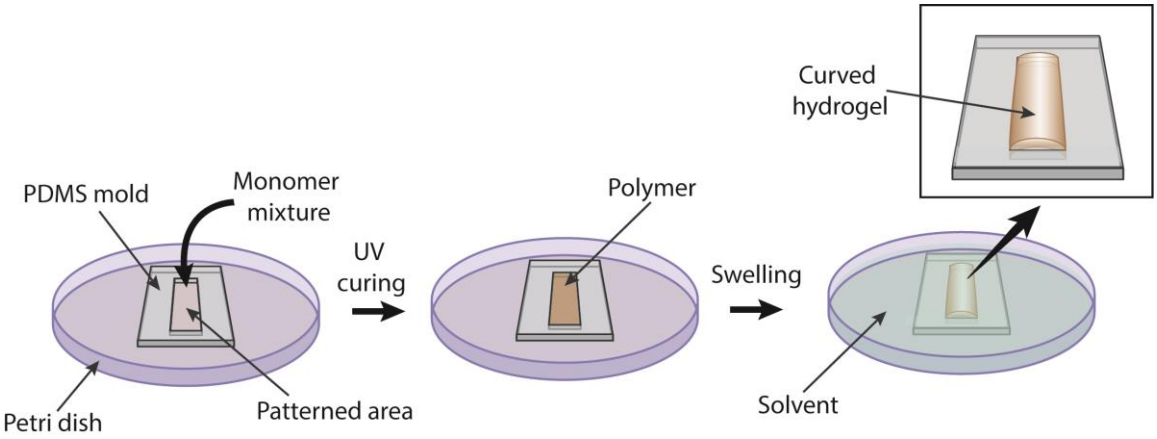

Figure 2-5. Transfer of micropillar patterns in PBS and DI water by immobilization of the PDMS mold onto a Petri dish.

2.3.2. Factors affecting self-delamination of the hydrogel from the PDMS mold

The previous experiments confirmed that the micropillar pattern can be successfully transferred onto the hydrogel samples through self-delamination of the hydrogel induced by swelling. Apart from the swelling medium, the dimensions, i.e. length, width, and depth, of the well in the PDMS mold can also influence the self-delamination of the hydrogel, thereby controlling the effectiveness and reproducibility of pattern transfer process.

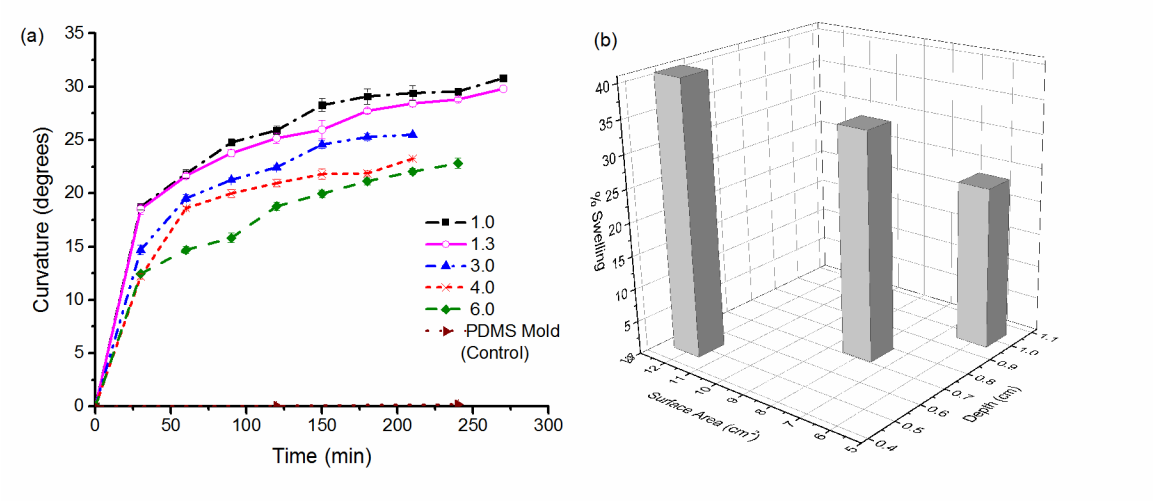

Figure 2-6. (a) The curvature of the hydrogel-PDMS composite as a function of time at different length to width ratios (1.0, 1.3, 3.0, 4.0, 6.0) of the PDMS well (or the hydrogel) at a constant depth and (b) 3-D graph that shows the percent swelling of the hydrogel based on depth of the well and surface area that is in direct contact with the swelling solvent.

2.3.2.1. Length to width ratio (aspect ratio) of the well

As depicted by the graph in **Figure 2-6(a)** the increase in length to width ratio decreases the maximum angle of the curvature of the hydrogel-PDMS composite, which was considered as the critical angle required for the self-delamination process. Increase in length to width ratio of the well from 1.0 to 6.0 decreased the critical angle from 30º to 22º. As well, the time required for self-delamination was slightly affected by the length to width ratio as the hydrogels took ~4.5 h at a ratio of 1.0 and ~3.5 h at the ratios of 3.0, 4.0, and 6.0 to delaminate from PDMS molds. The results clearly show that the rectangular shape (length to width ratio > 1) is more important than the square shape (length to width ratio = 1) to speed up the self-delamination process. The changes in length and width at a constant thickness lead to changes in the volume of the hydrogel monomer mixture poured onto the well. Thus, the amount of the polymer may influence the swelling subsequently affecting the delamination process.

2.3.2.2. The effect of the depth of the well and the surface area of the polymer on swelling

In this experiment, the length, width, and depth were changed, so as not to change the volume and hence the mass of the polymer. The constant amount of material used here eliminates any effect that can be caused by the polymer amount. The 3-D graph in **Figure 2-6(b)** shows that the largest area, which is in direct contact with the swelling solvent (24 cm^2) and the smallest depth (0.25 cm) resulted in the highest percent swelling which supported the fastest delamination of the hydrogel. A large amount of solvent can enter into the hydrogel when a large area is in direct contact with the swelling solvent and the solvent has to move a short distance to reach the opposite surface of the hydrogel. **Table 2-3** shows the dimensions of the PDMS molds (or hydrogel) and the time required for self-delamination.

Table 2-3. Dimensions of the PDMS well and the time required for self-delamination

Length (cm)	Width (cm)	Depth (cm)	Time (h)
3.0	2.0	1.0	72
4.0	2.0	0.75	60
4.0	3.0	0.5	48
6.0	4.0	0.25	24

2.3.3. Swelling of poly(HEMA/DMAEMA/TEGDMA) hydrogel at different temperatures

As the temperature varied from 30 °C to 40 °C, percent swelling of the hydrogel decreased from 28% to 17% (DI water), 26% to 16% (PBS), and 218% to 190% (60% ethanol). The percent swelling was slightly increased upon reaching 60 °C.

Previous studies report that the swelling of poly(HEMA)-based hydrogels reaches a minimum at temperatures between ~55 °C and ~60 °C and exhibits a high swelling below and above those temperatures.[79-81] When the polymer is in contact with water, hydrogen bonding between the

water molecules and the polymer chains allows water to enter into the polymer and the polymer swells. Upon swelling the polymer dilutes with water. Below 55 °C or 60 °C, the swelling is favored by the negative enthalpy of dilution (ΔH_{dil}) and high swelling is observed. As the temperature increases, the system absorbs heat from the surrounding and enters to a state of high enthalpy. Subsequently, the hydrogen bonding decreases and the bound water is converted to free water. The hydrogel deswells by expelling the free water from the network. Although the ΔH_{dil} is negative, the swelling is restricted, indicating unfavorable entropy of dilution ($\Delta S_{dil} < 0$). The decrease in ΔS_{dil} was attributed to interactions between the hydrophobic groups of the polymer network and water, which again results in penetration of water into the network. As a consequence, the swelling of the hydrogel increases as the temperature of the system exceeds the temperature that corresponds to the minimum swelling (~55 °C – ~60 °C).[80-81] Because of the small amount of DMAEMA used in the formulation, it is likely that swelling is nonionic.

2.3.4. Sorption kinetics of poly(HEMA/DMAEMA/TEGDMA) hydrogel

When a polymer sample is placed in a solvent, penetration of the solvent from the polymer surface creates a boundary separating the swollen region and the unswollen region. The solvent which diffuses through the polymer causes relaxation of the polymer chains and swelling of the polymer in front of the boundary.[73] The diffusion process can have Fickian, non-Fickian or Case II kinetics based on the rates of the solvent diffusion and polymer relaxation. In Fickian kinetics, the rate of the solvent diffusion is lower than the rate of polymer relaxation. A diffusion rate greater than the rate of polymer relaxation results in non-Fickian behavior, whereas case II kinetics is observed when both rates are closer to each other.[82]

As mentioned in the experimental section (**section 2.2.6**), the sorption mechanism of the polymer samples can be evaluated by fitting the data into the **Equation (2-3)**. A linear plot of swelling ratio, Q, vs square root of time is indicative of Fickian kinetics.[72] As seen in the graph in **Figure 2-7**, the linear plots of swelling ratio vs the square root of time (R^2 values > 0.994) obtained for all solvents reveal that the uptake of solvents by the poly(HEMA/DMAEMA/TEGDMA) exhibit Fickian kinetics.

As well, a more quantitative measure of sorption kinetics can be obtained by plotting log Q as a function of log T (T = time), where the kinetic exponent n is determined from the slope. If n = 0.5 the sorption mechanism is said to be Fickian and if n = 1 the sorption process is Case II. If n falls within 0.5 – 1 range the process follows non-Fickian or anomalous kinetics.[72] The n values calculated from the swelling data of this study are 0.5621 (±0.0168) (in DI water), 0.5435 (±0.0130) (in PBS), 0.6001 (±0.0050) (in 60% ethanol), and 0.5306 (±0.0135) (in absolute ethanol). The n values indicate slight deviations from the normal Fickian kinetics suggesting that the penetration is more toward diffusion controlled, but there might be a contribution from non-Fickian processes such as relaxation of polymer chains.[73] Nevertheless, in 60% ethanol, n = 0.6 implies more contribution from non-Fickian processes. A study published by Refojo reports that poly(HEMA) may have a secondary structure, which is stabilized by hydrophobic interactions, in addition to the chemically cross-linked primary structure.[83] The same study states that these hydrophobic interactions are broken in the presence of organic solvents such as alcohols and acetone and the swelling is remarkably increased. A similar phenomenon can be expected for the poly(HEMA/DMAEMA/TEGDMA) polymer when swollen in 60% ethanol and the penetration of solvent can be influenced by the solvation of hydrophobic interactions.

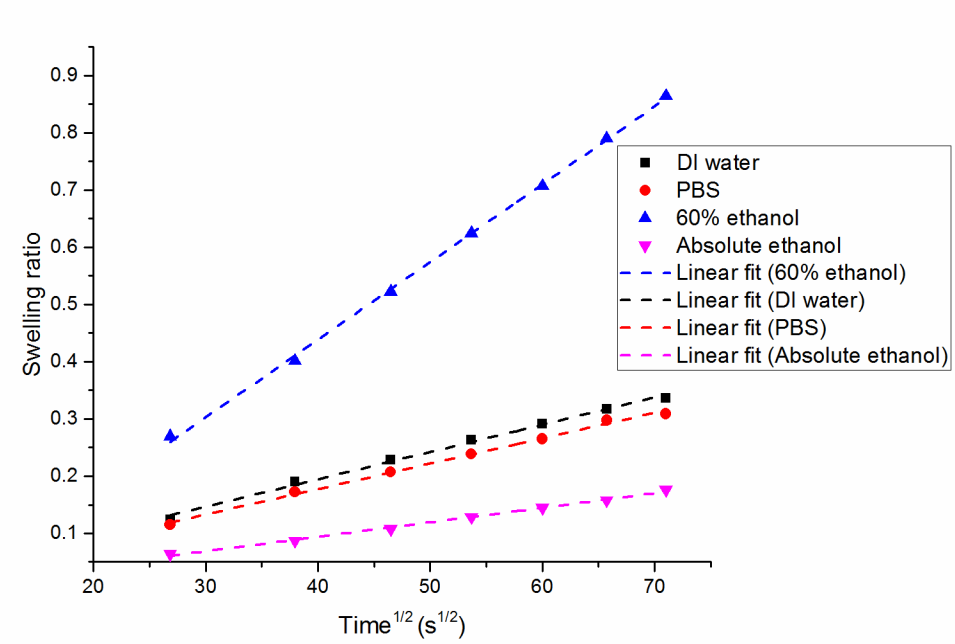

Figure 2-7. The graph of swelling ratio of hydrogels (in different solvents) as a function of square root of time. The R^2 values were 0.995 (DI water), 0.996 (PBS), 0.999 (60% ethanol), and 0.995 (absolute ethanol).

2.3.5. Investigation of compatibility of the poly(HEMA/DMAEMA/TEGDMA) hydrogel with sectioning protocols

2.3.5.1. Paraffin sectioning

Sectioning of the hydrogel samples with the cells was necessary to clearly visualize the cell aggregates attached to the hydrogels bearing micropillar patterns. To recognize the cells, the sections were stained with H & E (Hematoxylin and Eosin) and Alcian blue stains. The light microscopy images in **Figure 2-8** show the sections of hydrogel samples obtained from paraffin-sectioning. The photos demonstrate that the cell aggregates were detached from the hydrogel surface during sectioning process which involved several dehydration steps and solvent treatment steps; however, in some photos, the detached cell aggregates can be seen in the vicinity of the hydrogel section (**Figure 2-8(a) – (c)**). Although the micropillars are visible in some areas, they

seemed to be damaged. As well, twisting and tearing of the hydrogels was observed in some sections. However, as shown by the section stained with Alcian blue (**Figure 2-8(d)**), the sections of cell aggregates attached to the hydrogel were found occasionally. Overall, paraffin sectioning does not fulfill the initial requirement of better visualization of the cell aggregates on the hydrogels bearing micropillars as the cell aggregates and the microstructures were damaged.

Even though H & E staining is widely used in histology as a primary staining technique to evaluate the morphology, the pink color of hydrogel sections indicates that the stains were absorbed by the hydrogel. The absorption of stains by the hydrogel may interfere with microscopy of the cells.

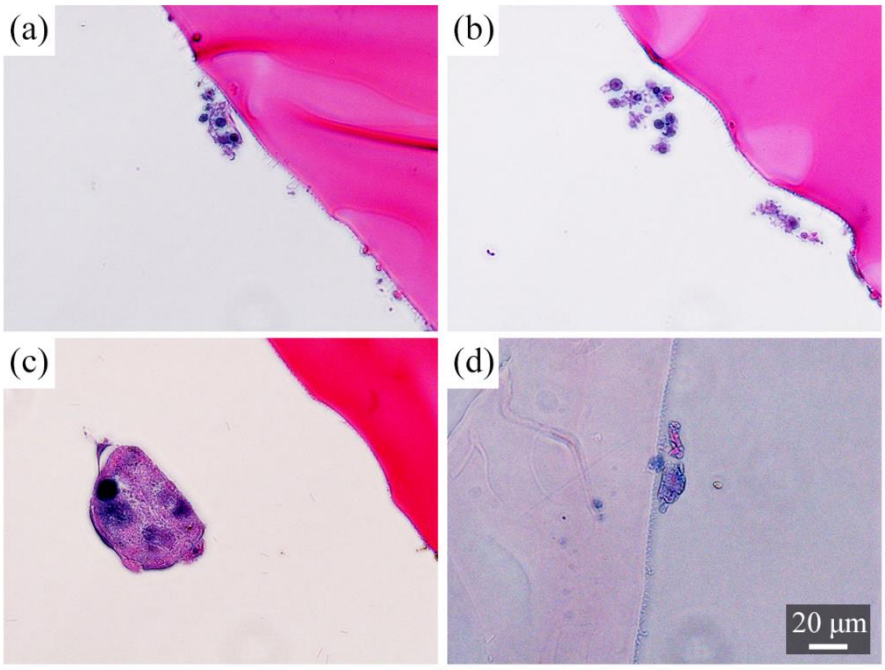

Figure 2-8. Light microscopy images of hydrogel samples subjected to paraffin-sectioning; (a), (b), (c) the sections were stained with H & E stain and show the cell aggregates detached from the hydrogel sample, and (d) a section with a cell aggregate stained by Alcian blue.

2.3.5.2. Cryosectioning

Cryosectioning is another technique which is recommended for sectioning hydrogels mainly because of the compatibility with hydrogels as the drying steps are not necessary. From the preliminary studies, cryosectioning did not appear to be a good method for the poly(HEMA/DMAEMA/TEGDMA) hydrogels mainly due to the difficulty of collecting and retaining the hydrogel sections on glass slides.

An issue common to both paraffin and cryosectioning techniques of the poly(HEMA-/DMAEMA/TEGDMA) system was that a large number of sections had to be collected since the cells form aggregates on the hydrogel sample, unlike a layer of cells uniformly spread over the entire sample. The tendency of not having good sections of the cell aggregates on a hydrogel section was very high. Since both sectioning techniques were not suitable, it was decided to stain the hydrogels with cultured cells directly (as described in **chapter 4**).

2.4. Conclusions

This study reports the investigation of factors critical to the transfer of micropillar pattern reproducibly and with high fidelity onto the poly(HEMA/DMAEMA/TEGDMA) hydrogel by the soft lithography technique. The self-delamination of the hydrogel from the PDMS mold induced by swelling was the key factor in the successful transfer of micropillar patterns with aspect ratios as high as 6. A detailed analysis of factors such as functionalization of PDMS molds, swelling solvent, as well as the dimensions of the mold provides a better control over the successful and effective transfer of microscale features onto the poly(HEMA/DMAEMA/TEGDMA) hydrogel. As well, the effect of temperature on swelling of the hydrogel and kinetics of swelling provides an insight of swelling of the hydrogel in different solvents. The other important aspect of this study is the evaluation of the compatibility of the system with two widely used histological

techniques: paraffin and cryosectioning, especially because of the potential biological applications of the poly(HEMA/DMAEMA/TEGDMA) hydrogel. This study further suggests that the direct application of staining procedures is an alternative approach for this system as none of the sectioning techniques were able to produce good sections of the fabricated poly(HEMA/DMAEMA/TEGDMA) hydrogel to clearly show the details of cells or cell-matrix interactions under the conditions used.

CHAPTER III

A SOFT-LITHOGRAPHY METHOD TO GENERATE ARRAYS OF MICROSTRUCTURES ONTO HYDROGEL SURFACES

Note: This chapter was published in Jayasinghe, H. G, Tormos, C. J., Khan, M., Madihally, S., and Vasquez, Y., (2018), A soft lithography method to generate arrays of microstructures onto hydrogel surfaces; Journal of Polymer Science Part B: Polymer Physics, 56, 1144-1157, (published by John Wiley & Sons, Inc., NJ), (DOI:10.1002/polb.24634)

3.1. Introduction

In nature, examples of surfaces with microscopic patterns having superior hydrophobic, self-cleaning and adhesive properties abound.[84-87] Examples include the ribbed structured skin of a shark,[88] the surface of a lotus leaf,[89] and the microscale setae of a gecko's foot pads.[90,91] Extensive research on synthetic mimics of these microstructures have resulted in surfaces that dynamically change rigidity,[92] adhesion,[93] or wettability,[94,95] to surfaces that function as anti-biofouling coatings.[96-97] Microstructured surfaces are also used in innovative applications that include force sensors,[92] biosensors,[98,99] drug delivery systems,[100] actuators,[101,102] photonic structures,[103] optoelectronics,[104] piezoelectric devices,[105] and in cellular adhesion,[44,106] migration,[107] and differentiation studies.[108-111] Use or implementation of microstructured surfaces for many biological applications is limited, however, by the types of materials that can be patterned with such fine features because many of these materials are not biodegradable and their mechanical properties are incompatible with natural tissues.

Hydrogels have been extensively studied for biological applications, because properties such as high retention of water, biocompatibility, biodegradability, and tunable mechanical properties enable hydrogels to mimic an endogenous cellular environment.[112-117] Some of the most successful techniques for patterning hydrogels include photolithography[60] and soft-lithography[35,118] methods, which includes microcontact printing,[119] embossing,[120] microfluidic patterning,[121] and micromolding.[122] Yet, patterning hydrogels with microscale features continues to be a challenge due to adhesion, low mechanical strength, and the characteristic swelling properties of the hydrogels themselves.[64,123] Typical hydrogels exhibit an elastic modulus of a few kPa but are only successfully patterned at the micron level when the elastic modulus of the polymer is on the order of a few GPa.[33,123] Additionally, hydrogel micromolding and related soft-lithography techniques make use of surface modification with adsorbed proteins or self-assembled monolayers to reduce or overcome adhesion between the gel and the mold.[64]

This chapter focuses on the fabrication of poly(HEMA/DMAEMA/TEGDMA) (HEMA = 2-hydroxyethyl methacrylate, DMAEMA = N,N-(dimethylaminoethyl)methacrylate and TEGDMA = tetraethylene glycol dimethacrylate) hydrogel patterned with micropillars by the soft-lithography technique. The surface-patterning process involves a very simple method that utilizes the swelling properties of the hydrogel itself to overcome the adhesion problem while allowing softer hydrogels (MPa) to be patterned using soft-lithography techniques. A hydrogel based on poly(HEMA) was chosen to pattern since poly(HEMA)-based hydrogels have been broadly studied for applications in drug delivery,[124] controlled release,[54] and as scaffolds for tissue engineering.[71] The formulation for the co-polymer, poly(HEMA/DMAEMA/TEGDMA), was adapted from the work published by You et al.[68] and yielded an elastic modulus of 8 MPa. Others have also previously reported the successful patterning of poly(dimethylsiloxane) (PDMS) and polyurethanes with micron and sub-micron feature sizes at the same elastic modulus.[123] Here, the

arrays of micropillars with a diameter (d) of 1 μm, pitch (d_{int}) of 3 μm, and a height (h) of either 2 μm or 6 μm were successfully replicated when a solvent with a moderate solubility parameter in the hydrogel was chosen as the swelling solvent such as phosphate buffered saline (PBS), deionized water (DI water), absolute ethanol, and 60% ethanol. The soft, elastomeric PDMS template was found to be a good confining material since it allows for nearly isotropic swelling of the hydrogel and relieves buckling without causing the hydrogel to crack or fail. Additionally, the biological properties (cell attachment and viability) of the fabricated hydrogel were evaluated by culturing HeLa cells on the hydrogel. It was revealed that the hydrogel is cytocompatible and the micropillars enhance the cell attachment properties of the hydrogel.

3.2. Experimental

3.2.1. Materials

SYLGARD™ 184 silicone elastomer (PDMS) was obtained from Dow Corning (Midland, MI). The chemicals 2-hydroxyethyl methacrylate (HEMA, 97% - the transduction monomer), N,N-(dimethylaminoethyl)methacrylate (DMAEMA, 98% - the functional co-monomer that makes the polymer pH sensitive), tetraethylene glycol dimethacrylate (TEGDMA, ≥ 90% - the cross-linker), 2-hydroxy-2-methylpropiophenone (97%), deuterated dimethylsulfoxide (DMSO-d_6), albumin from bovine serum (BSA), Tween® 20, Triton® X-100, and 10% neutral buffered formalin were purchased form Sigma-Aldrich (St. Louis, MO). Ethylene glycol and glass slides (7.5 × 2.5 × 0.1 cm) were purchased from Fisher Scientific (Fair Lawn, NJ). Ethanol (200 proof) was purchased from Pharmco-AAPER (Brookfield, CT). Epoxy OG142 was obtained from Epoxy Technology (Billerica, MA). Dulbecco's phosphate buffered saline (PBS) powder, Gibco™ Penicillin Streptomycin (Pen Strep), Trypsin-EDTA (0.05%), Molecular Probes™ Rhodamine phalloidin and Invitrogen™ 4′,6-diamidino-2-phenylindole (DAPI) were purchased from Life Technologies (Grand Island, NY). Gibco™ RPMI 1640 media and ReadyProbes® cell viability imaging kit

(blue/red) were obtained from Thermo Fisher Scientific, (Waltham, MA). Hyclone™ donor calf serum was purchased from GE Healthcare Life Sciences (Pittsburg, PA). Water was deionized at a resistance of 18.1 Ω/cm using a Barnstead Nanopure™ water purification system.

3.2.2. Generation of the surface pattern

Silicon (Si) micropillar arrays were fabricated by UV projection lithography and Bosch Deep Reactive Ion Etching (DRIE) of single crystal silicon wafers. A hexagonal array of micropillars was fabricated with features corresponding to the following dimensions: diameter (d) = 1 μm, height (h) = 2 μm or 6 μm, and interpillar spacing (d_{int}) = 3 μm. In order to transfer the pattern onto the other materials, i.e. epoxy or hydrogel, negative poly(dimethylsiloxane) (PDMS) molds of the original Si pattern were used. The PDMS molds were prepared as described elsewhere.[44,66,67] Briefly, Sylgard™ 184 silicone elastomer and curing agent were mixed thoroughly in a ratio of 10:1 wt. % and poured over the Si wafer, degassed in a vacuum to remove air bubbles, and thermally cured in an oven (Barnstead™) at 75 °C for 5 – 6 h. The PDMS molds were prepared in round petri dishes (60 mm × 10 mm) and had a diameter of 51.94 (±0.58) mm and a thickness of 4.78 (±0.58) mm.

More PDMS molds were generated using the epoxy replicates of the original pattern as the intermediate substrates so as not to damage the original Si wafer. The Aizenberg group has previously demonstrated that epoxy replicas can be easily produced from a PDMS mold with excellent fidelity.[67] Here, the epoxy replicas were generated by pouring a pre-polymer solution (Epotek OG142) into a negative PDMS mold of the original micropillar pattern and curing under 365 nm UV light using a Dymax™ light curing system (225 mW/cm^2, Model 5000 Flood) for 60 s. After cooling, the epoxy was removed from the mold and used to produce several other replica molds from PDMS.

3.2.3. Fabrication of surface-patterned poly(HEMA/DMAEMA/TEGDMA) hydrogel

The monomers HEMA, DMAEMA, TEGDMA were mixed with the initiator 2-hydroxy-2-methylpropiophenone in a ratio of 38:2:1:1 mol/mol respectively, and the solvent mixture containing water and ethylene glycol (1:1 mol/mol). The composition of the monomers for the hydrogel was adapted from the work published by You et al.[68] After mixing thoroughly, the mixture was poured over the PDMS mold and cured with 365 nm UV light for 90 s. After cooling to room temperature, the hydrogel was submerged in PBS, DI water, 60% ethanol or absolute ethanol and was allowed to swell until delaminated from the mold (**Scheme 3-1**).

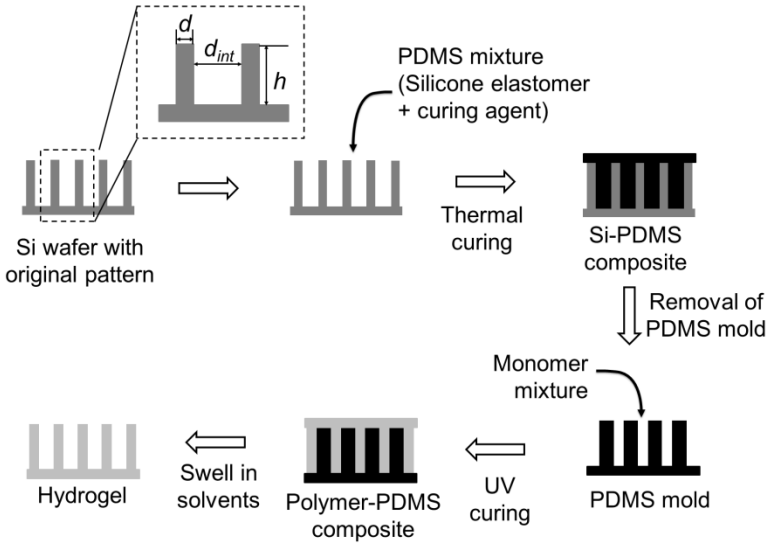

Scheme 3-1. Microstructured hydrogel samples were fabricated using soft-lithography. Micropillars with dimensions corresponding to a diameter (*d*) of 1 μm, a height (*h*) of 2 μm or 6 μm, and interpillar spacing (d_{int}), or pitch, of 3 μm were etched into a Si wafer. Negative molds of the micropillar pattern were produced in PDMS. A mixture of all the components used to synthesize poly(HEMA/DMAEMA/TEGDMA) was poured onto the negative PDMS mold and photopolymerized. The poly(HEMA/DMAEMA/TEGDMA) hydrogel was swollen in various solvents to promote delamination from the PDMS mold.

Hydrogels containing no microstructures, referred to as *blank* hydrogels, were also fabricated in the same manner except for using an unpatterned piece of Si wafer (2.5 cm × 1.0 cm × 3 mm) to prepare the initial PDMS mold. Hydrogels patterned with 2 μm pillars and the *blank* hydrogels had dimensions corresponding to 2.5 cm × 1.5 cm × 3 mm whereas hydrogels patterned with 6 μm pillars had dimensions corresponding to 2.5 cm × 1.0 cm × 3 mm.

3.2.4. Characterization of the structure of the polymer

The structure of the polymer was characterized by solution and solid-state nuclear magnetic resonance (NMR), and attenuated total reflectance Fourier transform infrared (ATR-FTIR) spectroscopy. Proton NMR (^{1}H NMR) spectra of the uncross-linked polymer were collected on a Bruker Avance III HD 400 MHz spectrometer. For solution-state NMR (^{1}H NMR), the polymer was prepared without the TEGDMA cross-linking agent, purified in DI water, dried at 120 °C, and dissolved in deuterated dimethylsulfoxide (DMSO-d_6). ^{13}C solid-state Magic Angle Spinning (MAS) NMR spectra of the dried, cross-linked polymer samples were obtained using a Bruker DSX Avance 300 MHz spectrometer. ATR-FTIR spectra of dehydrated, solid poly(HEMA/DMAEMA/TEGDMA) samples were taken on a Thermo Scientific Nicolet™ iS™ 50 FTIR spectrometer.

3.2.5. Confirmation of the micropillar pattern transfer

The transfer of the patterns was verified by imaging with an Environmental Scanning Electron Microscope (FEI Quanta 600 FE – ESEM). Prior to imaging with SEM, the hydrogel samples were serially dehydrated in a concentration series of absolute ethanol in water, critical point dried (BAL-TEC CPD030), and coated with Au/Pd (Balzers Union MED 010). Furthermore, the samples were imaged using a Leica SP2 confocal microscope with a 63× oil immersion objective to confirm the heights of the micropillars patterned on the hydrogels. Thin sections of patterned hydrogel samples were obtained using a sharp razor blade and mounted in water in a cavity slide

for optical imaging. The heights of micropillars were measured using ImageJ 1.47t software (Wayne Rasband, National Institutes of Health, USA).

3.2.6. Swelling studies

Swelling experiments were performed on free and PDMS confined hydrogel samples. The *blank* hydrogel samples were peeled off from the PDMS molds after UV curing and are referred to as the free hydrogels. The initial mass of the hydrogel samples was recorded prior to submerging in solvents. The mass of the swollen hydrogel was recorded at 2 h time intervals until the mass remained constant. Hydrogel samples were removed from the solvent and blotted with a paper towel prior to mass measurements. Five hydrogel samples were used for all swelling experiments unless otherwise indicated. Percent swelling (%Q) of poly(HEMA/DMAEMA/TEGDMA) hydrogels was calculated by means of solvent uptake using **Equation (3-1)**,

$$\%Q = \frac{W_s - W_i}{W_i} \times 100 \qquad \textbf{(3-1)}$$

where W_i is the initial mass of the hydrogel and W_s is the mass of the swollen hydrogel.[18,71]

The PDMS confined polymers are the polymer-PDMS composites where the polymer samples were not removed from the molds. The polymer-PDMS composites were also subjected to swelling experiments. The mass of the polymer-PDMS composites was recorded until a constant mass reached or the hydrogel delaminated from the mold. When the polymer was swelling inside the mold the composite became curved. The curvature of the composite was recorded every 2 h for 48 h or until the hydrogel delaminated from the mold. Digital images of the confined hydrogels were taken using a Nikon D3200 digital camera. ImageJ 1.47t software was used to determine the angle of curvature (θ) (**Figure 3-1**) of the PDMS mold using the low bond axisymmetric drop shape analysis (LB-ADSA) method of the drop analysis plug-in.

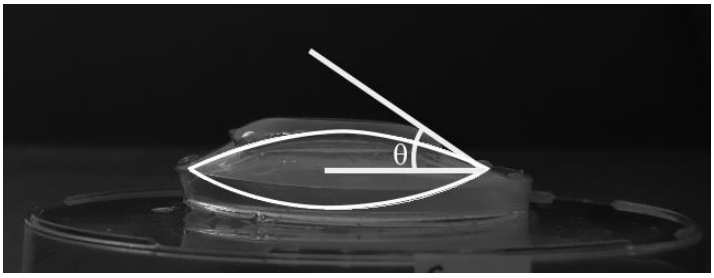

Figure 3-1. The polymer-PDMS composite was curved upon swelling of the polymer confined in the mold. The angle of curvature (θ) was measured to evaluate the swelling of the polymer in the mold.

3.2.7. Determination of solubility parameter (δ) of the hydrogel

As an extension of the swelling study, the solubility parameter of the poly(HEMA/DMAEMA/TEGDMA) was determined using the method developed by Gee.[125,126] The same technique was previously used by Çaykara et al. to determine the solubility parameter of poly(HEMA/IA) (IA = itaconoic acid - $CH_2(COOH)C(COOH)CH_2$) hydrogel.[127]

According to Gee, the relationship between the volumetric swelling ratio of a polymer in a solvent of solubility parameter δ is given by the **Equation (3-2)**:

$$\frac{Q_v}{Q_{v,max}} = e^{-aQ_v\,(\delta_{Solvent} - \delta_{Polymer})^2} \qquad \textbf{(3-2)}$$

Here, Q_v is the volumetric swelling ratio, $Q_{v,max}$ is the maximum volumetric swelling ratio, a is a constant, and $\delta_{Solvent}$ and $\delta_{Polymer}$ are the solubility parameters of the solvent and polymer, respectively. The solubility parameter of a polymer is the same value as the solvent in which the highest swelling is observed.

In order to determine the solubility parameter of the poly(HEMA/DMAEMA/TEGDMA) hydrogel, free, *blank* polymer samples were allowed to swell in solvents, with different δ values,

(Table 3-1) until the weight of the swollen hydrogel was constant. Then, the equilibrium swelling ratio by volume Q_v was calculated using **Equation (3-3)**:

$$Q_v = 1 + (\frac{W_s}{W_i} - 1)\frac{\rho_{polymer}}{\rho_{solvent}} \quad \textbf{(3-3)}$$

where W_i is the initial mass of the hydrogel, W_s is the mass of the swollen hydrogel, $\rho_{solvent}$ and $\rho_{polymer}$ are the densities of the solvent and polymer, respectively.[127] To determine the density of the polymer ($\rho_{Polymer}$), the volume of the polymer samples was measured by the solvent displacement method in hexane, a solvent that has a negligible effect on swelling of the hydrogel. Then the Q_v values were plotted against the δ of the solvents to infer the solubility parameter of the polymer.

Table 3-1. The solvents used for determination of $\delta_{Polymer}$ and their solubility parameter values (δ)[128]

Solvent	**Solubility Parameter [δ] ($MPa^{1/2}$)**
Triethanolamine	36.7
1-Butanol	23.2
Acetonitrile	24.4
Acetone	20.3
Isopropyl alcohol	23.5
Ethanol	26.6
Methanol	29.7
Ethylene glycol	32.9
DMF	24.8
DMSO	26.6

3.2.8. Mechanical testing

The mechanical properties of the hydrogel samples were evaluated by tensile tests performed using an INSTRON mechanical testing system (Model 5542). Hydrogel samples with dimensions of 7.0 cm × 2.5 cm × 0.3 cm were prepared using a PDMS mold as described previously. Mechanical properties of the polymer samples were evaluated in both the unswollen and swollen states. Poly(HEMA/DMAEMA/TEGDMA) samples were swollen in PBS, DI water, 60% ethanol, and absolute ethanol for 15 - 20 h prior to mechanical testing. Specimens were stretched at a constant rate of 5 mm/min. Data was collected every 50.00 mN and recorded using the associated Merlin (INSTRON) software. The elastic modulus was calculated from the slope of the linear portion of the stress–strain curve using a strain range of 0.0000 – 0.0006 for unswollen samples and 0.0000 – 0.0700 for swollen samples. A Mitutoyo Absolute Digimatic Caliper (Mitutoyo (UK) Ltd) was used to measure the dimensions of the samples before and after swelling. All data are presented as means ± standard deviation for n = 5. Statistical significance was determined using ANOVA analysis (single factor at $p < 0.05$).

3.2.9. Determination of weight-average molecular weight and network parameters

The weight-average molecular weight ($\overline{M_w}$) of the polymer was determined using the static light scattering (SLS, Malvern Zetasizer Nano system). The uncross-linked polymer, poly(HEMA/DMAEMA), was prepared as mentioned previously without adding the cross-linking agent TEGDMA. After UV curing the polymer was purified by immersing in DI water for 2 – 3 days followed by drying in a desiccator for about a week. Then the polymer was dissolved in N,N-dimethyl formamide (DMF) to prepare the stock solution (concentration of 0.01 g/mL). A series of polymer solutions with different concentrations (1.00, 2.50, 7.50, and 10.00 mg/mL) were prepared by diluting the required amounts of the stock solution with DMF. Toluene was used as the standard.

Effective cross-linking density and the molecular weight between cross-links were determined for the swollen hydrogel samples. The Flory-Huggins rubber elasticity model was used to determine the effective cross-linking density ($\overline{v_e}$) by plotting τ (in kPa) *vs.* (α-1/α^2) using the equation below:[129]

$$\tau = RT\overline{v_e}\phi^{-1/3}(\alpha - \frac{1}{\alpha^2}) \qquad \textbf{(3-4)}$$

Here, τ is the applied force per unit area of the swollen hydrogel, α is the ratio of deformed length to undeformed length of the swollen hydrogel. The cross-linking density was calculated from the slope of the resulting linear plot, and substituting; R is the universal gas constant (8.314 kPa·dm^3/mol·K), T temperature (294.1 K), and ϕ is the volume fraction of the polymer in the swollen hydrogels.

The dimensions of the polymer in swollen and unswollen states were measured by the caliper and ϕ was determined by the **Equation (3-5)**

$$\phi = \frac{Unswollen\ volume}{Swollen\ volume} \qquad \textbf{(3-5)}$$

The molecular weight between cross-links, $\overline{M_C}$, was calculated according to the **Equation (3-6)**,[2]

$$\tau = \frac{\rho RT}{\overline{M_C}}\ (1 - \frac{2\overline{M_C}}{\overline{M_N}})(\alpha - \frac{1}{\alpha^2})(\frac{\phi}{\phi_0})^{1/3} \qquad \textbf{(3-6)}$$

where ρ is the density of the polymer, $\overline{M_C}$ is the average molecular weight between cross-links, $\overline{M_N}$ is the number-average molecular weight of the uncross-linked polymer, ϕ and ϕ_0 are the polymer volume fraction in the fully swollen and relaxed states, respectively. The relaxed state refers to the polymer immediately after cross-linking, but before any swelling takes place. The volume fraction of the polymer at the relaxed state was found to be 0.83. Here, it is assumed that $\overline{M_N} >>> \overline{M_C}$. The weight-average molecular weight (M_w = 63000 g mol^{-1}) of uncross-linked polymer, poly(HEMA/DMAEMA), was determined by SLS; therefore, the assumption made in the above calculation was considered reasonable.

3.2.10. Evaluation of biological properties of synthesized hydrogel

Frozen HeLa cells (1×10^6 cells/mL, 1.00 mL) were recovered and expanded in T125 flask containing complete culture media (RPMI-1640 medium supplemented with 10% (v/v) donor calf serum (DCS), and 1% Pen Strep) at 37 °C and 5% CO_2 in a CO_2 supplied humidified incubator (Symphony 5.3 A, VWR, Radnor, PA). At 70% confluency, the cells were subcultured in T175 flasks containing complete culture media to produce enough cells for further studies.

For subculturing, the cells were detached from T125 tissue culture flask by incubating with trypsin-EDTA for 2 min at 37 °C and 5% CO_2. Complete culture media (double the volume of trypsin-EDTA) was added to deactivate trypsin and the cell suspension was centrifuged at 2000 rpm for 2 min. The cell pellet was dispersed in new growth media, mixed with Tryphan blue (Thermofisher Scientific) and the cell count was obtained using a Countess® automated cell counter (Thermo Fisher Scientific). The cells were divided into T175 flasks and cultured at 37 °C and 5% CO_2 in the humidified incubator until 70% confluent.

The biological properties (cell attachment and cytotoxicity) were evaluated by culturing HeLa cells on both unpatterned (*blank*) and patterned hydrogel samples (with 2 µm and 6 µm pillars). The hydrogel substrates were autoclaved in PBS and disks with a diameter of 10 mm were punched, using a cork borer, under sterile conditions. Prior to seeding cells, the hydrogel disks were pre-incubated overnight in complete culture media in 24-well plates. At the 70% confluency, the cells were detached, centrifuged, and counted as mentioned in the subculturing process.

The spent media was aspirated from the wells containing the hydrogel substrates and fresh media was added to each well. Then the samples were seeded with the HeLa cells. The seeding densities are mentioned below. The control experiments were carried out in the same way except for the culturing cells in the normal wells without hydrogel disks. Each cell experiment was done in triplicates.

For the attachment study, the seeding density was 8.0×10^3 cells/cm^2. The cells were incubated for one week while changing the media every other day. The attachment and proliferation of HeLa cells on each substrate were analyzed daily. Each day, a set of samples was fixed with 10% neutral buffered formalin for 30 min, permeabilized with Triton® X-100 in 0.1% BSA in PBS for 15 min, and stained with Rhodamine phalloidin (1:1000 dilution in 0.1% BSA and 0.1% Tween® 20 in PBS) for 2 h at room temperature in the dark. Each step was followed by two rinsing steps in 0.1% BSA in PBS. The nuclei were counterstained with DAPI (1:5000 dilution in 0.1% BSA and 0.1% Tween® 20 in PBS) for 5 min at room temperature in the dark. Finally, the samples were washed with PBS and imaged using an Olympus-IX83 inverted microscope. Bright-field and fluorescence images (through RFP and DAPI channels) of randomly selected fifteen fields of view were taken from each sample. The number of adherent cells in each spot was counted from the DAPI-stained photos by using the analyze particles built-in function of ImageJ 1.47t software.

The cell viability assay was carried out at two different time points: one day and seven days after seeding the cells (seeding densities 8.0×10^3 cells/cm^2 for the seven-day experiment and 2.6×10^4 cells/cm^2 for the one-day experiment). For the seven-day experiment, the growth media was refreshed every other day. At the end of each time period (one day or seven days) the cell viability was evaluated by using ReadyProbes™ cell viability imaging kit, blue/red, according to the manufacturer's instructions. Briefly, two drops of each NucBlue® Live and propidium iodide

were added to each well and incubated for 10 min at room temperature in the dark. Bright-field and fluorescence images (through RFP and DAPI channels) of randomly selected ten fields of view were taken from each sample. The number of total cells (from blue stained-image) and the dead cells (from red stained-image) were counted in each spot by using the analyze particles built-in function of ImageJ 1.47t software. The cell viability was calculated as the percentage of live cells in each spot.

3.3. Results and discussion

3.3.1. Synthesis and characterization of poly(HEMA/DMAEMA/TEGDMA) hydrogel

UV or visible light-initiated polymerizations are widely used in the synthesis of hydrogels due to ease of preparation, mild reaction conditions (e.g. ambient or physiological), and fast curing times.[130] Here, poly(HEMA/DMAEMA/TEGDMA) hydrogels were prepared by UV initiated radical polymerization to produce a network polymer as demonstrated in **Scheme 3-2**. All components–monomers, cross-linking agent, initiator, and solvents–are mixed together to generate randomly cross-linked networks upon UV irradiation for 90 s.[60] The hydrogel was prepared by mixing HEMA, DMAEMA, TEGDMA and 2-hydroxy-2-methylpropiophenone in a ratio of 38:2:1:1 mol/mol, respectively. The solvent mixture consisted of water and ethylene glycol in a ratio of 1:1 mol/mol.

Structural characterization of the polymer was performed using nuclear magnetic resonance (NMR) both in the solution and solid-state. The polymer was synthesized without the TEGDMA cross-linking agent and dissolved in deuterated dimethylsulfoxide (DMSO-d_6) in preparation for solution NMR (^{1}H NMR) studies. ^{1}H NMR spectra confirm the formation of the poly(HEMA/DMAEMA) polymer (**Figure 3-2**).

Furthermore, ATR-FTIR spectra (**Figure 3-3(a)**) and ^{13}C solid state NMR (**Figure 3-3(b)**) of the cross-linked polymer, poly(HEMA/DMAEMA/TEGDMA), confirm the presence of all three units; HEMA, DMAEMA, and TEGDMA in the network polymer.

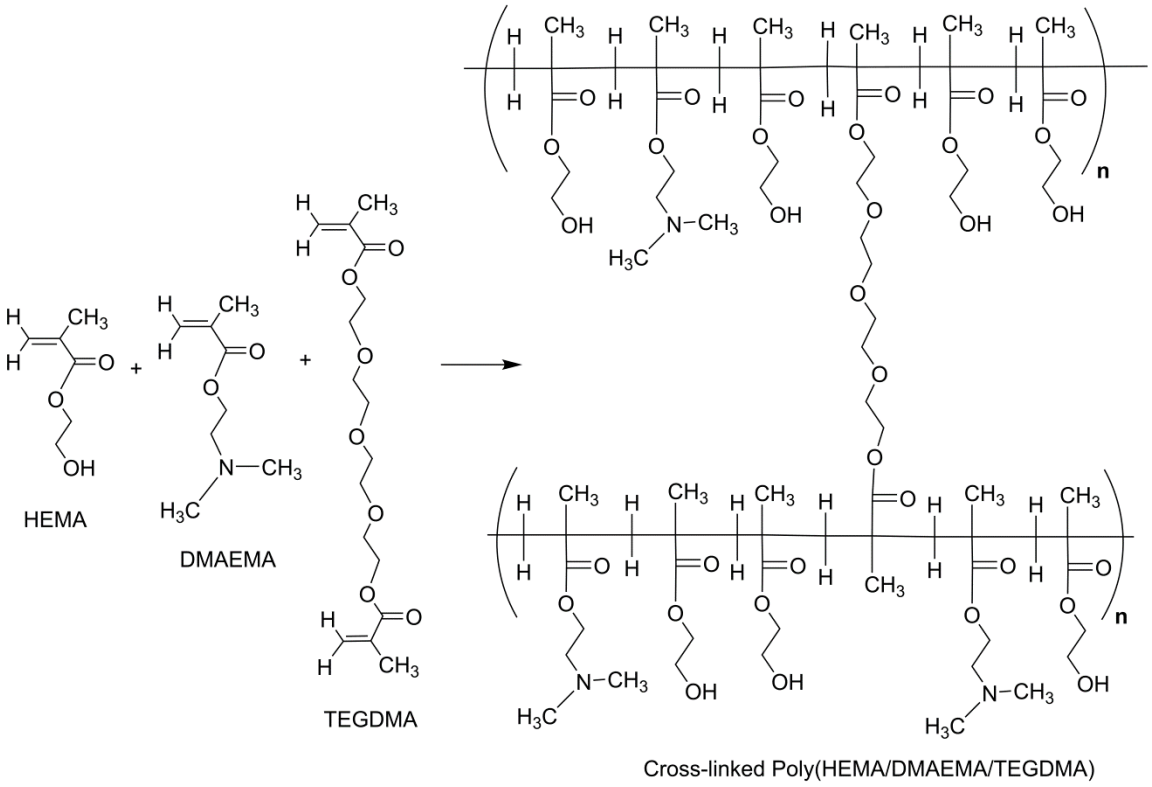

Scheme 3-2. Random co-polymerization of HEMA, DMAEMA, and TEGDMA results in a network polymer, poly(HEMA/DMAEMA/TEGDMA).

In the ^{1}H NMR spectrum, the peak (d), relevant to the proton on the OH of HEMA, (chemical shift, δ = 4.8 ppm) and the peak (b), relevant to Hs of CH_3 groups attached to N of DMAEMA (δ = 2.2 ppm) confirm the presence of both HEMA and DMAEMA in the polymer. Furthermore, the two peaks (a) present at δ = 0.8 ppm and δ = 1.0 ppm represent the Hs of CH_3 groups in both HEMA and DMAEMA units. As well, the peaks (c) at δ = 3.6 ppm and δ = 3.9 ppm are due to the Hs in CH_2 groups of the dangling groups of monomers. Generally, the peaks responsible for the double bond present in the monomer units appear between δ = 5.5 ppm and δ = 6.5 ppm.

Absence of any peaks in this area of the ^{1}H NMR spectrum of poly(HEMA/DMAEMA) further suggests the formation of a polymer.

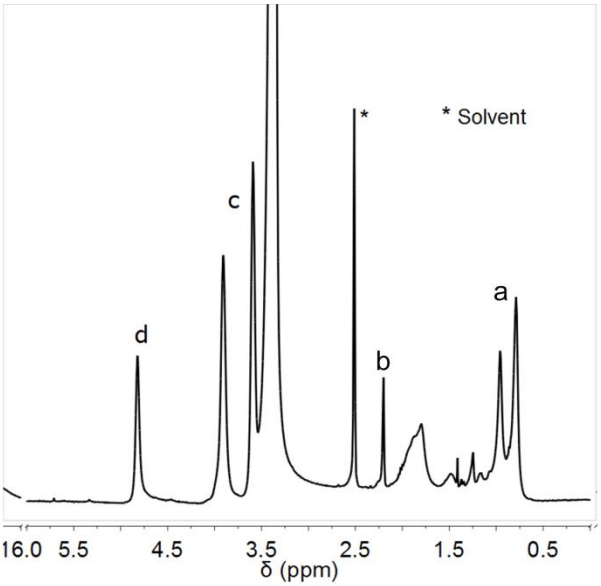

Figure 3-2. ^{1}H NMR spectrum of the poly(HEMA/DMAEMA) polymer without cross-linking agent (TEGDMA) (in DMSO-d_6; 400 MHz).

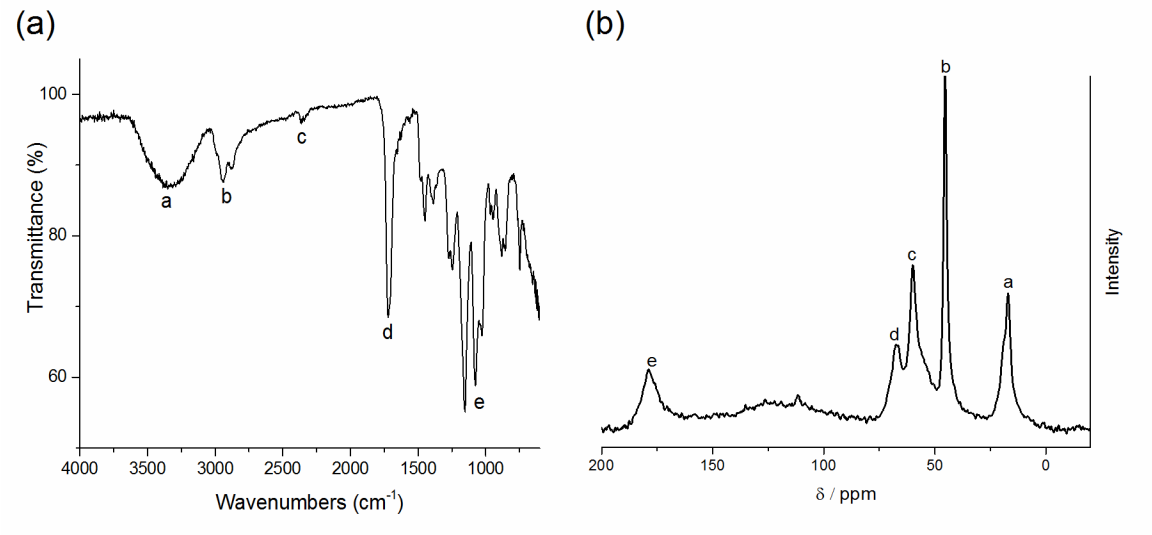

Figure 3-3. (a) ATR-FTIR spectrum and (b) ^{13}C NMR spectrum (Solid State; 300 MHz) of poly(HEMA/DMAEMA/TEGDMA) cross-linked polymer.

In the ATR-FTIR spectrum, the broad peak (a) present between 3250 and 3500 cm^{-1} represents the –OH group of HEMA units; peak (b) present ~3000 cm^{-1} represents the C-H (sp^3) bond; peak (c) at 2250 cm^{-1} represents the N-C bond, confirming the incorporation of DMAEMA units; peak (d) at 1700 cm^{-1} is the characteristic peak of -C=O groups; and peak (e) present ~1000 cm^{-1} represents the C-O-C bond of TEGDMA units.

In the ^{13}C NMR spectrum the peak (a) present at δ = 17 ppm represents the $–CH_3$ carbon in HEMA and DMAEMA units; peak (b) at δ = 45 ppm represents the Cs in CH_3 groups attached to N in DMAEMA, which confirms the presence of DMAEMA units in the polymer; peak (c) at δ = 59 ppm represents the Cs in $-CH_2$ groups in the polymer backbone; peak (d) present at δ = 67 ppm represents the C in –CO groups of TEGDMA and confirms the incorporation of TEGDMA units in to the network; and peak (e) is due to the –C=O groups present in the polymer.

3.3.2. Confirmation of the micropillar pattern transfer

Standard lithography and etching techniques were used to fabricate the micropillar array into a silicon wafer with the desired feature sizes and dimensions. Poly(HEMA/DMAEMA/TEGDMA) hydrogels were patterned with the micropillar structures using soft-lithography techniques, wherein a negative mold of the etched Si wafer is generated in PDMS.[57,100,108] The mixture of monomers, cross-linking agent, initiator, and solvents was cast onto the PDMS mold and UV cured. Patterned and unpatterned (*blank*) hydrogel samples were produced in the same fashion (see Experimental Section). Hydrogel replicas of the microstructures were swollen in a solvent, DI water, PBS, 60% ethanol, or absolute ethanol, until they delaminated from the mold. Peeling the hydrogels from the PDMS mold without initially swelling the hydrogel resulted in ripping, incomplete transfer of the micropillar pattern, clogging, or damage to the PDMS mold (**Figure 3-4**).

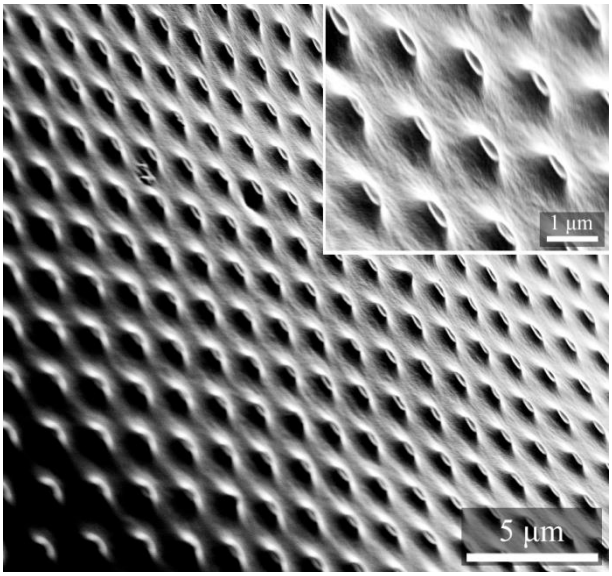

Figure 3-4. An SEM image of a hydrogel that was peeled off from the mold without swelling; the inset shows an enlarged SEM image; only the bases of the pillars can be seen as the micropillars were ripped off from the base due to the force applied when peeling off.

The SEM images shown in **Figure 3-5** confirm the successful transfer of the micropillar array pattern onto the hydrogel surface. The replication process was particularly fast and had the highest fidelity and reproducibility when 60% ethanol was used as the swelling solvent. Cross-sections of the patterned hydrogels were imaged using light microscopy to confirm that the micropillars were completely and successfully reproduced. Images in **Figure 3-5(e)** and **Figure 3-5(j)** illustrate that the micropillars on the hydrogel surface are replicas of the original micropillar patterns (d =1 µm; h = 2 µm, or 6 µm) etched into the master Si wafers.

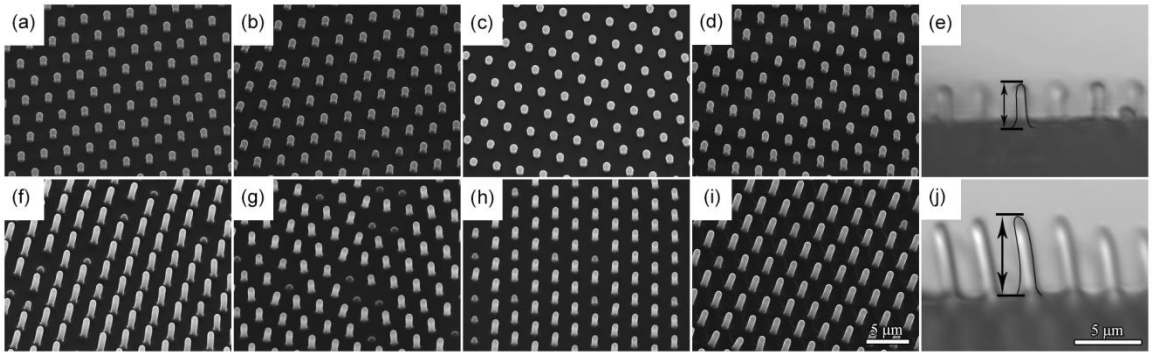

Figure 3-5. The SEM images of poly(HEMA/DMAEMA/TEGDMA) hydrogels patterned with micropillars. (a-d) Hydrogels patterned with micropillars of height = 2 µm and (f-j) height = 6 µm. Poly(HEMA/DMAEMA/TEGDMA) hydrogels were patterned with microstructures in a variety of swelling solvents including: (a, f) DI water, (b, g) PBS, (c, h) 60% ethanol, and (d, i) absolute ethanol. Light microscopy images of hydrogel cross-sections confirm that the heights of the micropillars patterned onto the hydrogel surface correspond to the original heights of (e) 2 µm and (j) 6 µm etched into the Si wafer.

3.3.3. Swelling studies

The graphs in **Figure 3-6** show the amount of time it takes for *blank* (unpatterned) poly(HEMA/DMAEMA/TEGDMA) hydrogels to swell in a particular solvent. At equilibrium, the percent mass swelling ratio (%Q) of free and *blank* hydrogels exceeds 200% and 100% in the solvents 60% ethanol and absolute ethanol, respectively (**Figure 3-6(a)** and **Figure 3-7**). This result was in agreement with published work by Guvendiren et al. on swelling studies of poly(HEMA) hydrogels in ethanolic solutions.[78] It took approximately 10 h for the free hydrogels to reach the maximum %Q in 60% ethanol and absolute ethanol. In DI water and PBS, it only took 2 h for the hydrogels to reach the equilibrium percent mass swelling ratio of 40% (**Figure 3-6(a)**). A significantly reduced %Q was observed in PDMS confined hydrogels upon swelling as compared to the free hydrogels (**Figure 3-6(b)**). This occurs due to the delamination of the hydrogel from the PDMS mold prior to complete swelling.

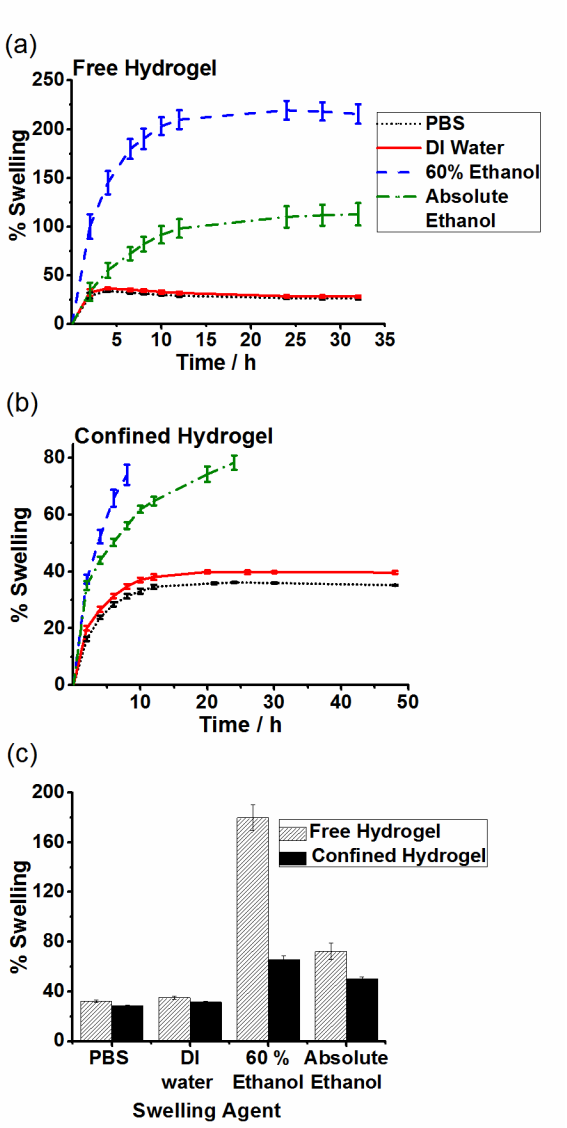

Figure 3-6. The swelling behavior of the poly(HEMA/DMAEMA/TEGDMA) hydrogel in DI water, PBS, 60% ethanol, and absolute ethanol. The percent mass swelling ratio (%Q) of (a) free and (b) PDMS-confined poly(HEMA/DMAEMA/TEGDMA) as a function of time; (c) A comparison of %Q of the free and PDMS-confined hydrogels in the various swelling solvents within a time span of 6 h. [Note: The experiments were performed with *blank* (unpatterned) hydrogels.]

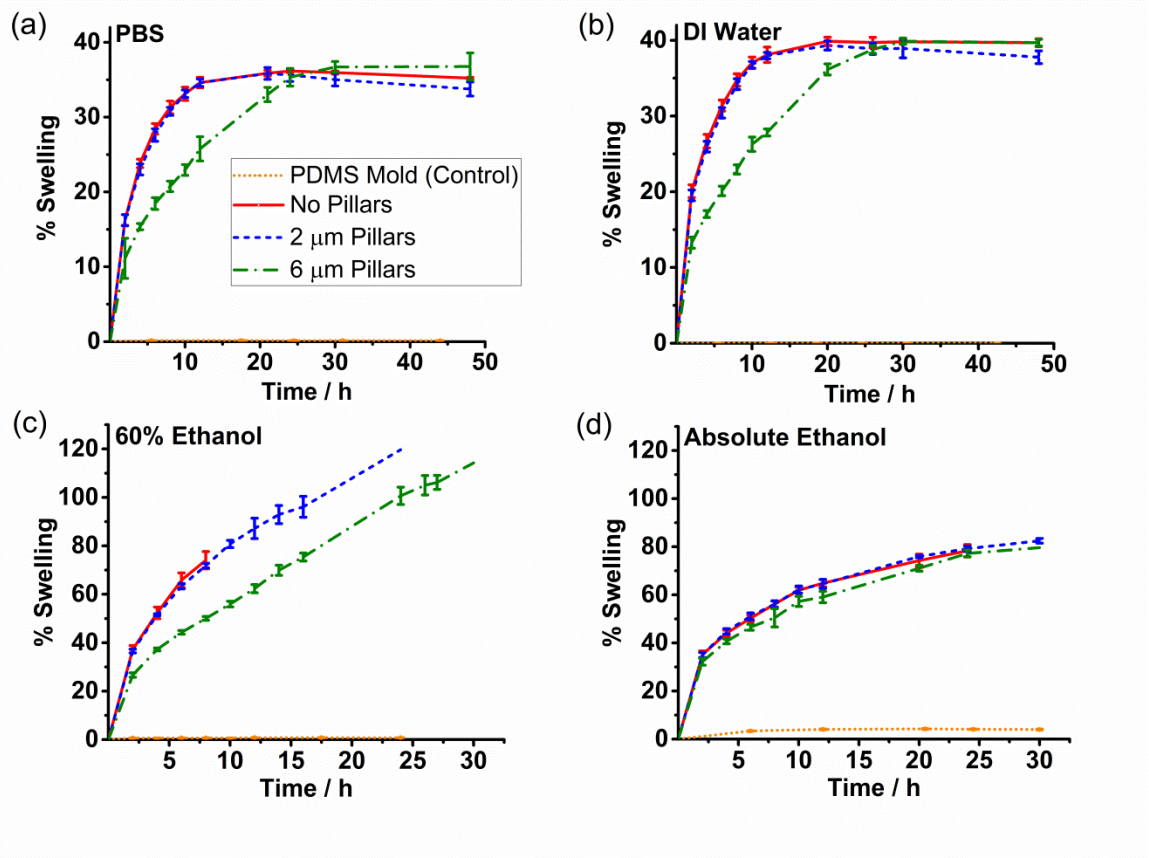

Figure 3-7. The percent mass swelling (%Q) of poly(HEMA/DMAEMA/TEGDMA) hydrogel-PDMS composites immersed in (a) PBS, (b) DI water, (c) 60% ethanol, and (d) absolute ethanol. PDMS molds and *blank* hydrogel samples are included for comparison. *Blank* samples and hydrogels patterned with micropillars of h = 2 μm show no significant difference in percent swelling. A larger difference in percent swelling is observed for surfaces patterned with micropillars of h = 6 μm, but this was attributed to the slightly different dimensions in these samples (see Experimental Section).

The mass swelling ratio decreased 1.5-fold in absolute ethanol and 3-fold in 60% ethanol when confined by PDMS (**Figure 3-6(b)** and **Figure 3-6(c)**). Such a change in %Q was not observed for swelling experiments carried out in either DI water or PBS (**Figure 3-6(c)**) since the %Q is only 40% and delamination of the hydrogel does not occur readily.

The poly(HEMA/DMAEMA/TEGDMA) hydrogels swollen in 60% ethanol delaminated from the PDMS mold before the 10 h mark (**Figure 3-6(b)**). Nevertheless, in both DI water and PBS, PDMS confined hydrogels took much longer (10 h) to reach the same equilibrium %Q (40%) when compared to free hydrogels (2 h) (**Figure 3-6(b)**). Similar swelling behavior was observed for hydrogels patterned with micropillar arrays irrespective of their height (**Figure 3-7**).

During the swelling experiments carried out for the PDMS-confined hydrogels, limited expansion of the hydrogel along the transverse direction generated a compressive stress inside the polymer network resulting in curvature of the PDMS mold upon swelling. **Figure 3-8(a)** shows representative images of the curvature of the hydrogel-PDMS composite with time for hydrogels swollen in 60% ethanol. The largest angle of curvature was found to be at $\theta = 29°$ (8 h) for the hydrogel-PDMS composite swollen in 60% ethanol, which is consistent with the maximum %Q observed in this system prior to delamination (**Figure 3-8(b)**).

Delamination occurs once the compressive stress exceeds the adhesive forces between the hydrogel and the substrate,[131-133] which for this system occurs when the angle of curvature of the swollen hydrogel and PDMS mold is greater than 20°, or at a volumetric swelling ratio of 2.01 (**Figure 3-9**). This angle is achieved in 60% ethanol or absolute ethanol and results in self-delamination (~2 h in 60% ethanol). When the hydrogels confined in the PDMS molds are swollen in PBS and DI water, the edges of the hydrogel are mechanically released from the mold and the PDMS is immobilized onto a surface to facilitate the delamination process. The swollen hydrogels delaminate from the mold after 3 - 4 days.

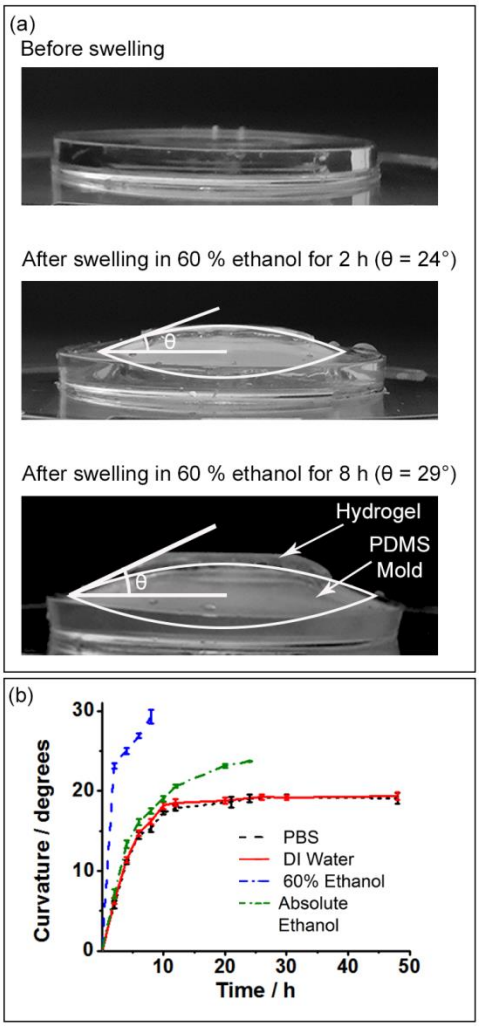

Figure 3-8. A curvature is induced in the PDMS mold as the confined hydrogel is swollen in solvent: (a) The digital photographs that show the curvature of the hydrogel-PDMS composite as it swells in 60% ethanol, (b) The angle (θ) of the hydrogel-PDMS composite as a function of time when the hydrogel swells in various solvents.

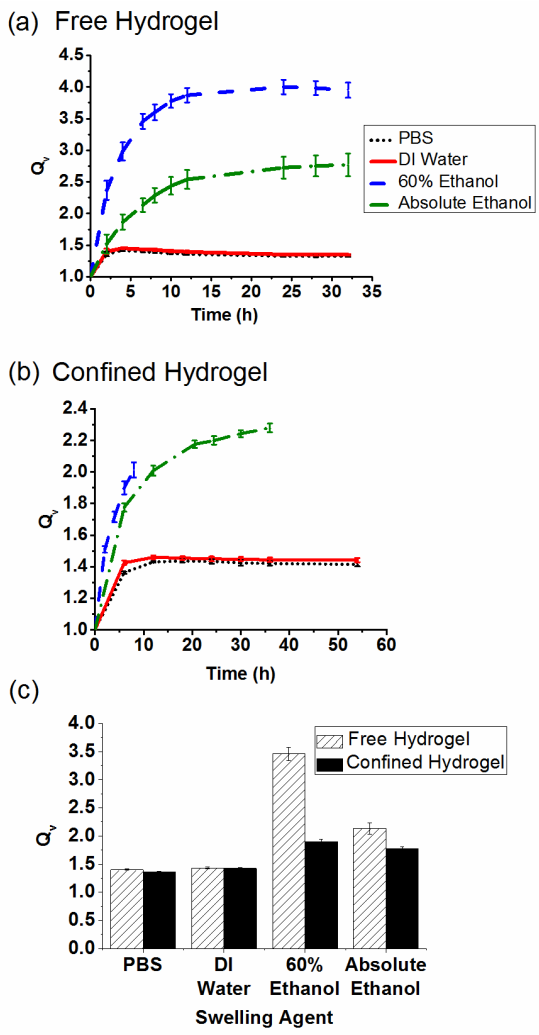

Figure 3-9. The volumetric swelling ratio (Q_v) of (a) *blank*, free (b) *blank*, PDMS-confined poly(HEMA/DMAEMA/TEGDMA) hydrogel in PBS, DI water, 60% ethanol, and absolute ethanol, (c) A comparison of Q_v of the free and confined hydrogels.

The curvature measurements follow the same trend as the %Q values where there is no significant effect from the pattern or the pillar height (**Figure 3-10**). When the composites are immersed in PBS and DI water the swelling of the hydrogels is insufficient for the delamination and the curvature measurements reach a plateau at ~30 h. In contrast, the swelling of the hydrogel facilitates self-delamination when swollen in 60% and absolute ethanol; however, the patterned hydrogels require a longer time to delaminate from the mold than the *blank* hydrogels.

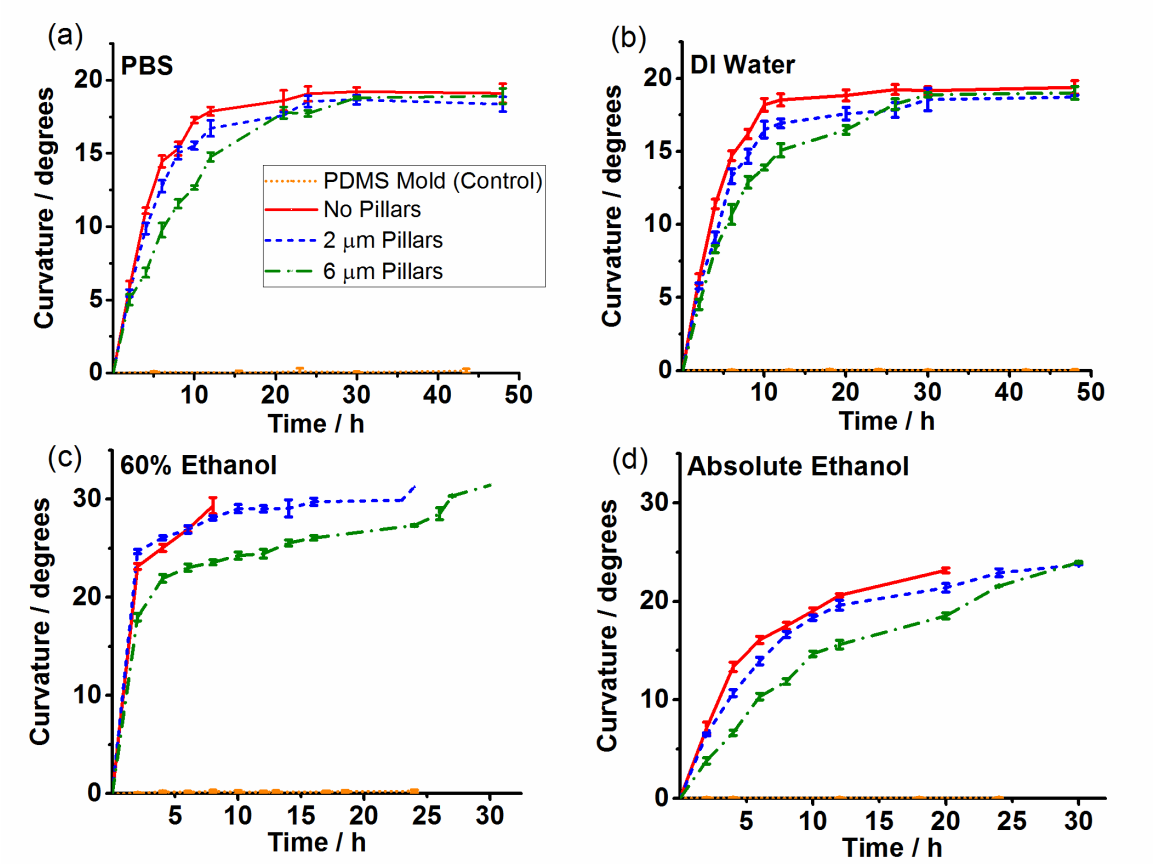

Figure 3-10. The curvature of poly(HEMA/DMAEMA/TEGDMA) hydrogel-PDMS composite immersed in (a) PBS, (b) DI water, (c) 60% ethanol, and (d) absolute ethanol. PDMS molds and unpatterned hydrogel samples are included for comparison. Unpatterned and patterned hydrogels with micropillars of h = 2 μm show no significant difference in curvature. A larger difference in curvature is observed for surfaces patterned with micropillars of h = 6 μm, but this was attributed to the slightly different dimensions in these samples (see Experimental Section).

3.3.4. Determination of solubility parameter of the hydrogel

Successful swelling of poly(HEMA/DMAEMA/TEGDMA) in ethanolic solutions is attributed to a favorable solubility parameter of the hydrogel in the solvent. As reported in previous studies, the maximum swelling is achieved when the solvent has the same solubility parameter (δ) as the polymer, ($\delta_{Solvent} \sim \delta_{Polymer}$).[125,126,134] The solubility parameter of the polymer, $\delta_{Polymer}$, by inference, is approximately the same value as the solvent having the highest affinity towards the polymer. The solubility parameter of the poly(HEMA/DMAEMA/TEGDMA) hydrogel ($\delta_{Polymer}$) was estimated to be 25 – 27 $MPa^{1/2}$ using the method developed by Gee[125] (**Figure 3-11**), since the highest swelling of the hydrogels was observed with solvents having an interaction parameter in this range. Additionally, the swelling of the hydrogels was evaluated in a series of ethanol-water mixtures (**Figure 3-12**). The maximum swelling ratio of this series of ethanolic solutions was obtained in 60% ethanol (the solubility parameter is approximately 35 $MPa^{1/2}$): a solvent that swells the hydrogel moderately. This result is in agreement with swelling studies of poly(HEMA) hydrogels previously published by Guvendiren et al.[78] Solvents having moderate to strong polar interactions will generally be good solvents for poly(HEMA/DMAEMA/TEGDMA), which can be attributed to the hydroxyl and amine pendant groups on the polymer chain. Consequently, 60% ethanol, as a solvent with a moderate solubility parameter in the hydrogel, allows for moderate swelling that results in delamination without ripping or tearing of the hydrogel.

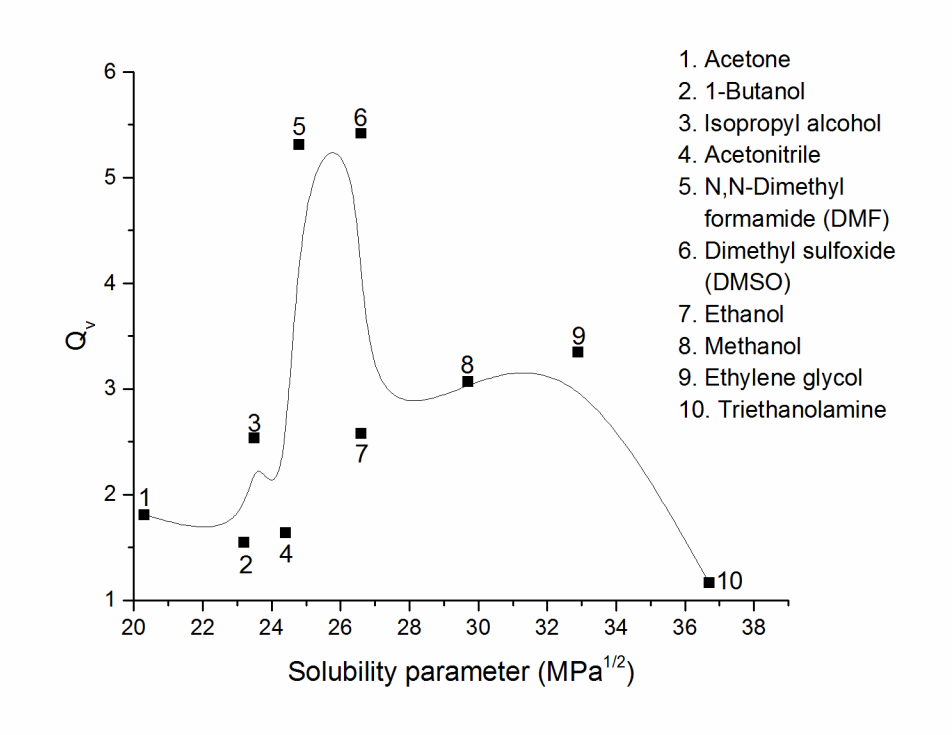

Figure 3-11. The volumetric swelling of the poly(HEMA/DMAEMA/TEGDMA) hydrogel vs solubility parameter in different solvents.

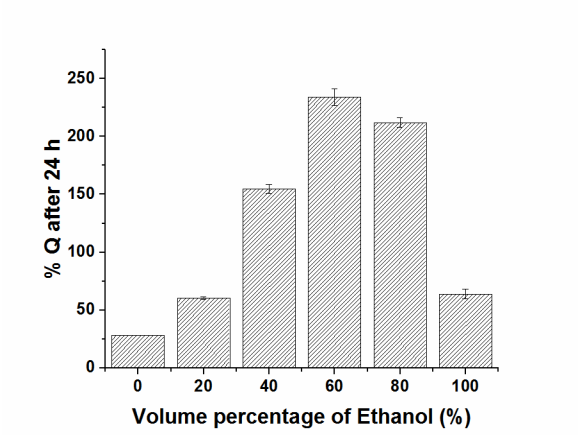

Figure 3-12. The percent mass swelling (%Q) in a series of ethanol-water mixtures.

3.3.5. Mechanical testing and determination of network parameters

The mechanical properties of the hydrogel are important to the replication process. The elastic modulus of ~8 MPa obtained for the poly(HEMA/DMAEMA/TEGDMA) hydrogels facilitates the fabrication process since this value is comparable to the elastic modulus of PDMS and other UV curable polyurethane polymers that have been successfully patterned with micro and nanoscale features.[115] Poly(HEMA/DMAEMA/TEGDMA) is one of the softest hydrogels to be patterned with such small features, although Chandra et al. previously demonstrated that poly(HEMA) based polymers could be patterned at the sub-micron level when the elastic modulus ranged from 1580 – 1790 MPa.[33,57] The mechanical properties of poly(HEMA/DMAEMA/TEGDMA) hydrogels are shown in **Figure 3-13** and were evaluated in both the swollen and unswollen states. Tensile tests were performed on the swollen hydrogel samples after they reached equilibrium swelling (15 – 20 h). The elastic modulus, ultimate tensile strength, and break strain were determined from stress-strain curves (**Figure 3-13(a)** and **Figure 3-13(b)**). As expected, the highest values for the elastic modulus (~8 MPa), ultimate tensile strength (~570 kPa), and break strain (~1.92 mm/mm) were obtained for the unswollen polymer samples (**Figure 3-13**). Additionally, when the poly(HEMA/DMAEMA/TEGDMA) samples were swollen in 60% ethanol, a 35-fold reduction in the elastic modulus was measured compared to the unswollen sample. Swelling the polymer in the other solvents resulted only in a 20-fold decrease in the elastic modulus: 414 kPa (in PBS), 357 kPa (in DI water), and 372 kPa (in absolute ethanol). Ultimate tensile strength decreased a marked 27- fold in 60% ethanol, but only by about an order of magnitude in the other solvents evaluated (**Table 3-2**). Similarly, the lowest break strain, 0.09 mm/mm, was measured in 60% ethanol (**Table 3-2**). Even though the polymerization was not rigorously controlled under an inert atmosphere, the mechanical properties of the random co-polymer poly(HEMA/DMAEMA/TEGDMA) were consistent (**Table 3-2**). The reduced mechanical properties of the hydrogel swollen in 60% ethanol likely result from stretching and rupture of some of the physical cross-links between the polymer chains

during swelling.[135,136] This can be verified in **Figure 3-13(c)** by a statistically significant reduction in the cross-linking density. The reduction in the mechanical properties upon swelling may also aid in the replication of the micropillar pattern by the soft-lithography process.[2,135,137]

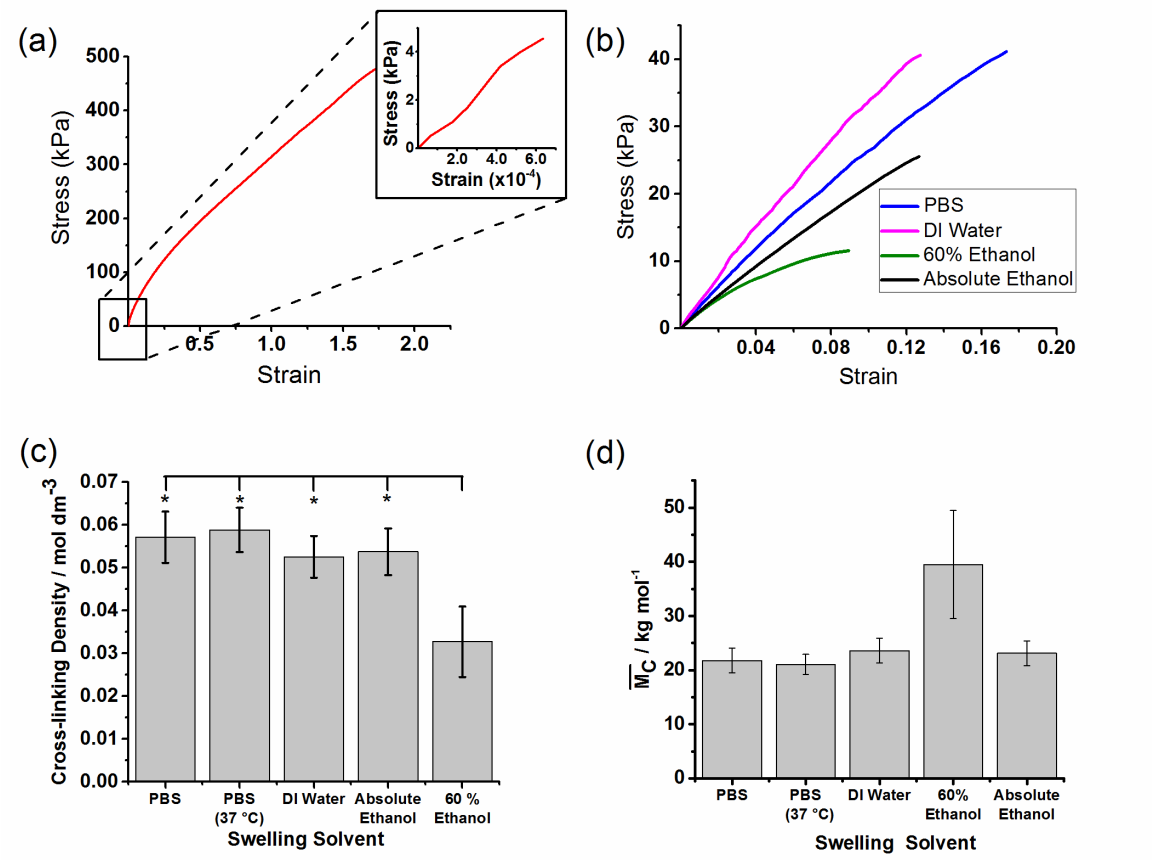

Figure 3-13. Evaluation of mechanical properties and the network parameters of poly(HEMA/DMAEMA/TEGDMA) hydrogels. Stress-strain curves of (a) unswollen and (b) swollen cross-linked polymers, (c) Cross-linking density (*$p < 0.01$ between the groups indicated) and (d) $\overline{M_C}$ of hydrogels was determined based on the swelling solvent.

Table 3-2. Elastic modulus, ultimate tensile strength, and break strain of poly(HEMA/DMAEMA/TEGDMA) hydrogels after swelling in each solvent for 15 – 20 h.

Swelling Solvent	**Elastic Modulus (kPa) ($\times 10^2$)**	**Ultimate Tensile Strength (kPa)**	**Break Strain (mm/mm)**
Unswollen	81.0 (±6.8)	570 (±97)	1.92 (±0.142)
PBS	4.14 (±0.74)	55.9 (±16.8)	0.150 (±0.035)
DI water	3.57 (±0.63)	52.8 (±10.3)	0.137 (±0.021)
60% Ethanol	2.20 (±0.36)	21.0 (±4.9)	0.090 (±0.028)
Absolute ethanol	3.72 (±0.37)	40.0 (±17.0)	0.215 (±0.007)

The elastic modulus was calculated from the slope of the linear part (initial slope) of the stress-strain curve
The ultimate tensile strength and the break strain were respectively determined from the stress and strain corresponding to the break point where the samples ruptured.

The weight-average molecular weight ($\overline{M_w}$) of the polymer, as determined by the static light scattering, was 63.1 (±2.17) kDa (the second virial coefficient, A_2, was 2.27×10^{-4} ($\pm 4.42 \times 10^{-5}$) mL mol/g^2).

3.3.6. Evaluation of biological properties

The cell attachment and cytotoxicity of poly(HEMA/DMAEMA/TEGDMA) hydrogel were evaluated using HeLa cells. The cells were cultured on *blank* (unpatterned) and patterned hydrogel substrates for seven days and the number of cells attached to the samples was assessed daily. **Figure 3-14** illustrates the attachment and viability of HeLa cells cultured on hydrogel substrates over seven days. As depicted by the graph in **Figure 3-14(a)**, at day 1, the attachment of HeLa cells onto the poly(HEMA/DMAEMA/TEGDMA) hydrogel was significantly enhanced when the hydrogel surface is patterned with micropillars. Interestingly, attachment of HeLa cells on the patterned hydrogels was comparable to the attachment of cells on tissue culture plastic (There is no statistical significance between the number of cells adhered to the control and

surface-patterned hydrogel when $p < 0.05$). **Figure 3-14(b)** shows a graph of the number of HeLa cells present on the hydrogel substrates and control wells over the seven days. The number of cells attached to the hydrogels with micropillar arrays is significantly greater than the *blank* (unpatterned) hydrogel throughout the experiment. This confirms that hydrogels with micropillar arrays support the retention of cells on the substrate. A similar trend was observed by Schulte et al. on starPEG (PEG = poly(ethylene glycol) hydrogels where the attachment of fibroblast cells increased when the hydrogels were patterned with pillars.[138] The improved attachment of cells on the patterned hydrogel surfaces can be attributed to the decreased hydrophilicity of the hydrogel due to the presence of the micropillars on the surface.[28,33]

The results show that the micropillar pattern promotes attachment of cells on the material; however, the height of the pillars did not appear to have a prominent effect on the attachment of HeLa cells. Furthermore, **Figure 3-14(b)** shows that the number of cells attached to the hydrogels increases, day by day, over the duration of the experiment. Hence, it is clear that poly(HEMA/DMAEMA/TEGDMA) hydrogel, at the composition used in this study, does not inhibit the proliferation of HeLa cells. The cytotoxicity of the material was further evaluated by the cell viability assay. The cell viability was determined at two time frames: 24 h and seven days. **Figure 3-14(c)** shows that more than 90% of the adhered cells on the hydrogel are viable at both time frames. Since the cell viability on poly(HEMA/DMAEMA/TEGDMA) is comparable to the viability of cells on tissue culture plastic, it is clear that the material is not toxic at the composition that was used in the fabrication process. The cell viability assay was performed on both *blank* (unpatterned) and patterned hydrogels (with 2 µm and 6 µm pillars). The viability remained the same in all hydrogels, regardless of the presence of the pillars or the pillar height. So that, the data obtained for hydrogel patterned with 2 µm pillars is shown for clarity (**Figure 3-15**).

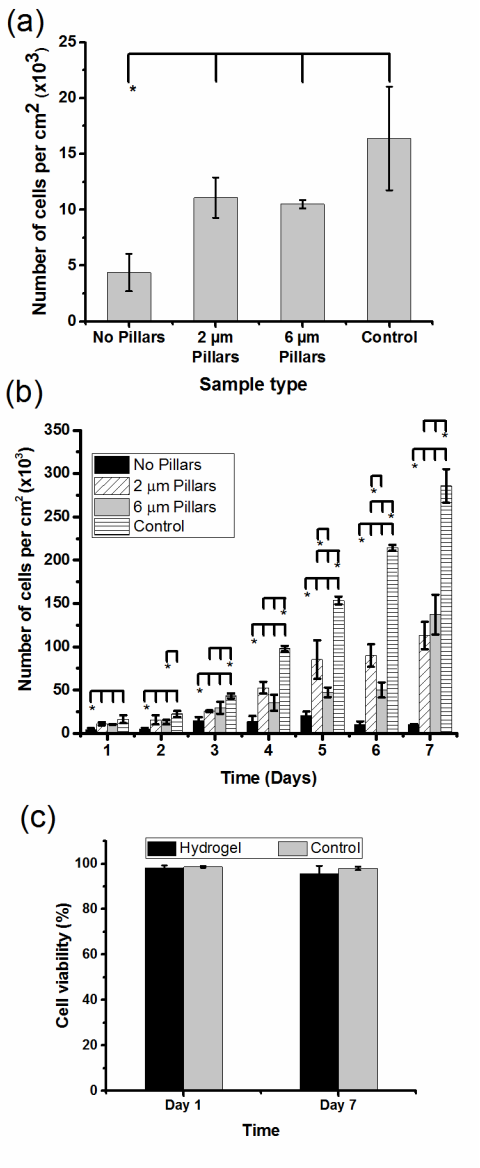

Figure 3-14. The attachment of HeLa cells onto hydrogels (a) after 24 h and (b) over 7 days; (c) Graph of the viability of HeLa cells grown on hydrogel samples with 2 µm pillars after 24 h and 7 days; Polystyrene or tissue culture plastic was used as the control. The statistical significance between the groups is indicated (*$p < 0.05$).

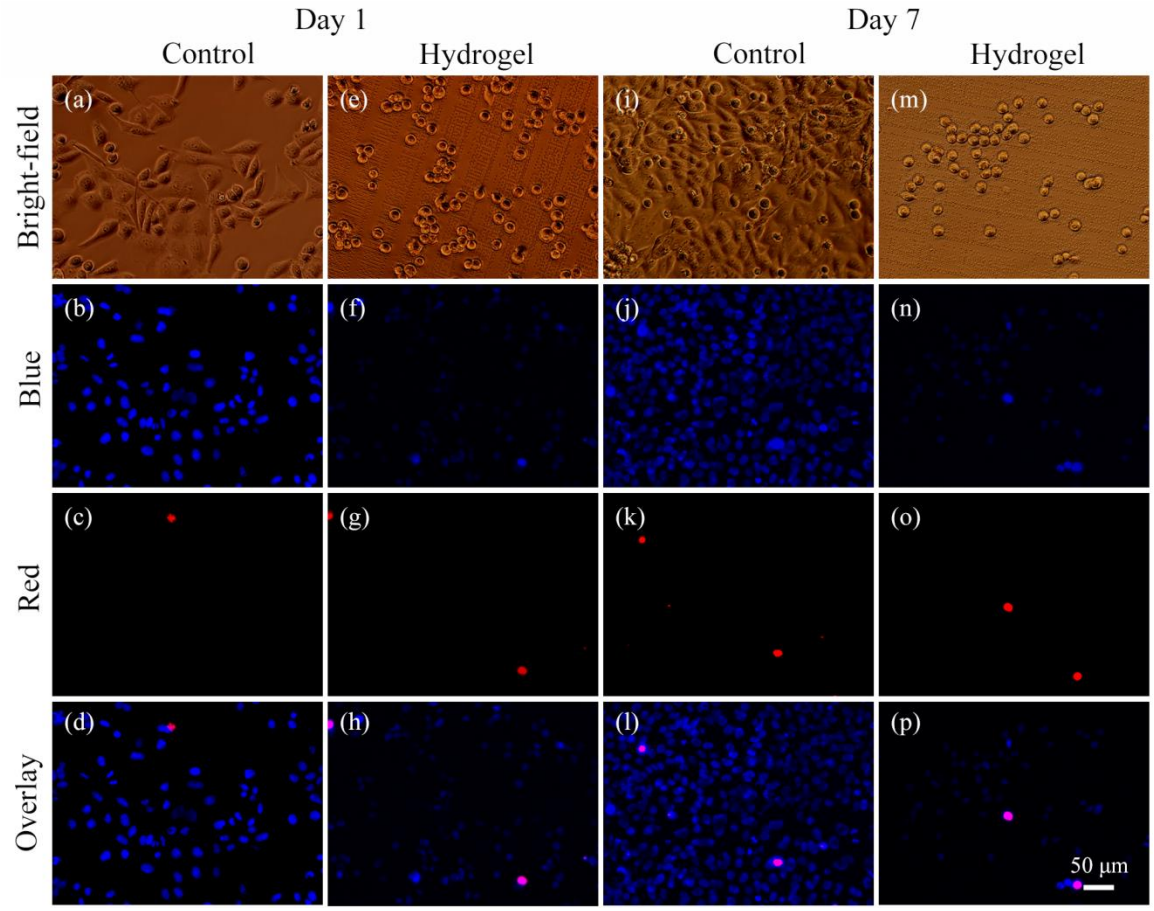

Figure 3-15. Viability of HeLa cells cultured on hydrogel samples for 1 day and 7 days; the blue stain (NucBlue® Live) stained the nuclei of all cells while the red stain (propidium iodide) stained the nuclei of dead cells.

Figure 3-16 illustrates the bright-field and fluorescence microscopy images of HeLa cells attached to the tissue culture plastic (a-d), *blank* hydrogel (e-h), and hydrogels patterned with micropillars of 2 µm (i-l), or 6 µm (m-p), at day 3. On the hydrogel substrates, the HeLa cells maintain mostly a rounded morphology with only some cells exhibiting elongated or spread morphologies (**Figure 3-16(e)-(p)**). In contrast, cells develop elongated or spread morphology on the tissue culture plastic (**Figure 3-16(a)-(d)**). As seen in the phalloidin-stained images, these rounded cells grew little protrusions that provide evidence for the attachment of cells on the hydrogel substrate. The rounded morphology of the HeLa cells is not indicative of cell death as

has been shown by Lyndon in his study where the mammalian cells were cultured on synthetic hydrogels with high equilibrium water content (70 – 90%).[27] Another interesting observation was that the cells formed clusters as they grew on the hydrogel substrates (**Figure 3-16**). The cells appeared to interact more strongly with each other rather than with the substrate, led to the formation of cell clusters.[138] An increase in cell number, growth of protrusions, formation of cell clusters, and viability data clearly show that the HeLa cells continuously grow and proliferate on the hydrogel substrates even though they do not have spread morphology. SEM images of surface-patterned hydrogels with HeLa cells also confirmed that the micropillars on the hydrogels remain intact even after seven days of cell culture (**Figure 3-17**).

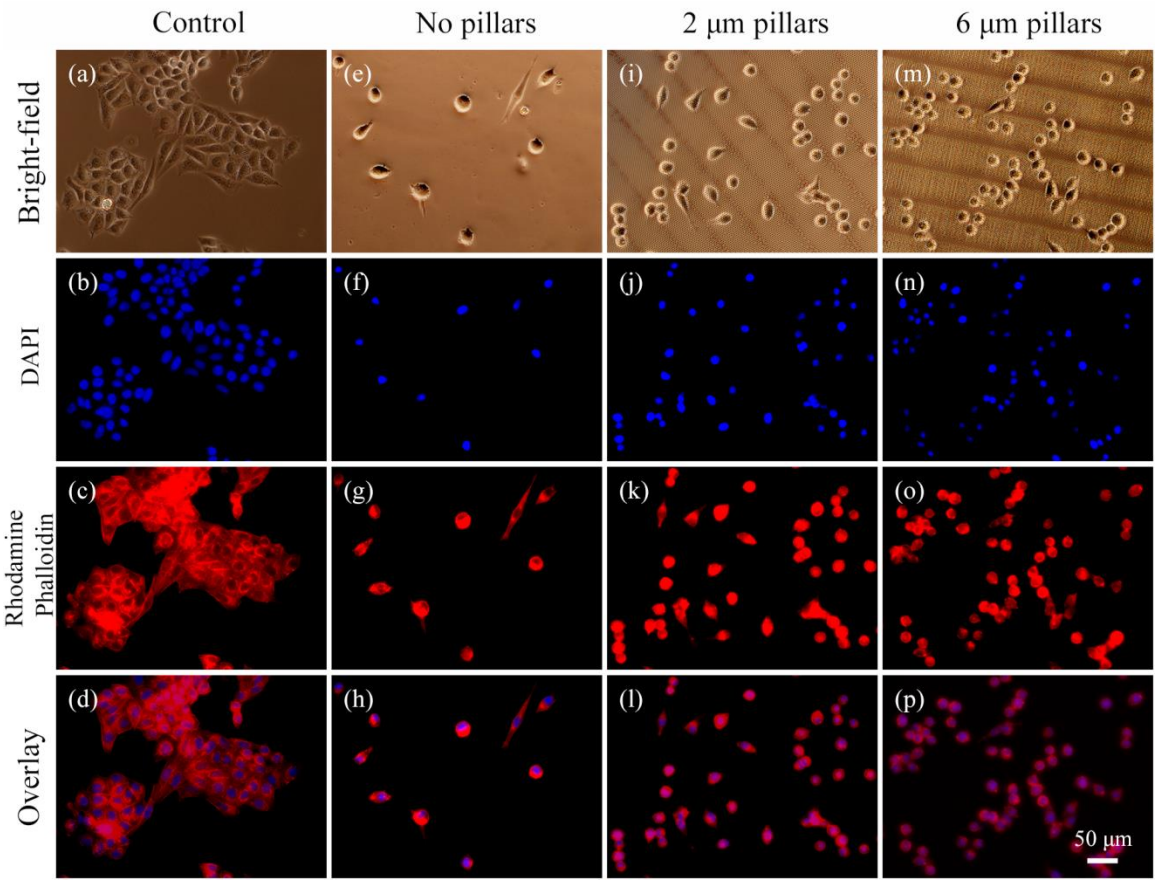

Figure 3-16. Fluorescence microscopy images of HeLa cells on hydrogels cultured for 3 days: (a-d) control experiment (polystyrene/tissue culture plastic), (e-h) *blank* (unpatterned) hydrogels, (i-l) hydrogels patterned with 2 μm pillars, and (m-p) hydrogels patterned with 6 μm pillars.

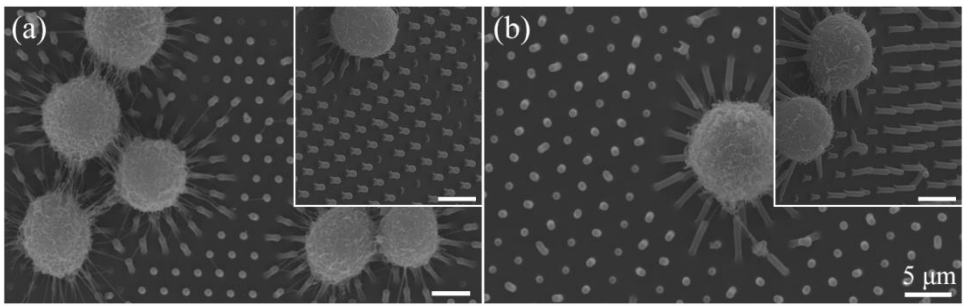

Figure 3-17. The SEM images of HeLa cells on hydrogel samples bearing (a) 2 µm pillars and (b) 6 µm pillars after 7 days of cell culture. The SEM images shown in the insets were taken at an angle of 45° to clearly show that the micropillars remain intact during the cell culture period.

3.4. Conclusions

This study demonstrated that micropillar arrays could be successfully and reproducibly patterned onto soft poly(HEMA/DMAEMA/TEGDMA) hydrogels by soft-lithography techniques when the hydrogels were swollen in solvents until delamination. The fabrication process is simple, less cumbersome, and results in the uniform and complete transfer of pattern onto the hydrogel surface. It is worthwhile to note that a soft poly(HEMA/DMAEMA/TEGDMA) hydrogel, which has an elastic modulus ~8 MPa, was patterned with a micropillar pattern of an aspect ratio as high as 6. The key factor was the utilization of solvents with moderate solubility parameters that are closer to the solubility parameter of the polymer, poly(HEMA/DMAEMA/TEGDMA). The PDMS serves a good material to utilize as a mold since it does not swell in many solvents,[139] allows for the isotropic swelling of hydrogel, and the dimensions of the mold can be easily designed.

The cell attachment and cytotoxicity studies show that the micropillar pattern on the hydrogel promoted the attachment of HeLa cells onto poly(HEMA/DMAEMA/TEGDMA) hydrogel, which is non-adhesive otherwise. *In vitro* studies show that the material is not toxic to the cells. It is anticipated that the surface pattern will support the attachment of other types of mammalian cells such as stem cells and hence poly(HEMA/DMAEMA/TEGDMA) hydrogel bearing micropillars, will be suitable for the potential applications in tissue engineering as scaffolding materials. This work is expected to facilitate the patterning of soft hydrogels for applications such as force sensors,[92] biosensors,[98,99] non-biofouling coatings,[140] drug delivery systems,[124] actuators,[102] and as scaffolds in tissue engineering.[111]

CHAPTER IV

SURFACE-PATTERNED POLY(HEMA/DMAEMA/TEGDMA) HYDROGELS TO CONTROL SIZE AND NUMBER OF STEM CELL AGGREGATES AS A POTENTIAL SCAFFOLDING MATERIAL

4.1. Introduction

Tissue engineering, an emerging area in biomedical sciences, has opened up new pathways to cure damaged or malfunctioning tissues by either *in vivo* regeneration or implantation of tissues grown *in vitro*.[37] The construction of a functional tissue, *in vivo* or *in vitro*, utilizes stem cells and biomaterials as scaffolds that directly interact with the tissue. The scaffolding material not only provides the structural support to growing tissues, but also can determine the fate of the cells.[141] Polymers,[142-144] ceramics,[145-146] and metals[147-149] are commonly used as biomaterials in tissue engineering for past few decades;[150-153] nevertheless, the incompatibilities,[154] in mechanical properties,[155] porosity,[156] and degradability,[157] of the material with surrounding tissues[158] and blood[159] causes complications and creates a need to improve the properties of existing biomaterials or to design novel materials with desirable characteristics.[160] As reported by Wichterle et al., among various polymeric materials, chemically or physically cross-linked hydrophilic polymer networks (or hydrogels) comprise the three key features that biomaterials should possess: desirable water content, resistance to biological reactions, and permeability to metabolic products.[161] Moreover, favorable mechanical properties, biocompatibility,

degradability, and the ability to cast into different shapes and sizes enable hydrogels to resemble the natural biological environment;[162] thus, hydrogels have been broadly studied for potential biological applications including scaffolds in tissue engineering,[142,163,164] delivery systems for therapeutic agents,[6,165,166] and in bionanotechnology.[167,168]

Use of hydrogels as scaffolding materials requires an excellent control over structure, surface chemistry, and physical properties that are crucial for regulating the responses of cells. Previous studies report that the mechanical properties,[42,169,170] surface topography,[138,171] wettability,[172] and surface functional groups[173,174] are some of the factors that direct adhesion,[172,175] orientation,[176,177] migration,[178] shape,[179] phenotype,[180,181] proliferation,[182,183] and differentiation of stem cells.[108,184] Hydrogels can be modified either chemically or physically by changing the composition[173,185] and patterning surfaces with different topographical features[138] respectively, to acquire the desired properties.

Since the surface topography controls the biological properties of materials, hydrogels patterned with nano and microscale features have been extensively studied to obtain a better understanding and manipulation of the functions of cells.[178,186] The topographical features on intrinsically non-adhesive hydrogel surfaces, such as poly(ethylene glycol) (PEG), were found to improve the attachment of cells.[138] Moreover, cells adopt a specific morphology based on the underlying structural features and subsequently differentiate along a distinct lineage. For an example, Guvendiren et al. reported that the hMSCs maintained an elongated shape when cultured on poly(2-hydroxyethyl methacrylate) (PHEMA) hydrogels bearing lamella-shaped wrinkles and round morphology on the hexagonal wrinkles. They have further observed that osteogenic differentiation was upregulated on the lamella pattern and adipogenic differentiation was upregulated on the hexagonal wrinkle pattern.[45] The morphology of cells, as demonstrated by previous research, is another important parameter that influences the differentiation pathway.[45,187]

A round morphology of stem cells induces adipogenesis or chondrogenesis whereas a well-spread, elongated morphology facilitates osteogenesis; however, for the chondrogenic differentiation of hMSCs, the formation of a three dimensional matrix is also important.[188]

Recently, several studies have reported utilization of three-dimensional cell culture conditions because the traditional two-dimensional culture systems fail to resemble the natural tissue environment.[189-191] Three-dimensional cell cultures have been commonly developed by various strategies, which include cell pellet culture,[192] forced aggregation technique,[193] as well as culturing cells on non-adhesive surfaces[194] and surfaces bearing nano[195] and micro[196] topographical features such as pillars, wells, and grooves. Among different topographical features, pillars supported the round morphology and aggregation of cells.[195,197] Even though, the effect of nano and micropillars on the morphology and differentiation of stem cells has been widely explored,[44,111,198] the manipulation of cell aggregates with the aid of pillar dimensions has not been broadly investigated.

In this work, the poly(HEMA/DMAEMA/TEGDMA) (DMAEMA = N,N-(dimethylaminoethyl)-methacrylate and TEGDMA = tetraethylene glycol dimethacrylate) hydrogels patterned with hexagonal arrays of micropillars with a diameter (d) of 1 μm, pitch (d_{int}) of 3 μm, and a height (h) of either 2 μm or 6 μm were utilized to induce aggregation of human mesenchymal stem cells (hMSCs), within 24 h after seeding the cells. (See Chapter 2 for the fabrication of surface-patterned poly(HEMA/DMEMA/TEGDMA) hydrogel.) Moreover, the use of the height of micropillars to control the number and size of the cell aggregates was studied. The largest cell aggregates were formed on hydrogels bearing 6 μm pillars whereas the 2 μm pillars yielded the highest number of cell aggregates. Furthermore, the differentiation studies revealed that the hMSCs are capable of differentiating along adipogenic and chondrogenic pathways on the

poly(HEMA/DMAEMA/TEGDMA) hydrogel. Overall, this work demonstrates that surface-patterned poly(HEMA/DMAEMA/TEGDMA) hydrogel has potential applications as a scaffolding material since the micropillars can be used to manipulate the number and size of hMSC aggregates while improving the cell attachment properties of the material.

4.2. Experimental

4.2.1. Materials

SYLGARD™ 184 silicone elastomer (PDMS) was purchased from Dow Corning (Midland, MI). Bone-marrow-derived human mesenchymal stem cells (hMSCs) at passage 2 were purchased from the Institute for Regenerative Medicine, Texas A&M University, College of Medicine (College Station, TX). Minimum essential medium α (α-MEM) and ethylene glycol were obtained from Thermo Fisher Scientific (Waltham, MA). Fetal bovine serum–premium select (FBS) and isopropyl alcohol 99% were purchased from Atlanta Biologicals (Flowery Branch, GA) and Pharmco-AAPER (Shelbyville, KY), respectively. HEMA, DMAEMA, TEGDMA, 2-hydroxy-2-methylpropiophenone, albumin from bovine serum (BSA), 2-phospho-L-ascorbic acid trisodium salt, dexamethasone, β-glycerol phosphate disodium salt pentahydrate, insulin (human recombinant), isobutylmethylxanthine, Oil Red O, goat serum donor herd, Pronase E, Fluorescein isothiocyanate (FITC)-conjugated goat anti-mouse Immunoglobulin secondary antibody (anti-mouse IgG (whole molecule)-FITC) produced in goat, 10% neutral buffered formalin solution, Triton® X-100, Tween® 20, and agarose low gelling temperature were purchased from Sigma-Aldrich (St. Louis, MO). Anti-collagen type II primary antibody (COLII) was obtained from Developmental Studies Hybridoma Bank, University of Iowa (Iowa City, IA) and mouse preimmune IgG was from Vector Laboratories (Burlingame, CA). Gibco™ Penicillin Streptomycin (Pen Strep), Trypsin-EDTA (0.05%), Dulbecco's phosphate buffered saline (PBS) powder, Molecular Probes™ Rhodamine phalloidin, and Invitrogen™ 4′,6-diamidino-2-phenylindole (DAPI) were purchased from Life Technologies (Grand Island, NY). Transforming

growth factor beta 1 (TGF β1) human recombinant (HEK) and Corning ITS + Premix universal culture supplement were obtained, respectively, from PromoCell GmbH (Heidelberg, Germany) and Corning Inc. (Corning, NY).

4.2.2. Fabrication of surface-patterned poly(HEMA/DMAEMA/TEGDMA) hydrogels

The hydrogel samples bearing surface patterns of micropillars of different heights (2 μm and 6 μm) were prepared using PDMS molds – the negative replicas of original surface-patterned Si wafers. (Generation of the surface pattern on Si wafer was described previously in chapter 2). The monomers HEMA, DMAEMA, TEGDMA were mixed with the initiator 2-hydroxy-2-methylpropiophenone in a ratio of 38:2:1:1 mol/mol respectively, and the solvent mixture containing water and ethylene glycol (1:1 mol/mol). The composition of the hydrogel was adapted from work published by You et al.[68] After mixing thoroughly, the mixture was poured over the PDMS molds, immobilized onto Petri dishes, and cured with 365 nm UV light using a Dymax™ light curing system (225 mW/cm^2, Model 5000 Flood) for 90 s. After cooling to room temperature, the polymer-PDMS composites were submerged in PBS and allowed to swell until delaminated from the molds. The edges of the hydrogels were mechanically released to facilitate the delamination process. After delamination, the hydrogels were stored in PBS until used for further experiments.

The unpatterned or *blank* hydrogel samples were generated from the same methodology except for using a piece of a bare silicon wafer in preparation of PDMS molds. The PDMS molds were prepared as mentioned elsewhere.[44,66,67] Briefly, Sylgard™ 184 silicone elastomer and curing agent were mixed thoroughly in a ratio of 10:1 wt. % and poured over the Si wafer, degassed in a vacuum to remove air bubbles, and thermally cured in an oven (Barnstead™) at 75 °C for 5 – 6 h.

4.2.3. Stem cell studies on surface-patterned poly(HEMA/DMAEMA/TEGDMA) hydrogels

4.2.3.1. Preparation of hydrogels and cells

After fabrication, the *blank* and surface-patterned hydrogel samples were sterilized by autoclaving in PBS (30 min, 121 °C). The disks were punched from the sterile hydrogel samples with a diameter of 5 mm or 10 mm to fit into wells of 24 and 96-well plates, respectively, using cork borers, under sterile conditions. Prior to seeding the cells, the hydrogel disks were placed in the well plates and pre-incubated in complete culture media (α-MEM, supplemented with 16.7% FBS, and 1% Pen Strep (v/v)) overnight at 37 °C and 5% CO_2 in a CO_2 supplied humidified incubator (Symphony 5.3 A, VWR, Radnor, PA). Each cell experiment was performed in triplicates unless otherwise mentioned.

Frozen hMSCs (5×10^5 cells/mL, 0.5 mL) at passage 3 were recovered and expanded in a T125 flask containing complete culture medium at 37 °C and 5% CO_2. At 70% confluency, the cells were subcultured in T175 flasks containing complete culture media to produce enough cells for further studies. For subculturing, the cells were detached from T125 tissue culture flask by incubating with trypsin-EDTA for 2 min at 37 °C and 5% CO_2. Complete culture media (double the volume of trypsin-EDTA) was added to deactivate trypsin and the cell suspension was centrifuged at 2000 rpm for 2 min. The cell pellet was dispersed in new growth media, mixed with Trypan blue (Thermo Fisher Scientific) and the cell count was obtained using a Countess® automated cell counter (Thermo Fisher Scientific). The cells were divided into T175 flasks and cultured at 37 °C and 5% CO_2 in the humidified incubator until 70% confluent, to produce enough cells for the experiments. All cell experiments were performed with cells at passage 4. Statistical analysis of cell experiments was determined by ANOVA (single factor at $p < 0.05$), unless otherwise mentioned.

4.2.3.2. The effect of surface pattern and seeding density on morphology of stem cells

The morphology of hMSCs on poly(HEMA/DMAEMA/TEGDMA) hydrogels was evaluated based on the micropillar pattern and seeding density. At 70% confluency, the cells were detached, centrifuged, and counted as mentioned in the subculturing process. The spent media was aspirated from the wells containing the hydrogels and new media was added to each well. Then the samples were seeded with hMSCs (seeding density = 1.0×10^4 cells/cm^2). Control experiments were carried out in the same way except for culturing cells on blank wells without hydrogel disks (tissue culture plastic). After 24 h, the cells were fixed with 10% neutral buffered formalin for 30 min, permeabilized with Triton® X-100 in 0.1% BSA in PBS for 15 min, and stained with Rhodamine phalloidin (1:1000 dilution in 0.1% BSA and 0.1% Tween® 20 in PBS) for 2 h at room temperature in the dark. Each step was followed by two rinsing steps in 0.1% BSA in PBS. The nuclei were counterstained with DAPI (1:5000 dilution in 0.1% BSA and 0.1% Tween® 20 in PBS) for 5 min at room temperature in the dark. Finally, the samples were washed with PBS and imaged using an Olympus-IX83 inverted microscope.

To evaluate the effect of seeding density on morphology, hMSCs were seeded on hydrogels, patterned with 2 µm pillars, at different seeding densities: 7.8×10^4 cells/cm^2, 1.6×10^5 cells/cm^2, 3.1×10^5 cells/cm^2, and 1.6×10^6 cells/cm^2. After 72 h of culture, the cells were fixed and stained with Rhodamine phalloidin and DAPI, and imaged from RFP and DAPI channels.

4.2.3.3. Evaluation of attachment of hMSCs onto hydrogels and effect of surface pattern

The hMSCs were cultured on the *blank* and surface-patterned hydrogels as previously mentioned. The seeding density was 3.0×10^4 cells/cm^2. The attachment and formation of cell aggregates were analyzed after 24 h of culture by fixing and staining the cells with DAPI. The DAPI-stained images were analyzed from ImageJ 1.47t software (Wayne Rasband, National Institutes of Health, USA) to quantify the cells present on the hydrogel surface. The sliding paraboloid method

was used to subtract background and the rolling ball radius was set to 50.0 pixels. After background subtraction, integrated density was measured for individual cell aggregates. The integrated density of an aggregate was divided from that of a single nucleus to quantify the number of nuclei in an aggregate. Similarly, the number of total nuclei was determined from the same method except for taking the nuclei present in the entire image into account.

Cell aggregates are loosely attached to the surface due to the hydrophilicity of the hydrogel and can be easily washed away during media exchange. To evaluate the loss of cell aggregates from media exchange, media was replaced either by aliquots (Method A) or completely (Method B) using a micropipette (seeding density was 3.1×10^4 cells/cm^2 and the cells were cultured for five days by refreshing media every other day). In Method A, a portion of spent media (250 µL) was removed and replaced with the same volume of new media ensuring that the hydrogel surface was covered throughout the entire time. The process was repeated 3 - 4 times to make sure that the spent media was replaced with sufficient new media. In Method B, the spent media was completely (1 mL at once) removed before adding new media. Bright-field images were taken before each media change. After five days, the aggregates were counted on each sample and compared to the number of aggregates present at day 1. Two methods were statistically compared using a Student T-test ($p < 0.05$).

4.2.4. Differentiation of hMSCs on poly(HEMA/DMAEMA/TEGDMA) hydrogels

4.2.4.1. Adipogenic differentiation

The hMSCs at passage 4 were seeded on hydrogel substrates at three different seeding densities (3.1×10^4 cells/cm^2, 1.6×10^5 cells/cm^2, and 2.6×10^6 cells/cm^2). After two days, the spent medium was replaced with either complete culture medium or adipogenic differentiation medium. The adipogenic differentiation medium consisted of α-MEM, 10% FBS, 1% Pen Strep, 1 µM dexamethasone, 0.5 mM isobutylmethylxanthine, and 1 µg/mL insulin. The media was refreshed every other day and the experiments were carried out for two weeks. For the control experiments, the hMSCs were cultured on blank wells without hydrogel disks.

After two weeks, the cells were fixed in 10% neutral buffered formalin for 2 h at room temperature and stained with Oil Red O according to the manufacturer's instructions to assess adipogenic differentiation. Briefly, 0.3% Oil Red O stock solution, prepared in isopropanol, was diluted with distilled water to generate a 0.18% working solution. The fixed cells were incubated in 60% isopropanol for 5 min followed by staining with the Oil Red O solution for 15 min at room temperature. Then the cells were washed with distilled water until the water became clear. Bright-field images of each sample were obtained from the Olympus-IX83 inverted microscope.

4.2.4.2. Chondrogenic differentiation

For chondrogenic differentiation experiments, hMSCs at passage 4 were seeded on hydrogel substrates at a seeding density of 1.6×10^5 cells/cm^2. The cells were allowed to grow for two days and the spent media was replaced with either complete culture medium or chondrogenic differentiation medium. The chondrogenic differentiation medium contained α-MEM provided with high glucose (4.5 g/L), 10% FBS, 1% Pen Strep, 1×10^{-7} M dexamethasone, 10% ITS + Premix tissue culture supplement, 50 µg/mL 2-phospho-L-ascorbic acid, and 10 ng/mL TGF β1. TGF β1 factor and 2-phospho-L-ascorbic acid were added to a mixture of α-MEM, glucose, FBS,

Pen Strep, dexamethasone, and ITS + Premix tissue culture supplement prior to use. The cells were incubated at 37 °C and 5% CO_2 for two weeks and the media was refreshed every other day.

For the positive control experiments, hMSC spheroids were formed as previously reported.[199] A 2% solution of agarose (in DMEM, 150 µL) was poured into the wells of a 96-well plate. After solidification of the agarose, cells were seeded at a density of 1.6×10^4 cells/mm^2 and incubated at 37 °C and 5% CO_2 for 24 h to form the spheroids. Then, the cell spheroids were transferred to centrifuge tubes containing either chondrogenic differentiation media or normal culture media and incubated at 37 °C and 5% CO_2 for two weeks. For the negative control experiments, the cells were seeded in wells without hydrogel disks for the same time period in either chondrogenic differentiation medium or normal culture medium.

Chondrogenic differentiation of the cells was confirmed by Alcian blue staining and immunostaining experiments. At the end of the experiment, the cells were fixed with 10% neutral buffered formalin for 2 h and washed with DI water. Then, the samples were incubated in the Alcian blue staining solution, prepared in 3% acetic acid solution (pH 2.5), for 4 h in the dark at room temperature. The samples were washed with the destaining solution (3% acetic acid) thrice. After each wash, the samples were left in DI water for 20 min and finally stored in PBS. Bright-field images of each sample were obtained from the Olympus-IX83 inverted microscope.

For immunostaining experiments, the cells were fixed and then digested in Pronase E solution for 20 min for epitope unmasking. After the Pronase E digestion, the cells were permeabilized with 0.1% Triton® X-100 in PBS for 15 min, rinsed with PBS, followed by incubation in 10% goat serum in PBS for 1 h. Then the samples were incubated in primary antibody solutions (anti-collagen type II primary antibody solution (COLII), 1:10 dilution in 1% goat serum or IgG, 1:2000 dilution in 1% goat serum) for 3 h at room temperature. After rinsing with PBS twice, the

samples were incubated in the secondary antibody (FITC-conjugated goat anti-mouse IgG) solution (1:50 dilution) in PBS with 0.05% Tween® 20 for 2 h at room temperature. The samples were washed with PBS three times, counterstained with DAPI for 5 min, and imaged by the Olympus-IX83 inverted microscope using GFP and DAPI channels.

4.2.5. Degradation of poly(HEMA/DMAEMA/TEGDMA) hydrogel

The degradation of the fabricated hydrogel under physiological conditions was evaluated for 8 weeks. After fabrication, the *blank* hydrogel samples were dried in a vacuum desiccator to a constant weight (w_1). Then the samples were immersed in PBS and incubated at 37 °C and 5% CO_2. The samples were removed from PBS on a weekly basis and dried in a vacuum desiccator to a constant weight (w_2). The percentage (%) weight loss was determined by the following equation:

$$\%\, weight\ loss = \frac{(w_1 - w_2)}{w_1} \times 100 \qquad \textbf{(4-1)}$$

4.2.6. Wettability of poly(HEMA/DMAEMA/TEGDMA) hydrogel

The wettability of *blank* and surface-patterned hydrogels was evaluated by measuring the water contact angle. Prior to contact angle measurements, the *blank* hydrogels were dried by several methods: oven-dried at 120 °C overnight, dried in a vacuum desiccator for 3 days, or blot-dried with a paper tissue, just before the measurements, to remove the excess solution on the surface [The samples were stored in PBS after fabrication and rinsed with DI water before drying.] The patterned hydrogel samples were also blot-dried with paper tissues to remove moisture on the surface [The patterned samples were not dried in the oven or desiccator since the drying process may result in the collapse of the micropillars.]

The contact angle was measured by the sessile drop method using a laboratory-made contact angle instrument which is equipped with a movable stage to hold the sample, a micropipette to deliver a water droplet onto the surface of the sample, and a high-resolution Proscope camera which can record 15 fps at a 640 × 480 resolution.[200] Images of deionized water droplets (5 μL) placed on at least four different spots on the top surface of a single hydrogel sample were used for contact angle analysis. Three samples were tested for each type of hydrogel. The contact angle was analyzed from low bond axisymmetric drop shape analysis (LB-ADSA) method of the drop analysis plug-in of ImageJ 1.47t software.

4.3. Results and discussion

4.3.1. Analysis of morphology of hMSCs on hydrogel samples

Poly(HEMA/DMAEMA/TEGDMA) hydrogels bearing hexagonal arrays of microscale pillars on the surface were fabricated using UV initiated radical polymerization and soft-lithography technique, as mentioned in the experimental section. The micropillar patterns have following dimensions: diameter (d) = 1 μm, height (h) = 2 μm or 6 μm, and interpillar spacing (d_{int}) = 3 μm. The behavior of hMSCs on the fabricated material was investigated by seeding cells on both *blank* or unpatterned and surface-patterned hydrogels.

The morphology of the hMSCs cultured on hydrogels was analyzed 24 h after seeding the cells. The fluorescent images in **Figure 4-1** depict an elongated morphology of cells on both *blank* and patterned hydrogels in contrast to the spread and flat morphology observed on the tissue culture plastic. The hMSCs cultured on hydrogels have small cell bodies compared to the tissue culture plastic; however, irrespective of the surface pattern, the cell bodies are relatively similar in size on all hydrogels. Moreover, the hMSCs grew flat lamellipodia-like extensions on the *blank* hydrogel whereas, on the patterned surfaces, thin filopodia-like structures were produced

(the arrowheads point out the flat (**Figure 4-1(a)**) and thin (**Figure 4-1(b)** and (**Figure 4-1(c)**) protrusions). The extensions show little or no difference in branching on the surface-patterned hydrogels in comparison to the *blank* hydrogels. Nevertheless, on the polystyrene surface, the cells formed actin stress fibers whereas on the hydrogel surface the actin stress fibers were not prominent.

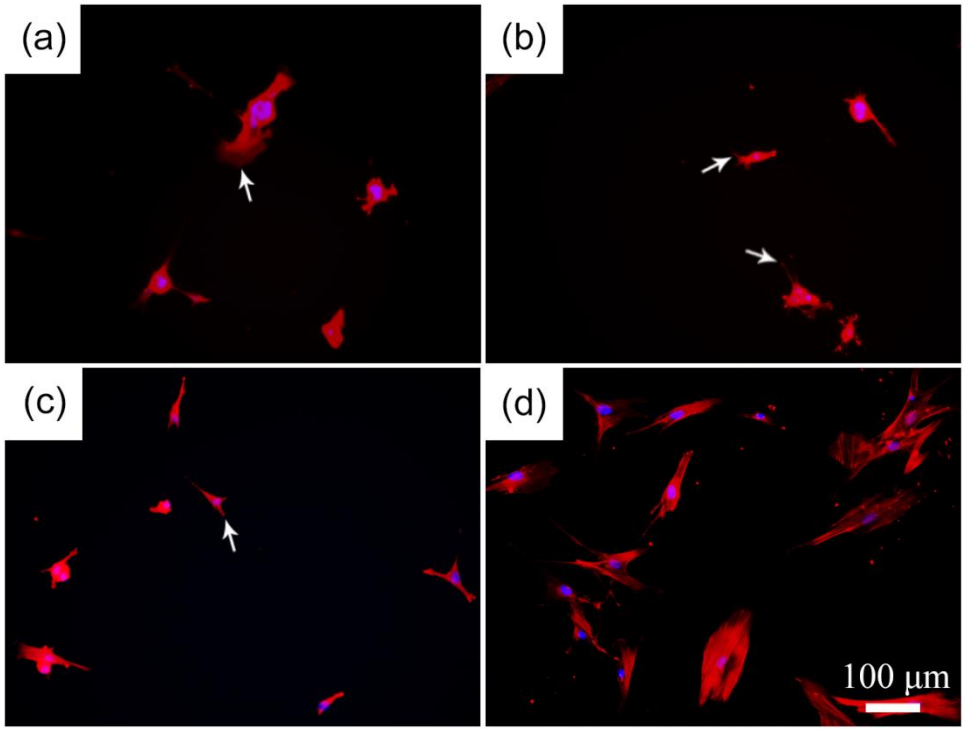

Figure 4-1. Fluorescent images (10×, imaged through RFP and DAPI channels) of hMSCs on hydrogels with (a) no pattern (*blank*), (b) 2 µm pillars, (c) 6 µm pillars, and (d) tissue culture plastic; the actin filaments and nuclei were stained with Rhodamine phalloidin and DAPI, respectively. The arrows indicate the spread and thin extensions grown from the cell bodies.

Interestingly, on the hydrogel samples, the majority of the cells tend to aggregate and form clusters (**Figure 4-1(a)-(c)**). The formation of cell aggregates can be attributed to the cell-cell interactions stronger than the cell-surface interactions.[138] **Figure 4-2** shows an enlarged image of a cell aggregate on a hydrogel sample with 2 µm pillars and highly branched-extensions grown

from the aggregate. In contrast, such extensions were hardly found on the *blank* hydrogels. Compared to the hydrogels patterned with 2 μm pillars, the cell aggregates produced more extensions on the samples with 6 μm pillars. The micropillars may serve as anchoring points to the cells, which may facilitate the attachment of the cell aggregates onto the hydrogel (**Figure 4-2(a), Figure 4-3(a)** and **Figure 4-3(b)**).

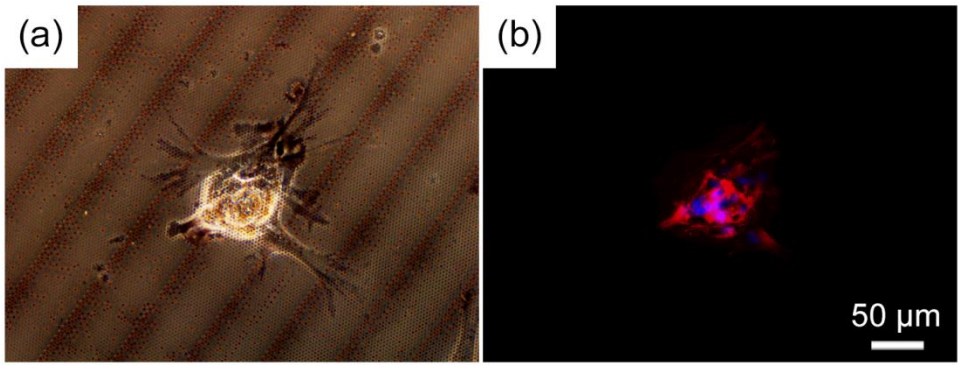

Figure 4-2. (a) Bright-field and (b) fluorescent images of a cell aggregate on a hydrogel surface bearing 2 μm pillars; actin and nuclei were stained with Rhodamine phalloidin and DAPI, respectively.

SEM images in **Figure 4-3** show that hMSCs cultured on the hydrogel surface tend to form either elongated (**Figure 4-3(a)**) or spheroid (**Figure 4-3(b)**) aggregates. Elongated cell aggregates formed thin, hair-like protrusions, which are few micrometers long whereas spheroid aggregates produced thin, short protrusions. In contrast to the cells attached to the hydrogels bearing micropillars, on the *blank* hydrogels, cells produced large and spread cell bodies (**Figure 4-3(c)**) and flat, branched extensions.

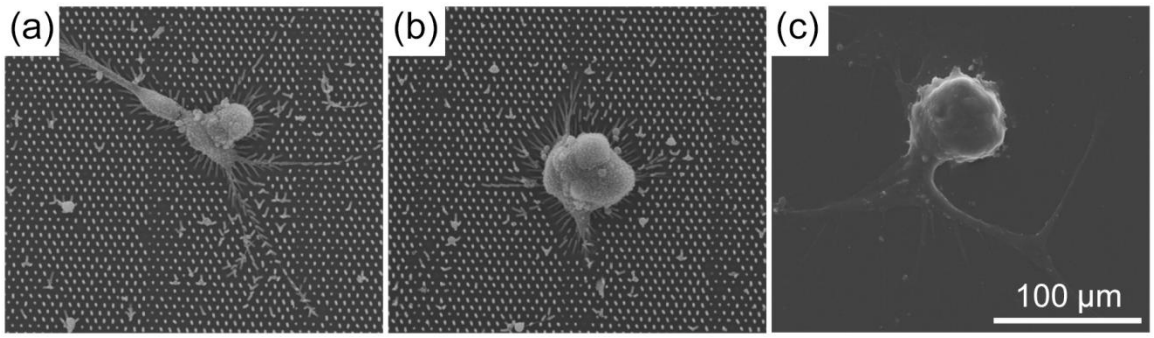

Figure 4-3. The SEM images of hMSCs aggregates on hydrogel samples bearing (a) 2 µm pillars, (b) 6 µm pillars and (c) no pillars (*blank*)

The effect of seeding density on the formation of cell aggregates was investigated using the following seeding densities: 7.8×10^4 cells/cm^2, 1.6×10^5 cells/cm^2, 3.1×10^5 cells/cm^2, and 1.6×10^6 cells/cm^2. At the low seeding density more single cells were observed; as the seeding density increased the number of single cells decreased and the formation of cell aggregates was prominent (**Figure 4-4**).

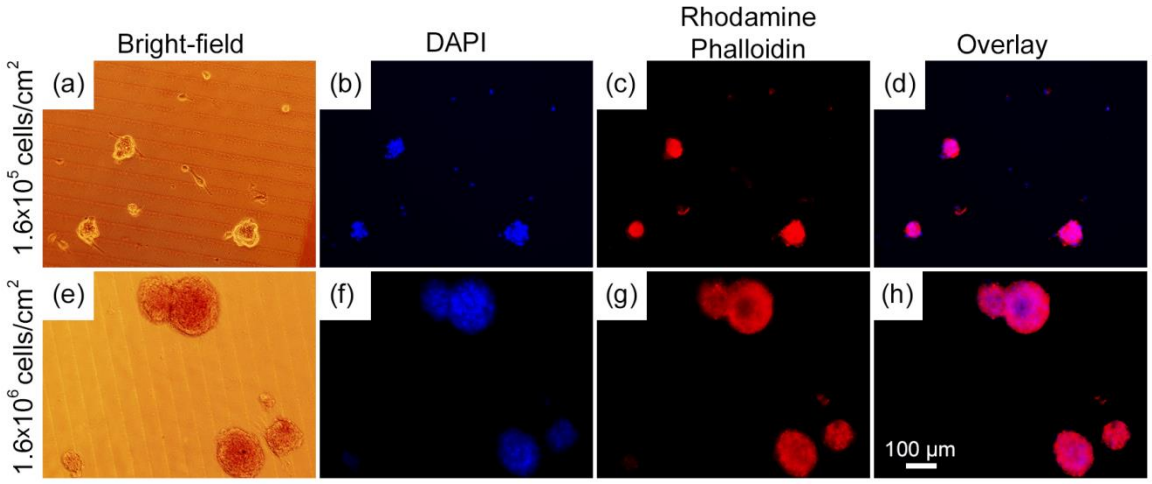

Figure 4-4. Morphology of hMSCs cultured on poly(HEMA/DMAEMA/TEGDMA) hydrogel samples at (a-d) low seeding density (1.6×10^5 cells/cm^2) and (e-h) high seeding density (1.6×10^6 cells/cm^2). At low seeding density single cells are observed on the hydrogels, but at high seeding densities, the aggregates are prominent.

The effect of surface pattern toward the formation of cell aggregates was evaluated from the DAPI-stained images of hMSCs cultured for 24 h on hydrogels. The intensity corresponding to the nuclei in a cell aggregate was divided by the intensity of the nucleus of a single cell to determine the number of nuclei (or cells) in an aggregate (x). Based on the number of nuclei in an aggregate, the cell aggregates were categorized into three classes: small, intermediate, and large. A small cell aggregate had less than 10 nuclei while a large one had more than 100 nuclei. An intermediate cell aggregate had between 10 to 100 nuclei.

As demonstrated by the graph in **Figure 4-5(a)** there is a noticeable difference in the number of small and large cell aggregates, depending on the surface pattern. On the *blank* hydrogels, the cells tend to form small and intermediate aggregates whereas on the surface-patterned hydrogels formation of large cell aggregates is prominent. Specifically, the formation of small aggregates was promoted by micropillars of 2 μm height while the 6 μm pillars facilitated the formation of large cell aggregates. Interestingly, there was no statistically significant effect from the micropillars for the formation of intermediate cell aggregates (10 to 100 nuclei) although the number of intermediate aggregates increased on the patterned hydrogels. The graph in **Figure 4-5(b)** shows the average number of cells attached to each type of hydrogel and indicates that the attachment of hMSCs was significantly enhanced by the micropillars on the hydrogel surface. Here, the total number of nuclei seen in the DAPI-stained images, which includes nuclei of both single cells and aggregates, was considered in the quantification.

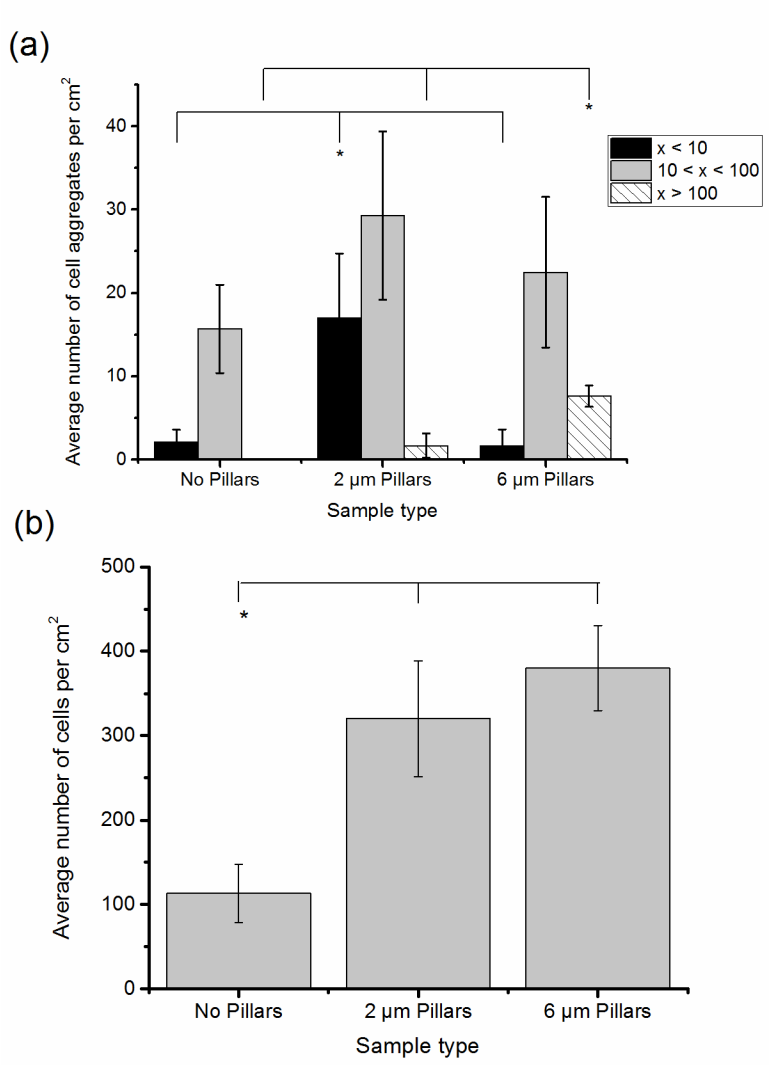

Figure 4-5. Attachment of hMSCs onto hydrogel samples after 24 h of seeding cells; (a) average number of cell aggregates (x is the number of nuclei in an aggregate) and (b) average number of cells on *blank* and surface-patterned hydrogel samples. *indicates the statistical significance between the groups ($p < 0.05$).

Several days of cell culture may cause the loss of cell aggregates during media exchanges. The loss of cell aggregates was evaluated by either changing media in aliquots (Method A), to ensure that the hydrogel surface was covered with media during the entire time, or completely (Method B). The comparison between the two methods showed that replacing the media in aliquots

(Method A) facilitates the retention of cell aggregates on hydrogels after five days of culture; however, the effect was statistically significant only on the hydrogels with 2 µm pillars (**Figure 4-6**). On the hydrogels bearing 6 µm pillars, the number of aggregates neither increased nor decreased considerably during the five days when the media was exchanged in aliquots. In contrast, the number of aggregates was increased on the *blank* hydrogels after five days. The complete removal of spent media (Method B) caused loss of cell aggregates on all hydrogels, but the effect was not prominent on the *blank* as compared to the patterned hydrogels. Moreover, both methods had a similar effect on the hydrogels patterned with 6 µm pillars (since there is no statistically significant difference at $p < 0.05$) although the retention of cell aggregates was slightly improved upon changing media in aliquots. Overall, the results suggest that the retention of cell aggregates on the poly(HEMA/DMAEMA/TEGDMA) hydrogel can be enhanced by slow and less-disturbed media changes. The key point is that one must ensure that the surface is covered with media during the entire media exchange and to minimize any disturbances.

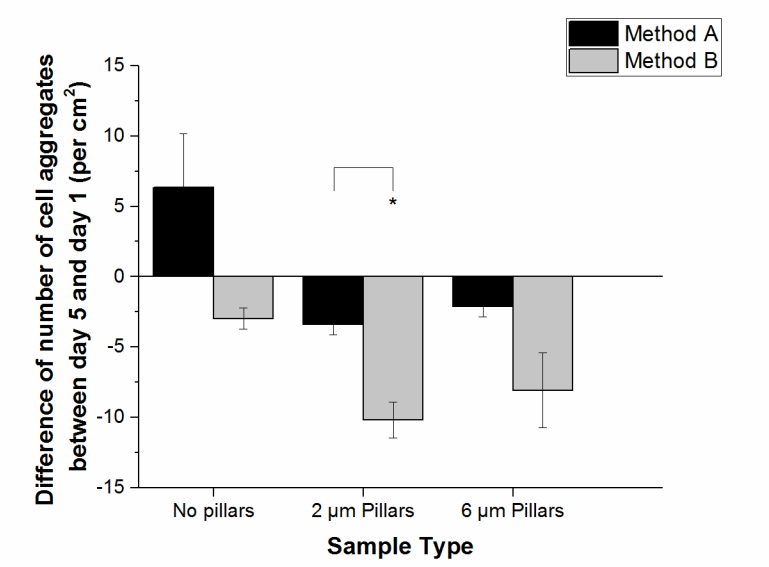

Figure 4-6. The effect of media change on retention of cell aggregates on hydrogel samples; Method A – media was changed in aliquots so that the hydrogel surface was covered by media entire time, Method B – spent media was completely removed before adding new media.

4.3.2. Differentiation of hMSCs on poly(HEMA/DMAEMA/TEGDMA) hydrogels

Here, the differentiation of hMSCs along chondrogenic and adipogenic differentiation pathways was investigated. Formation of cell aggregates on the poly(HEMA/DMAEMA/TEGDMA) hydrogel motivated the differentiation studies along chondrogenic lineage whereas the soft nature of the fabricated hydrogel inspired the adipogenic differentiation studies.

4.3.2.1. Adipogenic differentiation

Adipogenic differentiation was evaluated by staining cells with Oil Red O after two weeks of culture (**Figure 4-7**). Both single cells and aggregates cultured with adipogenic supplements showed positive staining for Oil Red O indicating adipogenic differentiation. The oil droplets stained with Oil Red O were clearly visible in single cells on hydrogels (**Figure 4-7(b)**), which were similar to the positive control experiment (**Figure 4-7(d)**). Individual oil droplets could not be imaged directly in the aggregates due to the high intensity caused by the large number of cells in an aggregate. Nevertheless, the dark red color of the cell aggregates (**Figure 4-7(c)**) was considered a positive indicator for adipogenic differentiation. The single cells on the hydrogels, which were treated with normal culture medium, stained very light red color showing little or no adipogenic differentiation. In the negative control experiments, the cells did not produce oil droplets as indicated by the lack of staining with Oil Red O (**Figure 4-7(h)**).

The effect of seeding density toward adipogenic differentiation of hMSCs was also studied. The cell aggregates were stained positively for adipogenesis, regardless of the seeding density. Interestingly, the large cell aggregates formed on the hydrogel samples with 6 μm pillars stained a dark red color even in the absence of adipogenic supplements (**Figure 4-8**). The red color appeared on the edges of the cell aggregates can be an indication of positive adipogenic differentiation and the black-brown color in the center is due to the poor penetration of light through the aggregate caused by the thickness of the aggregate.

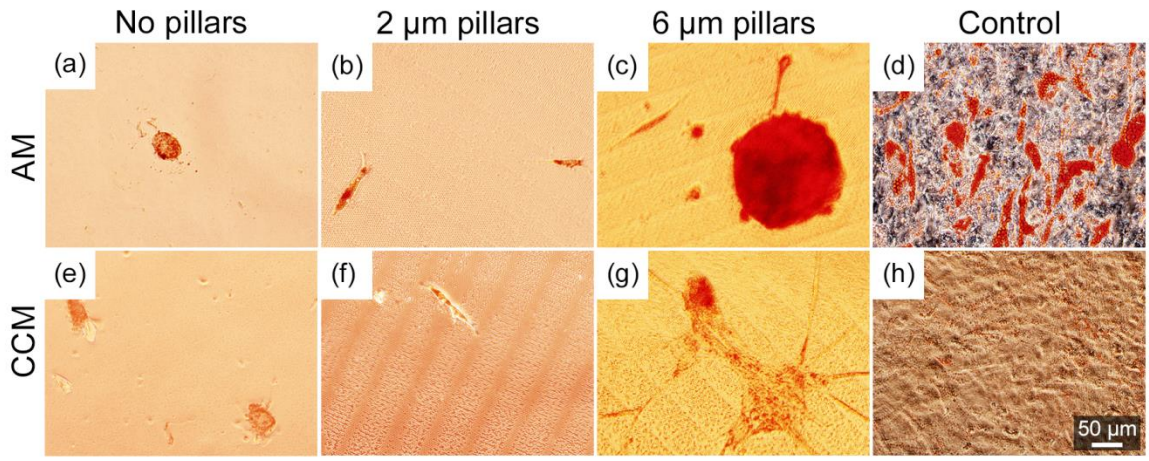

Figure 4-7. Light microscopy images of hMSCs stained with Oil Red O after two weeks of culture on (a, e) *blank* (unpatterned) hydrogels, (b, f) hydrogels patterned with 2 μm pillars, (c, g) hydrogels patterned with 6 μm pillars, and (d, h) control experiment (polystyrene/tissue culture plastic). AM = Adipogenic differentiation medium, CCM = complete culture medium

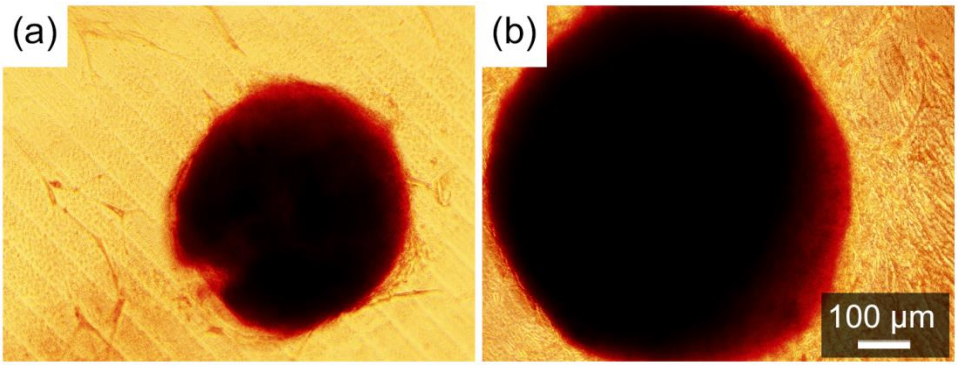

Figure 4-8. Light microscopy images of Oil Red O-stained, large cell aggregates formed on hydrogel samples bearing 6 μm pillars treated with normal culture medium at different seeding densities (a) 1.6×10^5 cells/cm^2 and (b) 2.6×10^5 cells/cm^2.

4.3.2.2. Chondrogenic differentiation

After two weeks of culture, chondrogenic differentiation of hMSCs was characterized by two methods: Alcian blue staining and immunostaining. The light microscopy (bright-field) images in **Figure 4-9** show the cell aggregates stained blue in color, a positive indicator of chondrogenic differentiation. Moreover, the cell aggregates formed on the hydrogels show the positive staining even in the absence of external growth factors (**Figure 4-9(e)-(g)**). Under both treatments, the cell aggregates were positively stained with Alcian blue, but not the single cells and the effect of pillar height was not appear to be prominent. In contrast, no positive staining was observed in the cells grown on tissue culture plastic in both chondrogenic and complete culture media (**Figure 4-9(d)** and **Figure 4-9(h)**). After 10 days of treatment with chondrogenic differentiation media, the cells on the tissue culture plastic started to detach from the wells which reduced the total number of cells (**Figure 4-9(d)**). This is in line with the observation made by Glennon-Alty and coworkers where the cells at the edge of the substrate detached and retracted to the center to form multilayers.[201]

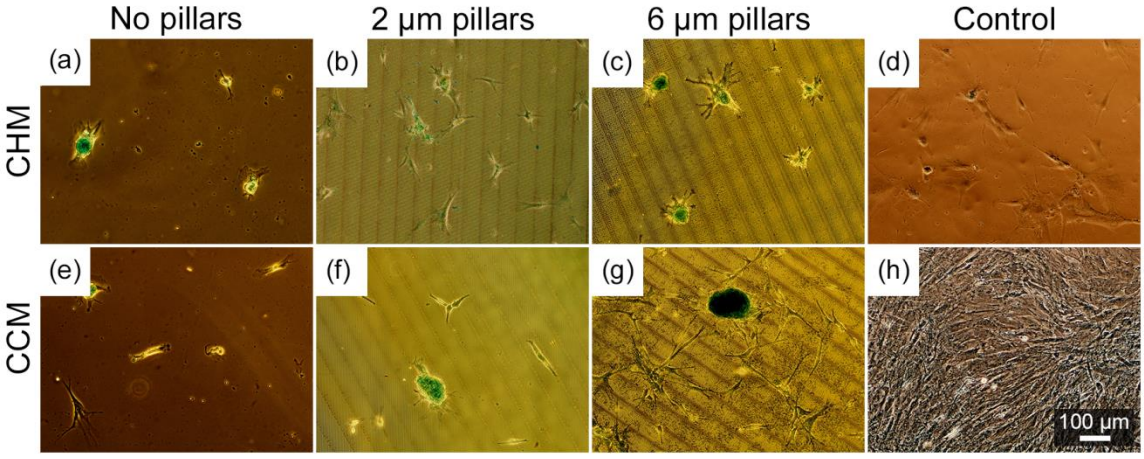

Figure 4-9. Light microscopy images of hMSCs stained with Alcian blue after two weeks of culture on (a, e) *blank* (unpatterned) hydrogels, (b, f) hydrogels patterned with 2 µm pillars, (c, g) hydrogels patterned with 6 µm pillars, and (d, h) control experiment (polystyrene/tissue culture plastic). CHM = Chondrogenic differentiation medium, CCM = complete culture medium

Immunostaining for type II collagen, the major extracellular component in cartilage,[167] was performed to further confirm the chondrogenic differentiation of hMSCs on poly(HEMA/DMAEMA/TEGDMA) hydrogel. Data obtained from Alcian blue staining and attachment study together suggest that the hydrogels patterned with 6 µm pillars are the most suitable for chondrogenic differentiation. [The former showed that the micropillar height did not significantly affect on differentiation of cells as long as aggregates were formed and the latter confirmed that hydrogels patterned with 6 µm pillars yielded large cell aggregates.] Since large spheres of hMSCs resulted a higher expression of chondrogenic markers, as observed by Lu et al.[202], hydrogels with 6 µm pillars were chosen for the immunostaining experiments. As shown by the fluorescence images in **Figure 4-10(c)** and **Figure 4-10(g)**, type II collagen was detected in the cell aggregates in both media. Unlike the chondrogenic differentiation medium which induces the differentiation of cells, the complete culture medium supports the continuous growth of cells; therefore, large cell aggregate can be seen on the hydrogel samples treated with normal culture medium. Similar to the cell aggregates on the hydrogels, the hMSC spheroids produced by the agarose well method were positively stained for type II collagen in both media. Type II collagen was not detected in the cells grown on tissue culture plastic (negative control).

Generally, *in vitro* chondrogenesis is performed in serum-free media mainly because of the poorly defined composition of serum and undesirable effects introduced by serum on differentiation experiments, which are highly dependent on external growth factors.[203-205] On the other hand, serum is essential for attachment and growth of cells.[205] In this study, the experiments performed in the serum-free chondrogenic medium failed due to the loss of cell aggregates after few days of culture (**Figure 4-11**). Since poly(HEMA/DMAEMA/TEGDMA) hydrogel itself has low cell attachment properties the FBS is crucial for maintaining the desired cell attachment. Therefore, the chondrogenic medium used for the above experiments required FBS.

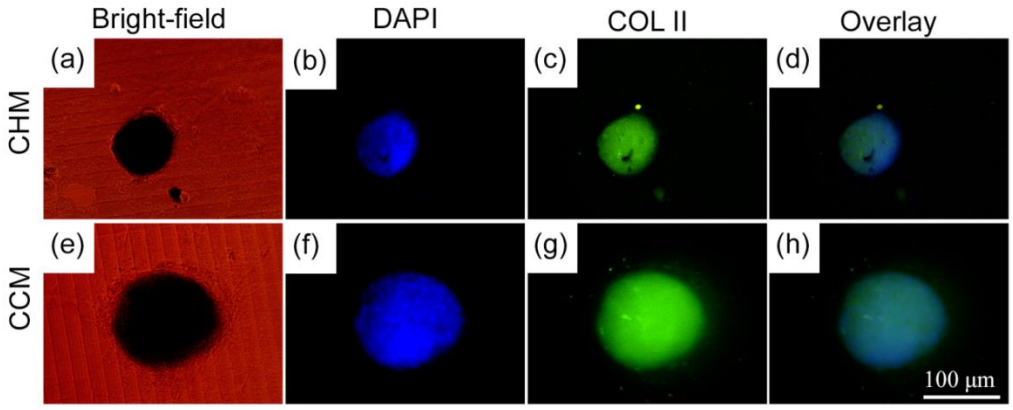

Figure 4-10. Light microscopy images of cell aggregates on hydrogels bearing 6 µm pillars: (a, e) bright-field, (b, f) DAPI, (c, g) immunostained for type II collagen (COL II), and (d, f) overlay of DAPI and COL II images. CHM = Chondrogenic differentiation medium, CCM = complete culture medium

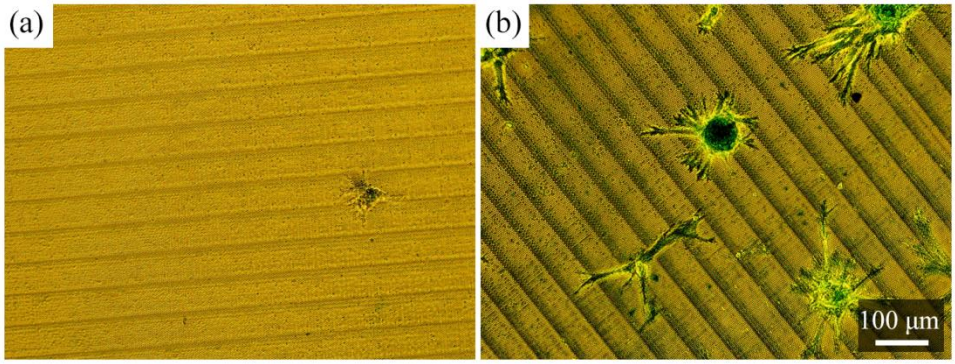

Figure 4-11. Light microscopy images of hMSCs cultured in chondrogenic differentiation medium (a) without FBS (serum-free) and (b) with FBS; the cells were stained with Alcian blue.

The immunostaining experiments were carried out in 24-well plates (diameter of hydrogel disks = 10 mm) since the initial experiments performed in 96-well plates (diameter of hydrogel disks = 5 mm) were unsuccessful due to the formation of one or two large aggregates instead of several small and intermediate aggregates. Most of these cell aggregates were loosely attached and washed away during media changes.

As seen in both adipogenic and chondrogenic differentiation experiments, the hMSCs differentiated along both lineages even in the absence of externally provided growth factors. Differentiation of hMSCs in the normal culture medium can be attributed to the endogenous production of growth factors by the cells and the modulation of differentiation pathway by the properties of the substrate, i.e. stiffness and surface chemistry.[201,206-208] On the other hand, Park, et al. reported that surface properties alone are unable to promote the differentiation along a specific lineage, especially to preferentially select between chondrogenesis and adipogenesis; thus the external growth factors are necessary.[209]

4.3.3. Degradation of poly(HEMA/DMAEMA/TEGDMA) hydrogel

The degradation study shows that the poly(HEMA/DMAEMA/TEGDMA) hydrogel is very stable at the physiological conditions. The experiment was performed for 8 weeks and the hydrogels showed only a 2.4% weight loss after 8 weeks of incubation in PBS at 37 °C **(Figure 4-12)**. Previous studies report that non-degradable hydrogels restrict cell spreading and promote round morphology, because the cells are incapable of degrading the polymer chains to obtain sufficient space for their spreading and movements, but the viability and proliferation of cells were not affected.[210-212] These studies suggest that, in addition to the surface chemistry, the low degradability of poly(HEMA/DMAEMA/TEGDMA) hydrogel may provide an extra support to the formation of aggregates by limiting spreading of the cells. However, introduction of biodegradable groups into the poly(HEMA/DMAEMA/TEGDMA) hydrogel, maintaining the ability to induce formation of cell aggregates, would be favorable in tissue engineering applications.

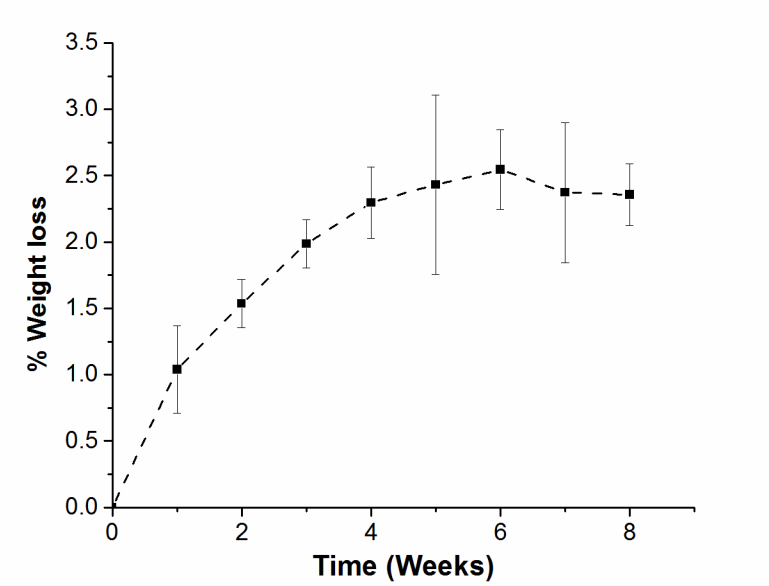

Figure 4-12. The graph of % weight loss for poly(HEMA/DMAEMA/TEGDMA) hydrogel as a function of time.

4.3.4. Wettability of poly(HEMA/DMAEMA/TEGDMA) hydrogel

The wettability of the fabricated hydrogel was determined by measuring contact angle from the sessile drop method. **Table 4-1** presents the contact angles obtained for *blank* and surface-patterned hydrogel samples. As expected, the contact angle of the hydrogel increased from ~55° (*blank*) to ~67° (2 µm pillars) and ~72° (6 µm pillars) indicating a decrease in hydrophilicity. However, drying of the samples in an oven at 120 °C completely evaporated water and the samples were completely dry; thus the surface became hydrophobic (contact angle ~95°). When the samples were blot-dried or dried in a vacuum desiccator, the contact angles were ~56° and ~57°, which might be due to the incomplete removal of water. An increase in hydrophobicity, resulting from the micropillars, supports the enhanced attachment of cells on the surface-patterned hydrogels.[28,33]

Table 4-1. Contact angle measurements of hydrogel samples subjected to various drying methods.

Hydrogel Sample	**Contact Angle (°)**
Blank (dried in a desiccator)	56.707 (±3.955)
Blank (blot-dried)	55.464 (±4.387)
2 μm pillars (blot-dried)	67.113 (±0.850)
6 μm pillars (blot-dried)	71.968 (±1.652)
Blank (oven-dried at 120 °C)	94.698 (±2.176)

4.4. Conclusions

This study shows that poly(HEMA/DMAEMA/TEGDMA) hydrogels patterned with micropillar arrays on the hydrogel surface provide excellent control over the size of the cell aggregates. Micropillars also enhance the attachment of cells to the hydrogel surface. It is noteworthy that the manipulation of morphology and size of the aggregates was achieved by physical cues without chemically modifying the hydrogel. Furthermore, this study suggests that the retention of cell aggregates can be increased by slow, less-disturbed media exchanges to ensure the hydrogel surface is covered with media during the entire time. Finally, the differentiation studies revealed that the poly(HEMA/DMAEMA/TEGDMA) hydrogel does not inhibit the differentiation of hMSCs aggregates along both adipogenic and chondrogenic lineages regardless of the presence of the external growth factors. Overall, this study demonstrates that the surface-patterned poly(HEMA/DMAEMA/TEGDMA) hydrogels can be potentially used as a scaffolding material for engineering adipose and cartilage tissues.

CHAPTER V

SUMMARY, CONCLUSIONS, AND FUTURE DIRECTIONS

In this study, a hydrogel based on 2-hydroxyethyl methacrylate (HEMA), N,N-(dimethyl-aminoethyl)methacrylate (DMAEMA), and tetraethylene glycol dimethacrylate (TEGDMA) was synthesized. The hexagonal arrays of microscale pillars with dimensions of diameter (d) = 1 μm, height (h) = 2 μm or 6 μm, and interpillar spacing (d_{int}) = 3 μm were transferred onto the surface of hydrogels using a soft-lithography technique. Here, a poly(dimethylsiloxane) (PDMS) mold was used as the intermediate stamp which had the negative of the original pattern. This study revealed that the swelling of the hydrogel until delamination was successful for transferring the micropillars onto the hydrogel, instead of the lift-off method which is generally used for demolding in soft-lithography. The fastest method for pattern transfer was found to be the immersion in 60% ethanol due to notable swelling. In deionized water and phosphate buffered saline (PBS) the swelling was insufficient to promote self-delamination; thus, the PDMS mold was immobilized onto a Petri dish and the hydrogels were mechanically released from the edges to facilitate the delamination.

The swelling of the hydrogel confined in the PDMS mold induced a curvature in the hydrogel-PDMS composite. The hydrogel itself delaminated from the PDMS mold when the angle of curvature exceeded 20 °, therefore, the angle can be used as a successful measure to predict the self-delamination of the hydrogel. Furthermore, properties such as swelling of the hydrogel in

different solvents, network parameters, solubility parameter, and mechanical properties were determined to better understand the structure and swelling behavior of the fabricated hydrogel. As well, the study was further extended to explore the temperature dependency of swelling of the hydrogel and swelling kinetics. Among the swelling solvents used in the study, 60% ethanol was found to be the best solvent for the poly(HEMA/DMAEMA/TEGDMA) hydrogel. The solubility parameter was estimated to be between 25 - 27 $MPa^{1/2}$ and the elastic modulus was ~8 MPa. The mechanism of initial absorption of solvents was likely to have more contribution from Fickian kinetics and the swelling behavior based on the temperature follows the typical trend where the swelling passes through a minimum between 40 - 50 °C.

As the poly(HEMA)-based hydrogels are well known for biological applications such as tissue engineering, the cell attachment and cytotoxicity of the fabricated hydrogel were evaluated using HeLa cells and human mesenchymal stem cells. The studies of HeLa cells demonstrated that the hydrogel is not cytotoxic and the micropillars improved the attachment of cells to the hydrogel. Furthermore, the stem cells aggregated on the poly(HEMA/DMAEMA/TEGDMA) hydrogel indicating low attachment. However, the micropillar patterns were able to improve the number of cell aggregates compared to the *blank* hydrogel. Moreover, the height of the micropillars influences the number and size of the cell aggregates as the 2 μm pillars facilitated the formation of small and intermediate cell aggregates while the 6 μm pillars supported large aggregates. The differentiation studies confirm that the adipogenic and chondrogenic differentiation of stem cells can be promoted on the hydrogel. The micropillar arrays indirectly affect the differentiation of the stem cells by controlling the formation of aggregates. Overall, the surface-patterned poly(HEMA/DMAEMA/TEGDMA) hydrogel was fabricated using the soft-lithography technique and the properties of the hydrogel were analyzed in detail to have a better understanding of the network structure and swelling behavior. As well, the potential of the biological applications of this hydrogel was demonstrated from cell studies.

As future studies, the poly(HEMA/DMAEMA/TEGDMA) polymer can be synthesized with different ratios of HEMA:DMAEMA:TEGDMA in the monomer feed to tune the properties of the material. Changing the composition will alter the swelling properties of the hydrogel which may affect the pattern-transfer process. As well, the change in composition may further enhance the cell attachment properties of the material. Obtaining the desired cell adhesion properties yet maintaining the aggregation of stem cells will be an interesting direction for future investigations related to biological applications. Furthermore, cell attachment properties can be improved by introducing extracellular matrix components such as collagen or fibronectin. Once the *in vitro* studies successfully show the potential tissue engineering applications of the poly(HEMA/DMAEMA/TEGDMA) polymer, this study can be extended to *in vivo* studies.

REFERENCES

1. A. M. Lowman and N. A. Peppas, In *Encyclopedia of controlled drug delivery*; E. Mathiowitz, Ed.; John Wiley & Sons, Inc: New York, **1999**, 397.

2. B. V. Slaughter, S. S. Khurshid, O. Z. Fisher, A. Khademhosseini and N. A. Peppas, Hydrogels in regenerative medicine, *Advanced Materials* **2009**, *21*, 3307.

3. N. A. Peppas, Y. Huang, M. Torres-Lugo, a. J. H. Ward and J. Zhang, Physicochemical Foundations and Structural Design of Hydrogels in Medicine and Biology, *Annual Review of Biomedical Engineering* **2000**, *2*, 9.

4. R. Langer and N. A. Peppas, Advances in biomaterials, drug delivery, and bionanotechnology, *AIChE Journal* **2003**, *49*, 2990.

5. O. Okay, In *Hydrogel Sensors and Actuators: Engineering and Technology*; G. Gerlach; K.-F. Arndt, Eds.; Springer Berlin Heidelberg: Berlin, Heidelberg, **2010**, 1.

6. W. E. M. Noteborn, G. Yue, J. Wim, K. Alexander and R. E. Kieltyka, Dual-crosslinked human serum albumin-polymer hydrogels for affinity-based drug delivery, *Macromolecular Materials and Engineering* **2017**, *302*, 1700243.

7. H. R. Culver, J. R. Clegg and N. A. Peppas, Analyte-responsive hydrogels: Intelligent materials for biosensing and drug delivery, *Accounts of Chemical Research* **2017**, *50*, 170.

8. Y. Qiu and K. Park, Environment-sensitive hydrogels for drug delivery, *Advanced Drug Delivery Reviews* **2001**, *53*, 321.

9. I. M. El-Sherbiny and M. H. Yacoub, Hydrogel scaffolds for tissue engineering: Progress and challenges, *Global Cardiology Science & Practice* **2013**, *2013*, 316.

10. M. Liu, X. Zeng, C. Ma, H. Yi, Z. Ali, X. Mou, S. Li, Y. Deng and N. He, Injectable hydrogels for cartilage and bone tissue engineering, *Bone Research* **2017**, *5*, 17014.

11. N. A. Peppas and E. W. Merrill, Crosslinked poly(vinyl alcohol) hydrogels as swollen elastic networks, *Journal of Applied Polymer Science* **1977**, *21*, 1763.

12. O. V. Khutoryanskaya, Z. A. Mayeva, G. A. Mun and V. V. Khutoryanskiy, Designing temperature-responsive biocompatible copolymers and hydrogels based on 2-hydroxyethyl(meth)acrylates, *Biomacromolecules* **2008**, *9*, 3353.

13. B. D. Ratner and A. S. Hoffman, In *Hydrogels for Medical and Related Applications*; American Chemical Society, **1976**, 1.

14. J.-P. Montheard, M. Chatzopoulos and D. Chappard, 2-Hydroxyethyl methacrylate (HEMA): Chemical properties and applications in biomedical fields, *Journal of Macromolecular Science, Part C* **1992**, *32*, 1.

15. L. Yong-Yong, Z. Xian-Zheng, C. Han, Z. Jing-Ling, C. Si-Xue and Z. Ren-Xi, Self-assembled, thermosensitive PCL-g-P(NIPAAm-co-HEMA) micelles for drug delivery, *Macromolecular Rapid Communications* **2006**, *27*, 1913.

16. P. A. Faccia and J. I. Amalvy, Synthesis, characterization, and swelling behavior of new pH-sensitive hydrogels derived from copolymers of 2-hydroxyethyl methacrylate and 2-(diisopropylamino)ethylmethacrylate, *Journal of Applied Polymer Science* **2013**, *127*, 1974.

17. Y. J. Lee and P. V. Braun, Tunable inverse opal hydrogel pH sensors, *Advanced Materials* **2003**, *15*, 563.

18. C. Yanfeng and Y. Min, Swelling kinetics and stimuli-responsiveness of poly(DMAEMA) hydrogels prepared by UV-irradiation, *Radiation Physics and Chemistry* **2001**, *61*, 65.

19. I. Kazuhiko and M. Kiyohide, Glucose-responsive insulin release from polymer capsule1, *Journal of Polymer Science Part C: Polymer Letters* **1986**, *24*, 413.

20. L. M. Söderqvist, E. Ranucci and A. C. Albertsson, Biodegradable polymers from renewable sources. New hemicellulose-based hydrogels, *Macromolecular Rapid Communications* **2001**, *22*, 962.

21. S. Atzet, S. Curtin, P. Trinh, S. Bryant and B. Ratner, Degradable poly(2-hydroxyethyl methacrylate)-co-polycaprolactone hydrogels for tissue engineering scaffolds, *Biomacromolecules* **2008**, *9*, 3370.

22. S. D. Bruck, Aspects of three types of hydrogels for biomedical applications, *Journal of Biomedical Materials Research* **1973**, *7*, 387.

23. S.-D. Lee, G.-H. Hsiue, C.-Y. Kao and P. C.-T. Chang, Artificial cornea: surface modification of silicone rubber membrane by graft polymerization of pHEMA via glow discharge, *Biomaterials* **1996**, *17*, 587.

24. C.-D. Young, J.-R. Wu and T.-L. Tsou, Fabrication and characteristics of polyHEMA artificial skin with improved tensile properties, *Journal of Membrane Science* **1998**, *146*, 83.

25. J. Song, E. Saiz and C. R. Bertozzi, Preparation of pHEMA–CP composites with high interfacial adhesion via template-driven mineralization, *Journal of the European Ceramic Society* **2003**, *23*, 2905.

26. C. Prati, R. Mongiorgi, G. Valdrè and G. Montanari, Hydroxyethyl-methacrylate dentin bonding agents: Shear bond strength, marginal microleakage and SEM analysis, *Clinical Materials* **1991**, *8*, 137.

27. M. J. Lyndon, Synthetic hydrogels as substrata for cell adhesion studies, *British Polymer Journal* **1986**, *18*, 22.

28. P. B. van Wachem, A. H. Hogt, T. Beugeling, J. Feijen, A. Bantjes, J. P. Detmers and W. G. van Aken, Adhesion of cultured human endothelial cells onto methacrylate polymers with varying surface wettability and charge, *Biomaterials* **1987**, *8*, 323.

29. J. S. Burmeister, J. D. Vrany, W. M. Reichert and G. A. Truskey, Effect of fibronectin amount and conformation on the strength of endothelial cell adhesion to HEMA/EMA copolymers, *Journal of Biomedical Materials Research* **1996**, *30*, 13.

30. L. Civerchia-Perez, B. Faris, G. LaPointe, J. Beldekas, H. Leibowitz and C. Franzblau, Use of collagen-hydroxyethylmethacrylate hydrogels for cell growth, *Proceedings of the National Academy of Sciences* **1980**, *77*, 2064.

31. E. Brynda, M. Houska, J. Kysilka, M. Přádný, P. Lesný, P. Jendelová, J. Michálek and E. Syková, Surface modification of hydrogels based on poly(2-hydroxyethyl methacrylate) with extracellular matrix proteins, *Journal of Materials Science: Materials in Medicine* **2009**, *20*, 909.

32. F. Chiellini, R. Bizzarri, C. K. Ober, D. Schmaljiohann, T. Yu, W. M. Saltzman, R. Solaro and E. Chiellini, Surface patterning and biological evaluation of semi-interpenetrated poly(HEMA)/poly(alkyl β-malolactonate)s, *Macromolecular Symposia* **2003**, *197*, 369.

33. D. Chandra, J. A. Taylor and S. Yang, Replica molding of high-aspect-ratio (sub-)micron hydrogel pillar arrays and their stability in air and solvents, *Soft Matter* **2008**, *4*, 979.

34. P. Krsko, T. E. McCann, T.-T. Thach, T. L. Laabs, H. M. Geller and M. R. Libera, Length-scale mediated adhesion and directed growth of neural cells by surface-patterned poly(ethylene glycol) hydrogels, *Biomaterials* **2009**, *30*, 721.

35. Y. Xia and G. M. Whitesides, Soft lithography, *Annual Review of Materials Science* **1998**, *28*, 153.

36. D. Qin, Y. Xia and G. M. Whitesides, Soft lithography for micro- and nanoscale patterning, *Nature Protocols* **2010**, *5*, 491.

37. R. Langer and J. P. Vacanti, Tissue engineering, *Science* **1993**, *260*, 920.

38. D. Howard, L. D. Buttery, K. M. Shakesheff and S. J. Roberts, Tissue engineering: strategies, stem cells and scaffolds, *Journal of Anatomy* **2008**, *213*, 66.

39. M. Vemuri, L. G. Chase and M. S. Rao. Mesenchymal stem cell assays and applications; Springer Science+Business Media, LLC 2011: Springer New York Dordrecht Heidelberg London, **2011**

40. A. J. Rosenbaum, D. A. Grande and J. S. Dines, The use of mesenchymal stem cells in tissue engineering: A global assessment, *Organogenesis* **2008**, *4*, 23.

41. C. McKee and G. R. Chaudhry, Advances and challenges in stem cell culture, *Colloids and Surfaces B: Biointerfaces* **2017**, *159*, 62.

42. A. J. Engler, S. Sen, H. L. Sweeney and D. E. Discher, Matrix elasticity directs stem cell lineage specification, *Cell* **2006**, *126*, 677.

43. H. J. Anderson, J. K. Sahoo, R. V. Ulijn and M. J. Dalby, Mesenchymal stem cell fate: Applying biomaterials for control of stem cell behavior, *Frontiers in Bioengineering and Biotechnology* **2016**, *4*, 38.

44. M. A. Bucaro, Y. Vasquez, B. D. Hatton and J. Aizenberg, Fine-tuning the degree of stem cell polarization and alignment on ordered arrays of high-aspect-ratio nanopillars, *ACS Nano* **2012**, *6*, 6222.

45. M. Guvendiren and J. A. Burdick, The control of stem cell morphology and differentiation by hydrogel surface wrinkles, *Biomaterials* **2010**, *31*, 6511.

46. J. Oju and A. Eben, Regulation of Stem Cell Fate in a Three-Dimensional Micropatterned Dual-Crosslinked Hydrogel System, *Advanced Functional Materials* **2013**, *23*, 4765.

47. Y. Hu, J.-O. You and J. Aizenberg, Micropatterned hydrogel surface with high-aspect-ratio features for cell guidance and tissue growth, *ACS Applied Materials & Interfaces* **2016**, *8*, 21939.

48. M. Caldorera-Moore, M. K. Kang, Z. Moore, V. Singh, S. V. Sreenivasan, L. Shi, R. Huang and K. Roy, Swelling behavior of nanoscale, shape- and size-specific, hydrogel particles fabricated using imprint lithography, *Soft Matter* **2011**, *7*, 2879.

49. H. Feil, Y. H. Bae, J. Feijen and S. W. Kim, Mutual influence of pH and temperature on the swelling of ionizable and thermosensitive hydrogels, *Macromolecules* **1992**, *25*, 5528.

50. N. Bouklas and R. Huang, Swelling kinetics of polymer gels: comparison of linear and nonlinear theories, *Soft Matter* **2012**, *8*, 8194.

51. Z. Maolin, L. Jun, Y. Min and H. Hongfei, The swelling behavior of radiation prepared semi-interpenetrating polymer networks composed of polyNIPAAm and hydrophilic polymers, *Radiation Physics and Chemistry* **2000**, *58*, 397.

52. M. K. Kang and R. Huang, Swell-induced surface instability of confined hydrogel layers on substrates, *Journal of the Mechanics and Physics of Solids* **2010**, *58*, 1582.

53. A. M. Mathur, K. F. Hammonds, J. Klier and A. B. Scranton, Equilibrium swelling of poly(methacrylic acid-g-ethylene glycol) hydrogels: Effect of swelling medium and synthesis conditions, *Journal of Controlled Release* **1998**, *54*, 177.

54. T. Traitel, Y. Cohen and J. Kost, Characterization of glucose-sensitive insulin release systems in simulated in vivo conditions, *Biomaterials* **2000**, *21*, 1679.

55. L. Klouda and A. G. Mikos, Thermoresponsive hydrogels in biomedical applications, *European Journal of Pharmaceutics and Biopharmaceutics* **2008**, *68*, 34.

56. T. R. Hoare and D. S. Kohane, Hydrogels in drug delivery: Progress and challenges, *Polymer* **2008**, *49*, 1993.

57. D. Chandra and S. Yang, Stability of high-aspect-ratio micropillar arrays against adhesive and capillary forces, *Accounts of Chemical Research* **2010**, *43*, 1080.

58. F. D. Benedetto, A. Biasco, D. Pisignano and R. Cingolani, Patterning polyacrylamide hydrogels by soft lithography, *Nanotechnology* **2005**, *16*, S165.

59. Y. Li, S. Dai, J. John and K. R. Carter, Superhydrophobic surfaces from hierarchically structured wrinkled polymers, *ACS Applied Materials & Interfaces* **2013**, *5*, 11066.

60. T. Yu and C. K. Ober, Methods for the topographical patterning and patterned surface modification of hydrogels based on hydroxyethyl methacrylate, *Biomacromolecules* **2003**, *4*, 1126.

61. X.-M. Zhao, Y. Xia and G. M. Whitesides, Soft lithographic methods for nano-fabrication, *Journal of Materials Chemistry* **1997**, *7*, 1069.

62. G. M. Whitesides, E. Ostuni, S. Takayama, X. Jiang and D. E. Ingber, Soft lithography in biology and biochemistry, *Annual Review of Biomedical Engineering* **2001**, *3*, 335.

63. D.-H. Kim, K. Han, K. Gupta, K. W. Kwon, K.-Y. Suh and A. Levchenko, Mechanosensitivity of fibroblast cell shape and movement to anisotropic substratum topography gradients, *Biomaterials* **2009**, *30*, 5433.

64. M. D. Tang, A. P. Golden and J. Tien, Molding of three-dimensional microstructures of gels, *Journal of the American Chemical Society* **2003**, *125*, 12988.

65. J.-L. Ruan, N. L. Tulloch, V. Muskheli, E. E. Genova, P. D. Mariner, K. S. Anseth and C. E. Murry, An improved cryosection method for polyethylene glycol hydrogels used in tissue engineering, *Tissue Engineering. Part C, Methods* **2013**, *19*, 794.

66. R. S. Kane, S. Takayama, E. Ostuni, D. E. Ingber and G. M. Whitesides, Patterning proteins and cells using soft lithography, *Biomaterials* **1999**, *20*, 2363.

67. B. Pokroy, A. K. Epstein, M. C. M. Persson-Gulda and J. Aizenberg, Fabrication of bioinspired actuated nanostructures with arbitrary geometry and stiffness, *Advanced Materials* **2009**, *21*, 463.

68. J.-O. You and D. T. Auguste, Conductive, physiologically responsive hydrogels, *Langmuir* **2010**, *26*, 4607.

69. M. Zhang, J. Wu, L. Wang, K. Xiao and W. Wen, A simple method for fabricating multi-layer PDMS structures for 3D microfluidic chips, *Lab on a Chip* **2010**, *10*, 1199.

70. M. D. Borysiak, K. S. Bielawski, N. J. Sniadecki, C. F. Jenkel, B. D. Vogt and J. D. Posner, Simple replica micromolding of biocompatible styrenic elastomers, *Lab on a chip* **2013**, *13*, 2773.

71. J. Kroupová, D. Horák, J. Pacherník, P. Dvořák and M. Šlouf, Functional polymer hydrogels for embryonic stem cell support, *Journal of Biomedical Materials Research Part B: Applied Biomaterials* **2006**, *76B*, 315.

72. N. Subramaniam, F. D. Blum and L. R. Dharani, Effects of moisture and other contaminants in friction composites, *Polymer Engineering & Science* **1993**, *33*, 1204.

73. B. A. Firestone and R. A. Siegel, Kinetics and mechanisms of water sorption in hydrophobic, ionizable copolymer gels, *Journal of Applied Polymer Science* **1991**, *43*, 901.

74. J.-K. Chen, F.-H. Ko, K.-F. Hsieh, C.-T. Chou and F.-C. Chang, Effect of fluoroalkyl substituents on the reactions of alkylchlorosilanes with mold surfaces for nanoimprint lithography, *Journal of Vacuum Science & Technology B: Microelectronics and Nanometer Structures Processing, Measurement, and Phenomena* **2004**, *22*, 3233.

75. J. P. Rolland, E. C. Hagberg, G. M. Denison, K. R. Carter and J. M. De Simone, High-resolution soft lithography: Enabling materials for nanotechnologies, *Angewandte Chemie International Edition* **2004**, *43*, 5796.

76. K. Haubert, T. Drier and D. Beebe, PDMS bonding by means of a portable, low-cost corona system, *Lab on a Chip* **2006**, *6*, 1548.

77. A. J. Bowman, J. R. Scherrer and R. S. Reiserer, Note: A single-chamber tool for plasma activation and surface functionalization in microfabrication, *The Review of Scientific Instruments* **2015**, *86*, 066106.

78. M. Guvendiren, J. A. Burdick and S. Yang, Solvent induced transition from wrinkles to creases in thin film gels with depth-wise crosslinking gradients, *Soft Matter* **2010**, *6*, 5795.

79. M. F. Refojo and H. Yasuda, Hydrogels from 2-hydroxyethyl methacrylate and propylene glycol monoacrylate, *Journal of Applied Polymer Science* **1965**, *9*, 2425.

80. T. C. Warren and W. Prins, Polymer-diluent interaction in cross-linked gels of poly(2-hydroxyethyl methacrylate), *Macromolecules* **1972**, *5*, 506.

81. L. Wen-Fu and L. Yu-Hung, pH-reversible hydrogels. IV. Swelling behavior of the 2-hydroxyethyl methacrylate-co-acrylic acid-co-sodium acrylate copolymeric hydrogels, *Journal of Applied Polymer Science* **2001**, *81*, 1360.

82. A. K. Bajpai and M. Shrivastava, Swelling kinetics of a hydrogel of poly(ethylene glycol) and poly(acrylamide-co-styrene), *Journal of Applied Polymer Science* **2002**, *85*, 1419.

83. M. F. Refojo, Hydrophobic interaction in poly(2-hydroxyethyl methacrylate) homogeneous hydrogel, *Journal of Polymer Science Part A-1: Polymer Chemistry* **1967**, *5*, 3103.

84. L. Feng, S. Li, Y. Li, H. Li, L. Zhang, J. Zhai, Y. Song, B. Liu, L. Jiang and D. Zhu, Super-hydrophobic surfaces: from natural to artificial, *Advanced Materials* **2002**, *14*, 1857.

85. C. Neinhuis and W. Barthlott, Characterization and distribution of water-repellent, self-cleaning plant surfaces, *Annals of Botany* **1997**, *79*, 667.

86. W. Barthlott and C. Neinhuis, Purity of the sacred lotus, or escape from contamination in biological surfaces, *Planta* **1997**, *202*, 1.

87. L. F. Boesel, C. Greiner, E. Arzt and A. del Campo, Gecko-inspired surfaces: A path to strong and reversible dry adhesives, *Advanced Materials* **2010**, *22*, 2125.

88. P. Ball, Engineering Shark skin and other solutions, *Nature* **1999**, *400*, 507.

89. H. E. Jeong, S. H. Lee, J. K. Kim and K. Y. Suh, Nanoengineered multiscale hierarchical structures with tailored wetting properties, *Langmuir* **2006**, *22*, 1640.

90. W. R. Hansen, K. Autumn and J. Israelachvili, Evidence for self-cleaning in gecko setae, *Proceedings of the National Academy of Sciences of the United States of America* **2005**, *102*, 385.

91. X. Gao and L. Jiang, Biophysics: Water-repellent legs of water striders, *Nature* **2004**, *432*, 36.

92. J. Fu, Y.-K. Wang, M. T. Yang, R. A. Desai, X. Yu, Z. Liu and C. S. Chen, Mechanical regulation of cell function with geometrically modulated elastomeric substrates, *Nature Methods* **2010**, *7*, 733.

93. Y. Wang, H. Hu, J. Shao and Y. Ding, Fabrication of well-defined mushroom-shaped structures for biomimetic dry adhesive by conventional photolithography and molding, *ACS Applied Materials & Interfaces* **2014**, *6*, 2213.

94. D. Öner and T. J. McCarthy, Ultrahydrophobic surfaces. Effects of topography length scales on wettability, *Langmuir* **2000**, *16*, 7777.

95. Z. Yoshimitsu, A. Nakajima, T. Watanabe and K. Hashimoto, Effects of surface structure on the hydrophobicity and sliding behavior of water droplets, *Langmuir* **2002**, *18*, 5818.

96. X. Li, H. Tian, J. Shao, Y. Ding and H. Liu, Electrically modulated microtransfer molding for fabrication of micropillar arrays with spatially varying heights, *Langmuir* **2013**, *29*, 1351.

97. A. del Campo and E. Arzt, Fabrication approaches for generating complex micro- and nanopatterns on polymeric surfaces, *Chemical Reviews* **2008**, *108*, 911.

98. J. K. Ng, E. S. Selamat and W.-T. Liu, A spatially addressable bead-based biosensor for simple and rapid DNA detection, *Biosensors and Bioelectronics* **2008**, *23*, 803.

99. V. Penmatsa, T. Kim, M. Beidaghi, H. Kawarada, L. Gu, Z. Wang and C. Wang, Three-dimensional graphene nanosheet encrusted carbon micropillar arrays for electrochemical sensing, *Nanoscale* **2012**, *4*, 3673.

100. Y. Ito, H. Hasuda, M. Morimatsu, N. Takagi and Y. Hirai, A microfabrication method of a biodegradable polymer chip for a controlled release system, *Journal of Biomaterials Science, Polymer Edition* **2005**, *16*, 949.

101. K. Morishima, Y. Tanaka, M. Ebara, T. Shimizu, A. Kikuchi, M. Yamato, T. Okano and T. Kitamori, Demonstration of a bio-microactuator powered by cultured cardiomyocytes coupled to hydrogel micropillars, *Sensors and Actuators B: Chemical* **2006**, *119*, 345.

102. Y. Yu and T. Ikeda, Soft actuators based on liquid-crystalline elastomers, *Angewandte Chemie International Edition* **2006**, *45*, 5416.

103. C.-S. Kee, M.-Y. Jang, S.-I. Kim, I. Park and H. Lim, Tuning and widening of stop bands of microstrip photonic band gap ring structures, *Applied Physics Letters* **2005**, *86*, 181109.

104. E. Garnett and P. Yang, Light trapping in silicon nanowire solar cells, *Nano Letters* **2010**, *10*, 1082.

105. X. Chen, X. Li, J. Shao, N. An, H. Tian, C. Wang, T. Han, L. Wang and B. Lu, High-performance piezoelectric nanogenerators with imprinted P(VDF-TrFE)/BaTiO3 nanocomposite micropillars for self-powered flexible sensors, *Small* **2017**, *13*, 1604245.

106. M. Goto, T. Tsukahara, K. Sato, T. Konno, K. Ishihara, K. Sato and T. Kitamori, Nanometer-scale patterned surfaces for control of cell adhesion, *Analytical Sciences* **2007**, *23*, 245.

107. H. Jeon, S. Koo, W. M. Reese, P. Loskill, C. P. Grigoropoulos and K. E. Healy, Directing cell migration and organization via nanocrater-patterned cell-repellent interfaces, *Nature Materials* **2015**, *14*, 918.

108. Z. Li, Y. Gong, S. Sun, Y. Du, D. Lü, X. Liu and M. Long, Differential regulation of stiffness, topography, and dimension of substrates in rat mesenchymal stem cells, *Biomaterials* **2013**, *34*, 7616.

109. S.-W. Kuo, H.-I. Lin, J. Hui-Chun Ho, Y.-R. V. Shih, H.-F. Chen, T.-J. Yen and O. K. Lee, Regulation of the fate of human mesenchymal stem cells by mechanical and stereo-topographical cues provided by silicon nanowires, *Biomaterials* **2012**, *33*, 5013.

110. S. Gobaa, S. Hoehnel, M. Roccio, A. Negro, S. Kobel and M. P. Lutolf, Artificial niche microarrays for probing single stem cell fate in high throughput, *Nature Methods* **2011**, *8*, 949.

111. K. S. Brammer, C. Choi, C. J. Frandsen, S. Oh and S. Jin, Hydrophobic nanopillars initiate mesenchymal stem cell aggregation and osteo-differentiation, *Acta Biomaterialia* **2011**, *7*, 683.

112. A. Asti and L. Gioglio, Natural and synthetic biodegradable polymers: different scaffolds for cell expansion and tissue formation, *The International Journal of Artificial Organs* **2014**, *37*, 187.

113. D. W. Hutmacher, Scaffolds in tissue engineering bone and cartilage, *Biomaterials* **2000**, *21*, 2529.

114. M. Nikkhah, F. Edalat, S. Manoucheri and A. Khademhosseini, Engineering microscale topographies to control the cell–substrate interface, *Biomaterials* **2012**, *33*, 5230.

115. H. Yeganeh, M. M. Lakouraj and S. Jamshidi, Synthesis and properties of biodegradable elastomeric epoxy modified polyurethanes based on poly(ε-caprolactone) and poly(ethylene glycol), *European Polymer Journal* **2005**, *41*, 2370.

116. F.-L. Jin and S.-J. Park, Impact-strength improvement of epoxy resins reinforced with a biodegradable polymer, *Materials Science and Engineering: A* **2008**, *478*, 402.

117. N. A. Peppas, J. Z. Hilt, A. Khademhosseini and R. Langer, Hydrogels in biology and medicine: from molecular principles to bionanotechnology, *Advanced Materials* **2006**, *18*, 1345.

118. D. B. Weibel, W. R. DiLuzio and G. M. Whitesides, Microfabrication meets microbiology, *Nature Reviews Microbiology* **2007**, *5*, 209.

119. A. G. Castano, V. Hortiguela, A. Lagunas, C. Cortina, N. Montserrat, J. Samitier and E. Martinez, Protein patterning on hydrogels by direct microcontact printing: application to cardiac differentiation, *RSC Advances* **2014**, *4*, 29120.

120. S. Kobel, M. Limacher, S. Gobaa, T. Laroche and M. P. Lutolf, Micropatterning of hydrogels by soft embossing, *Langmuir* **2009**, *25*, 8774.

121. S. Allazetta, S. Cosson and M. P. Lutolf, Programmable microfluidic patterning of protein gradients on hydrogels, *Chemical Communications* **2011**, *47*, 191.

122. J. Yeh, Y. Ling, J. M. Karp, J. Gantz, A. Chandawarkar, G. Eng, J. Blumling Iii, R. Langer and A. Khademhosseini, Micromolding of shape-controlled, harvestable cell-laden hydrogels, *Biomaterials* **2006**, *27*, 5391.

123. H. N. Kim, D.-H. Kang, M. S. Kim, A. Jiao, D.-H. Kim and K.-Y. Suh, Patterning methods for polymers in cell and tissue engineering, *Ann. Biomed. Eng.* **2012**, *40*, 1339.

124. J. H. Kou, D. Fleisher and G. L. Amidon, Modeling drug release from dynamically swelling poly(hydroxyethyl methacrylate-co-methacrylic acid) hydrogels, *Journal of Controlled Release* **1990**, *12*, 241.

125. G. Gee. Thermodynamics of rubber solutions and gels in advances in colloid science; Interscience: New York, **1946**

126. G. Gee, Interaction between rubber and liquid. IV. Factors governing the absorption of oil by rubber, *Transactions, Institute of the rubber industry, London* **1943**, *18*, 266.

127. T. Çaykara, C. Özyürek, Ö. Kantoğlu and O. Güven, Influence of gel composition on the solubility parameter of poly(2-hydroxyethyl methacrylate-itaconic acid) hydrogels, *Journal of Polymer Science Part B: Polymer Physics* **2002**, *40*, 1995.

128. J. Brandrup and E. H. Immergut. Polymer Handbook; John Wiley & Sons: New York, **1989**

129. T. P. Davis and M. B. Huglin, Effect of crosslinker on properties of copolymeric N-vinyl-2-pyrrolidone/methyl methacrylate hydrogels and organogels, *Die Makromolekulare Chemie* **1990**, *191*, 331.

130. N. A. Peppas, P. Bures, W. Leobandung and H. Ichikawa, Hydrogels in pharmaceutical formulations, *European Journal of Pharmaceutics and Biopharmaceutics* **2000**, *50*, 27.

131. G. Lin, S. Chang, C. H. Kuo, J. Magda and F. Solzbacher, Free swelling and confined smart hydrogels for applications in chemomechanical sensors for physiological monitoring, *Sensors and Actuators B: Chemical* **2009**, *136*, 186.

132. S. K. Basu, A. V. McCormick and L. E. Scriven, Stress generation by solvent absorption and wrinkling of a cross-linked coating atop a viscous or elastic base, *Langmuir* **2006**, *22*, 5916.

133. K. M. Crosby and R. M. Bradley, Pattern formation during delamination and buckling of thin films, *Phys. Rev. E* **1999**, *59*, R2542.

134. A. F. M. Barton, Solubility parameters, *Chemical Reviews* **1975**, *75*, 731.

135. K. S. Anseth, C. N. Bowman and L. Brannon-Peppas, Mechanical properties of hydrogels and their experimental determination, *Biomaterials* **1996**, *17*, 1647.

136. Q. Xing, K. Yates, C. Vogt, Z. Qian, M. C. Frost and F. Zhao, Increasing mechanical strength of gelatin hydrogels by divalent metal ion removal, *Scientific Reports* **2014**, *4*.

137. P. J. Flory. Principles of Polymer Chemistry; George Banta Publishing Company: Cornell University Press, **1953**

138. V. A. Schulte, M. Díez, M. Möller and M. C. Lensen, Surface topography induces fibroblast adhesion on intrinsically nonadhesive poly(ethylene glycol) substrates, *Biomacromolecules* **2009**, *10*, 2795.

139. J. N. Lee, C. Park and G. M. Whitesides, Solvent compatibility of poly(dimethylsiloxane)-based microfluidic devices, *Analytical Chemistry* **2003**, *75*, 6544.

140. L. M. Granhag, J. A. Finlay, P. R. Jonsson, J. A. Callow and M. E. Callow, Roughness-dependent removal of settled spores of the Green Alga Ulva (syn. Enteromorpha) exposed to hydrodynamic forces from a water jet, *Biofouling* **2004**, *20*, 117.

141. N. J. Walters and E. Gentleman, Evolving insights in cell–matrix interactions: Elucidating how non-soluble properties of the extracellular niche direct stem cell fate, *Acta Biomaterialia* **2015**, *11*, 3.

142. S. Ahadian, L. Davenport Huyer, M. Estili, B. Yee, N. Smith, Z. Xu, Y. Sun and M. Radisic, Moldable elastomeric polyester-carbon nanotube scaffolds for cardiac tissue engineering, *Acta Biomaterialia* **2017**, *52*, 81.

143. C. Y. Jeong, C. S. Kwang, H. C. Man, S. I. Soo, P. S. Nie, H. S. Hwa, P. H. Ki, P. Y. Hwan, S. Youngsook and N. Insup, Evaluations of blood compatibility via protein adsorption treatment of the vascular scaffold surfaces fabricated with polylactide and surface-modified expanded polytetrafluoroethylene for tissue engineering applications, *Journal of Biomedical Materials Research Part A* **2005**, *75A*, 824.

144. Y. Ji, K. Ghosh, X. Z. Shu, B. Li, J. C. Sokolov, G. D. Prestwich, R. A. F. Clark and M. H. Rafailovich, Electrospun three-dimensional hyaluronic acid nanofibrous scaffolds, *Biomaterials* **2006**, *27*, 3782.

145. T. J. Webster, C. Ergun, R. H. Doremus, R. W. Siegel and R. Bizios, Enhanced functions of osteoblasts on nanophase ceramics, *Biomaterials* **2000**, *21*, 1803.

146. L. L. Hench, Bioceramics, *Journal of the American Ceramic Society* **1998**, *81*, 1705.

147. C. Di Mario, H. Griffiths, O. Goktekin, N. Peeters, J. Verbist, M. Bosiers, K. Deloose, B. Heublein, R. Rohde, V. Kasese, C. Ilsley and R. Erbel, Drug-eluting bioabsorbable magnesium stent, *Journal of Interventional Cardiology* **2004**, *17*, 391.

148. M. Peuster, C. Hesse, T. Schloo, C. Fink, P. Beerbaum and C. von Schnakenburg, Long-term biocompatibility of a corrodible peripheral iron stent in the porcine descending aorta, *Biomaterials* **2006**, *27*, 4955.

149. Y. Okazaki, A new Ti–15Zr–4Nb–4Ta alloy for medical applications, *Current Opinion in Solid State and Materials Science* **2001**, *5*, 45.

150. B. Dhandayuthapani, Y. Yoshida, T. Maekawa and D. S. Kumar, Polymeric scaffolds in tissue engineering application: A review, *International Journal of Polymer Science* **2011**, *2011*.

151. M. T. Lam and J. C. Wu, Biomaterial applications in cardiovascular tissue repair and regeneration, *Expert Review of Cardiovascular Therapy* **2012**, *10*, 1039.

152. A. H. Yusop, A. A. Bakir, N. A. Shaharom, M. R. Abdul Kadir and H. Hermawan, Porous biodegradable metals for hard tissue scaffolds: A review, *International Journal of Biomaterials* **2012**, *2012*, 10.

153. K. Alvarez and H. Nakajima, Metallic scaffolds for bone regeneration, *Materials* **2009**, *2*, 790.

154. C.-H. Chang, F.-H. Lin, T.-F. Kuo and H.-C. Liu, Cartilage tissue engineering, *Biomedical Engineering: Applications, Basis and Communications* **2005**, *17*, 61.

155. M. Wang, Developing bioactive composite materials for tissue replacement, *Biomaterials* **2003**, *24*, 2133.

156. T. M. Freyman, I. V. Yannas and L. J. Gibson, Cellular materials as porous scaffolds for tissue engineering, *Progress in Materials Science* **2001**, *46*, 273.

157. H. Liu, E. B. Slamovich and T. J. Webster, Less harmful acidic degradation of poly(lactic-co-glycolic acid) bone tissue engineering scaffolds through titania nanoparticle addition, *International Journal of Nanomedicine* **2006**, *1*, 541.

158. D. S. Kohane and R. Langer, Polymeric biomaterials in tissue engineering, *Pediatric Research* **2008**, *63*, 487.

159. S. Venkatraman, F. Boey and L. L. Lao, Implanted cardiovascular polymers: Natural, synthetic and bio-inspired, *Progress in Polymer Science* **2008**, *33*, 853.

160. N. A. Peppas and R. Langer, New Challenges in Biomaterials, *Science* **1994**, *263*, 1715.

161. O. Wichterle and D. Lim, Hydrophilic gels for biological use, *Nature* **1960**, *185*, 117.

162. A. M. Kloxin, C. J. Kloxin, C. N. Bowman and K. S. Anseth, Mechanical properties of cellularly responsive hydrogels and their experimental determination, *Advanced Materials* **2010**, *22*, 3484.

163. M. Mehdi, T. Ashish, P. C. Pablo, T. Sepehr, A. Ayyoob, N. Mehdi and D. P. Alireza, Nanoreinforced hydrogels for tissue engineering: Biomaterials that are compatible with load-bearing and electroactive tissues, *Advanced Materials* **2017**, *29*, 1603612.

164. W. S. Kim, D. J. Mooney, P. R. Arany, K. Lee, N. Huebsch and J. Kim, Adipose tissue engineering using injectable, oxidized alginate hydrogels, *Tissue Engineering Part A* **2012**, *18*, 737.

165. M. R. Battig, B. Soontornworajit and Y. Wang, Programmable release of multiple protein drugs from aptamer-functionalized hydrogels via nucleic acid hybridization, *Journal of the American Chemical Society* **2012**, *134*, 12410.

166. T. Lin, J. Wu, X. Zhao, H. Lian, A. Yuan, X. Tang, S. Zhao, H. Guo and Y. Hu, In situ floating hydrogel for intravesical delivery of adriamycin without blocking urinary tract, *Journal of Pharmaceutical Sciences* **2014**, *103*, 927.

167. X. Ma, H. Tao, K. Yang, L. Feng, L. Cheng, X. Shi, Y. Li, L. Guo and Z. Liu, A functionalized graphene oxide-iron oxide nanocomposite for magnetically targeted drug delivery, photothermal therapy, and magnetic resonance imaging, *Nano Research* **2012**, *5*, 199.

168. C. Yi, P. Xiao-Hui and D. Chang-Ming, Dual stimuli-responsive supramolecular polypeptide-based hydrogel and reverse micellar hydrogel mediated by host–guest chemistry, *Advanced Functional Materials* **2010**, *20*, 579.

169. C. F. Deroanne, C. M. Lapiere and B. V. Nusgens, In vitro tubulogenesis of endothelial cells by relaxation of the coupling extracellular matrix-cytoskeleton, *Cardiovascular Research* **2001**, *49*, 647.

170. W. J. Hadden, J. L. Young, A. W. Holle, M. L. McFetridge, D. Y. Kim, P. Wijesinghe, H. Taylor-Weiner, J. H. Wen, A. R. Lee, K. Bieback, B.-N. Vo, D. D. Sampson, B. F. Kennedy, J. P. Spatz, A. J. Engler and Y. S. Choi, Stem cell migration and mechanotransduction on linear stiffness gradient hydrogels, *Proceedings of the National Academy of Sciences* **2017**, *114*, 5647.

171. M. Guvendiren, S. Fung, J. Kohn, C. De Maria, F. Montemurro and G. Vozzi, The control of stem cell morphology and differentiation using three-dimensional printed scaffold architecture, *MRS Communications* **2017**, *7*, 383.

172. C. Lensen Marga, A. Schulte Vera, J. Salber, M. Diez, F. Menges and M. Möller. In Pure and Applied Chemistry, **2008**, p 2479.

173. D. S. W. Benoit, M. P. Schwartz, A. R. Durney and K. S. Anseth, Small functional groups for controlled differentiation of hydrogel-encapsulated human mesenchymal stem cells, *Nature Materials* **2008**, *7*, 816.

174. G. Pan, B. Guo, Y. Ma, W. Cui, F. He, B. Li, H. Yang and K. J. Shea, Dynamic introduction of cell adhesive factor via reversible multicovalent phenylboronic acid/cis-diol polymeric complexes, *Journal of the American Chemical Society* **2014**, *136*, 6203.

175. E. N. Mpoyi, M. Cantini, P. M. Reynolds, N. Gadegaard, M. J. Dalby and M. Salmerón-Sánchez, Protein adsorption as a key mediator in the nanotopographical control of cell behavior, *ACS Nano* **2016**, *10*, 6638.

176. E. K. F. Yim, R. M. Reano, S. W. Pang, A. F. Yee, C. S. Chen and K. W. Leong, Nanopattern-induced changes in morphology and motility of smooth muscle cells, *Biomaterials* **2005**, *26*, 5405.

177. A. I. Teixeira, P. F. Nealey and C. J. Murphy, Responses of human keratocytes to micro- and nanostructured substrates, *Journal of Biomedical Materials Research Part A* **2004**, *71A*, 369.

178. J. Deng, C. Zhao, J. P. Spatz and Q. Wei, Nanopatterned adhesive, stretchable hydrogel to control ligand spacing and regulate cell spreading and migration, *ACS Nano* **2017**, *11*, 8282.

179. E. Lamers, X. Frank Walboomers, M. Domanski, J. te Riet, F. C. M. J. M. van Delft, R. Luttge, L. A. J. A. Winnubst, H. J. G. E. Gardeniers and J. A. Jansen, The influence of nanoscale grooved substrates on osteoblast behavior and extracellular matrix deposition, *Biomaterials* **2010**, *31*, 3307.

180. M. Floren, W. Bonani, A. Dharmarajan, A. Motta, C. Migliaresi and W. Tan, Human mesenchymal stem cells cultured on silk hydrogels with variable stiffness and growth factor differentiate into mature smooth muscle cell phenotype, *Acta Biomaterialia* **2016**, *31*, 156.

181. P.-Y. Wang, W.-T. Li, J. Yu and W.-B. Tsai, Modulation of osteogenic, adipogenic and myogenic differentiation of mesenchymal stem cells by submicron grooved topography, *Journal of Materials Science: Materials in Medicine* **2012**, *23*, 3015.

182. D. Khang, J. Choi, Y.-M. Im, Y.-J. Kim, J.-H. Jang, S. S. Kang, T.-H. Nam, J. Song and J.-W. Park, Role of subnano-, nano- and submicron-surface features on osteoblast differentiation of bone marrow mesenchymal stem cells, *Biomaterials* **2012**, *33*, 5997.

183. J. A. Wood, I. Ly, D. L. Borjesson, P. F. Nealey, P. Russell and C. J. Murphy, The modulation of canine mesenchymal stem cells by nano-topographic cues, *Experimental Cell Research* **2012**, *318*, 2438.

184. E. H. Ahn, Y. Kim, Kshitiz, S. S. An, J. Afzal, S. Lee, M. Kwak, K.-Y. Suh, D.-H. Kim and A. Levchenko, Spatial control of adult stem cell fate using nanotopographic cues, *Biomaterials* **2014**, *35*, 2401.

185. S. J. Bryant and K. S. Anseth, Hydrogel properties influence ECM production by chondrocytes photoencapsulated in poly(ethylene glycol) hydrogels, *Journal of Biomedical Materials Research* **2002**, *59*, 63.

186. S. Vignesh, A. Gopalakrishnan, P. M.R, S. V. Nair, R. Jayakumar and U. Mony, Fabrication of micropatterned alginate-gelatin and k-carrageenan hydrogels of defined shapes using simple wax mould method as a platform for stem cell/induced Pluripotent Stem Cells (iPSC) culture, *International Journal of Biological Macromolecules* **2018**, *112*, 737.

187. B. M. Spiegelman and C. A. Ginty, Fibronectin modulation of cell shape and lipogenic gene expression in 3t3-adipocytes, *Cell* **1983**, *35*, 657.

188. A. E. Grigoriadis, J. N. Heersche and J. E. Aubin, Differentiation of muscle, fat, cartilage, and bone from progenitor cells present in a bone-derived clonal cell population: effect of dexamethasone, *The Journal of Cell Biology* **1988**, *106*, 2139.

189. J. Oju and A. Eben, Regulation of stem cell fate in a three-dimensional micropatterned dual-crosslinked hydrogel system, *Advanced Functional Materials* **2013**, *23*, 4765.

190. W.-J. Li, R. Tuli, C. Okafor, A. Derfoul, K. G. Danielson, D. J. Hall and R. S. Tuan, A three-dimensional nanofibrous scaffold for cartilage tissue engineering using human mesenchymal stem cells, *Biomaterials* **2005**, *26*, 599.

191. F. Grinnell and W. M. Petroll, Cell motility and mechanics in three-dimensional collagen matrices, *Annual Review of Cell and Developmental Biology* **2010**, *26*, 335.

192. B. Johnstone, T. M. Hering, A. I. Caplan, V. M. Goldberg and J. U. Yoo, In vitro chondrogenesis of bone marrow-derived mesenchymal progenitor cells, *Experimental Cell Research* **1998**, *238*, 265.

193. P. R. Baraniak and T. C. McDevitt, Scaffold-free culture of mesenchymal stem cell spheroids in suspension preserves multilineage potential, *Cell and Tissue Research* **2012**, *347*, 701.

194. S. Kale, S. Biermann, C. Edwards, C. Tarnowski, M. Morris and M. W. Long, Three-dimensional cellular development is essential for ex vivo formation of human bone, *Nature Biotechnology* **2000**, *18*, 954.

195. Y.-N. Wu, J. B. K. Law, A. Y. He, H. Y. Low, J. H. P. Hui, C. T. Lim, Z. Yang and E. H. Lee, Substrate topography determines the fate of chondrogenesis from human mesenchymal stem cells resulting in specific cartilage phenotype formation, *Nanomedicine: Nanotechnology, Biology and Medicine* **2014**, *10*, 1507.

196. D. Gallego-Perez, N. Higuita-Castro, S. Sharma, R. K. Reen, A. F. Palmer, K. J. Gooch, L. J. Lee, J. J. Lannutti and D. J. Hansford, High throughput assembly of spatially controlled 3D cell clusters on a micro/nanoplatform, *Lab on a Chip* **2010**, *10*, 775.

197. C.-H. Choi, S. H. Hagvall, B. M. Wu, J. C. Y. Dunn, R. E. Beygui and C.-J. "Cj" Kim, Cell interaction with three-dimensional sharp-tip nanotopography, *Biomaterials* **2007**, *28*, 1672.

198. X. Liu, R. Liu, B. Cao, K. Ye, S. Li, Y. Gu, Z. Pan and J. Ding, Subcellular cell geometry on micropillars regulates stem cell differentiation, *Biomaterials* **2016**, *111*, 27.

199. F. Langenbach, K. Berr, C. Naujoks, A. Hassel, M. Hentschel, R. Depprich, N. R. Kubler, U. Meyer, H.-P. Wiesmann, G. Kögler and J. Handschel, Generation and differentiation of microtissues from multipotent precursor cells for use in tissue engineering, *Nature Protocols* **2011**, *6*, 1726.

200. B. R. Sedai, B. K. Khatiwada, H. Mortazavian and F. D. Blum, Development of superhydrophobicity in fluorosilane-treated diatomaceous earth polymer coatings, *Applied Surface Science* **2016**, *386*, 178.

201. L. Glennon-Alty, R. Williams, S. Dixon and P. Murray, Induction of mesenchymal stem cell chondrogenesis by polyacrylate substrates, *Acta Biomaterialia* **2013**, *9*, 6041.

202. T.-J. Lu, F.-Y. Chiu, H.-Y. Chiu, M.-C. Chang and S.-C. Hung, Chondrogenic differentiation of mesenchymal stem cells in three-dimensional chitosan film culture, *Cell Transplantation* **2017**, *26*, 417.

203. J. S. Fitzsimmons, A. Sanyal, C. Gonzalez, T. Fukumoto, V. R. Clemens, S. W. O'Driscoll and G. G. Reinholz, Serum-free media for periosteal chondrogenesis in vitro, *Journal of Orthopaedic Research* **2004**, *22*, 716.

204. D. Barnes and G. Sato, Methods for growth of cultured cells in serum-free medium, *Analytical Biochemistry* **1980**, *102*, 255.

205. M. Wong and R. S. Tuan, Nuserum, a synthetic serum replacement, supports chondrogenesis of embryonic chick limb bud mesenchymal cells in micromass culture, *In Vitro Cellular & Developmental Biology-Animal* **1993**, *29A*, 917.

206. J. Rossignol, C. Boyer, R. Thinard, S. Remy, A. S. Dugast, D. Dubayle, N. D. Dey, F. Boeffard, J. Delecrin, D. Heymann, B. Vanhove, I. Anegon, P. Naveilhan, G. L. Dunbar and L. Lescaudron, Mesenchymal stem cells induce a weak immune response in the rat striatum after allo or xenotransplantation, *Journal of Cellular and Molecular Medicine* **2009**, *13*, 2547.

207. H. Liu, K. Lu, P. A. MacAry, K. L. Wong, A. Heng, T. Cao and D. M. Kemeny, Soluble molecules are key in maintaining the immunomodulatory activity of murine mesenchymal stromal cells, *Journal of Cell Science* **2012**, *125*, 200.

208. H. Park, X. Guo, J. S. Temenoff, Y. Tabata, A. I. Caplan, F. K. Kasper and A. G. Mikos, Effect of swelling ratio of injectable hydrogel composites on chondrogenic differentiation of encapsulated rabbit marrow mesenchymal stem cells in vitro, *Biomacromolecules* **2009**, *10*, 541.

209. J. S. Park, J. S. Chu, A. D. Tsou, R. Diop, Z. Tang, A. Wang and S. Li, The effect of matrix stiffness on the differentiation of mesenchymal stem cells in response to TGF-β, *Biomaterials* **2011**, *32*, 3921.

210. Y. Lei, S. Gojgini, J. Lam and T. Segura, The spreading, migration and proliferation of mouse mesenchymal stem cells cultured inside hyaluronic acid hydrogels, *Biomaterials* **2011**, *32*, 39.

211. R. J. Seelbach, P. Fransen, M. Peroglio, D. Pulido, P. Lopez-Chicon, F. Duttenhoefer, S. Sauerbier, T. Freiman, P. Niemeyer, C. Semino, F. Albericio, M. Alini, M. Royo, A. Mata and D. Eglin, Multivalent dendrimers presenting spatially controlled clusters of binding epitopes in thermoresponsive hyaluronan hydrogels, *Acta Biomaterialia* **2014**, *10*, 4340.

212. A. M. Kloxin, M. W. Tibbitt, A. M. Kasko, J. A. Fairbairn and K. S. Anseth, Tunable hydrogels for external manipulation of cellular microenvironments through controlled photodegradation, *Advanced Materials* **2010**, *22*, 61.

VITA

Hasani G. J. Jayasinghe Arachchige Dona

Candidate for the Degree of
Doctor of Philosophy

Thesis: FABRICATION, SWELLING, AND BIOLOGICAL PROPERTIES OF SURFACE-PATTERNED HYDROGELS BASED ON POLY(2-HYDROXYETHYL METHACRYLATE)

Major Field: Chemistry

Biographical:
Education:

- Completed the requirements for the Doctor of Philosophy in Chemistry at Oklahoma State University, Stillwater, Oklahoma in December, 2018.
- Completed the requirements for the Bachelor of Science in Chemistry at University of Kelaniya, Kelaniya, Sri Lanka in 2010.

Experience:
Graduate Teaching/Research Assistant, Oklahoma State University (2012-2018)

- Research fields – Patterning polymer surfaces with microstructures using soft lithography, Polymer chemistry, Scanning electron microscopy, Culturing, differentiation, and immunostaining of stem cells on hydrogels
- Teaching – General Chemistry I and II, and Organic Chemistry I laboratories

Teaching Assistant, Open University of Sri Lanka, Sri Lanka (2011-2012)

- Organic Chemistry laboratories, Physical Chemistry laboratories

Teaching Assistant, University of Kelaniya, Sri Lanka (2010-2011)

- Analytical Chemistry laboratory, Biochemistry laboratory, Environmental and Industrial Chemistry aboratory,

Fellowships and Awards:

- NSF Fellowship to attend PolyChar23 short course and conference, May 2015, Lincoln, Nebraska
- First place for outstanding and exemplary paper presentation, Physical Sciences and Technology Division, 25th Annual OSU Research Symposium 2014

Professional Memberships: American Chemical Society (2014 – Present)
Golden Key International Honor Society (2014 – Present)